Aus dem LMU Genzentrum
Institut der Ludwig-Maximilians-Universität München

Dissertation

zum Erwerb des Doctor of Philosophy (Ph.D.)

an der Medizinischen Fakultät der
Ludwig-Maximilians-Universität München

TNF-α and IFN-γ Differentially Regulate AML Cell Susceptibility to CD70-Antibody-Mediated Cytotoxicity

vorgelegt von:
Monika Sponheimer

aus:
Bonn / Deutschland

Jahr:
2026

Mit Genehmigung der Medizinischen Fakultät der
Ludwig-Maximilians-Universität München

Erstes Gutachten von:	Prof. Dr. Marion Subklewe
Zweites Gutachten von:	Prof. Dr. Elfriede Nößner
Drittes Gutachten von:	Prof. Dr. Barbara Schraml-Schotta
Viertes Gutachtes:	Prof. Dr. Dr. Daniel Kotlarz

Dekan: **Prof. Dr. med. Thomas Gudermann**

Datum der Verteidigung:

16.01.2026

Table of content

Abstract

Despite advances in acute myeloid leukemia (AML) treatment, relapse rates remain high, leading to poor outcomes. While antibody and CAR-T cell therapies have transformed the treatment landscape in B-cell malignancies, translation to AML has been limited due to the lack of leukemia-specific surface antigens and the risk of on-target-off-leukemia toxicity. Among the candidate targets under clinical investigation, CD70 has gained attention due to its expression on both AML bulk and leukemic stem cells, with restricted expression in normal tissues.

This preclinical study evaluated CD70 as a target for NK cell-based immunotherapy in AML utilizing a sugar-engineered antibody targeting CD70 (SEA-CD70). Flow cytometry analysis showed CD70 expression ranging from 0.2 % to 89.6 % (mean = 15.1 %, n = 86) in primary AML cells across different genetic subgroups. Importantly, CD70 expression remained conserved at time of relapse (0.3 – 90.3 % $CD70^+$, mean = 25.4, n = 14). SEA-CD70 demonstrated potent cytotoxicity against AML cell lines, primary AML cells, and in a mouse model. Cytotoxic activity was dose-dependent and correlated with antigen expression levels. Given CD70's role as co-stimulatory molecule, we assessed the efficacy of CD70-based NK-cell therapy within the dynamics of inflammatory responses, particularly the pro-inflammatory cytokine milieu. Interestingly, we observed an upregulation of CD70 on AML cells upon exposure to conditioned medium (CM) from CD33xCD3 activated T cells. As expected, the cytokine profile of the CM showed high levels of tumor necrosis factor alpha (TNF-α) and interferon gamma (IFN-γ; 1.7 ng/ml and > 9 ng/ml respectively, n = 6). Further investigation on the impact of defined cytokines revealed a TNF-α dependent upregulation of CD70 on AML cells leading to enhanced antibody-dependent cellular cytotoxicity (ADCC) against primary AML cells (specific lysis without conditioning = 17.9 %, n = 15 vs. TNF- α = 34.3 %, n = 13, p = 0.0048) However, IFN-γ exposure of AML cells lead to a markedly reduced ADCC (specific lysis without conditioning: 17.9 % vs. IFN-γ = 9.2 %, n = 15). Mechanistically this observation was shown to be mediated by a significant upregulation of the NK cell inhibitory receptor ligands (MFI ratio HLA-ABC without conditioning = 65.8 vs. IFN-γ = 139.1 n = 16, p = < 0.0001, HLA-E without conditioning = 2.4 vs. IFN-γ = 4.9, n = 11, p = 0.0045). Blocking of the NK inhibitory receptors (KIR and NKG2A) by lirilumab and monalizumab partially reversed the reduced ADCC (without 8.3 % vs. IFN-γ: 1.1 % vs. IFN-g + lirilumab: 6.5 %, IFN-γ + monalizumab: 3.3 %, n = 6). Utilizing a CD33 directed antibody, similar findings were observed, indicating a universal adaptive resistance mechanisms of AML cells to ADCC.

Our findings provide mechanistic insight into resistance to antibody-mediated immunotherapy in AML and may help contextualize limited efficacy observed in early clinical trials so far. Biomarker studies in patients receiving mAbs are warranted to further understand IFN- γ dependent upregulation of human leukocyte antigen (HLA) molecules as a mode of resistance in AML.

List of figures

List of tables

List of abbreviations

ALL	Acute lymphoblastic leukemia
AML	Acute myeloid leukemia
ADCs	Antibody drug conjugates
ADCC	Antibody dependent cellular cytotoxicity
ADCP	Antibody-dependent cellular phagocytosis
ASXL1	additional sex combs-like 1
BCL-2	B cell lymphoma 2
BiTE	Bispecific T-cell engager
BsAb	Bispecific antibody
CAR	Chimeric antigen receptor
CEBPA	CCAAT/enhancer binding protein alpha
CLL-1	C-type lectin-like molecule-1
CR	Complete response
CSF1R	Colony-stimulating factor 1 receptor
DCs	Dendritic cells
DEG	Differentially expressed genes
DNMT3A	DNA methyltransferase 3A
DLBCL	Diffuse large B cell lymphoma
ELN	European leukemia network
E:T	Effector-to-target
EZH2	Enhancer of zeste 2
FasL	Fas ligand
FBS	Fetal bovine serum
FDA	U.S. food and drug administration
FLT3	Fms-like tyrosine kinase 3
GvHD	Graft versus host disease
GvL	Graft versus leukemia
HDs	Healthy donors
HLH	Hemophagocytic lymphohistocytosis
HMA	Hypomethylating agents
HLA	Human leukocyte antigen

HSC	Hematopoietic stem cell
HSCT	Hematopoietic stem cell transplantation
IDH	Isocitrate dehydrogenase
IFN-γ	Interferon-γ
IL	Interleukin
iPSCs	Induced pluripotent stem cells
JAK-STAT	Janus-kinase-signal transducer and activator of transcription
JNK	c-Jun-N-terminal kinase
KMT2A	Lysine methyltransferase 2a
KO	Knock out
LBCL	Large B cell lymphoma
LMU	Ludwig-Maximilians-University
LSCs	Leukemic stem cells
mAb	Monoclonal antibody
MCL	Mantle cell lymphoma
MICA	MHC class I polypeptide-related sequence A
MM	Multiple myeloma
MLLT3	Mixed lineage leukemia translocated to 3
MRD	Measurable residual disease
mTECs	Medullary thymic epithelial cells
NHL	Non-Hodkin lymphoma
NK	Natural killer
NPM1	Nucleophosmin 1
NRAS	Neuroblastoma RAS viral oncogene homolog
PBMCs	Peripheral blood mononuclear cells
PD-1	Programmed cell death protein 1
PD-L1	Programmed death ligand 1
PSG	Penicillin–streptomycin–glutamine
r/r	Relapse/refractory
RAS	Rat-sarcoma
RAF	Rapidly accelerated fibrosarcoma
RCC	Renal cell carcinoma
RNPs	Ribonucleoproteins

RUNX1	Runt-related transcription factor 1
sAML	Secondary AML
sCD27	Soluble CD27
scFv	Single chain variable fragments
SCID	Severe combined immunodeficiency
tAML	Therapy related AML
TCR	T cell receptor
TET2	Tet methylcytosine dioxygenase 2
Tg	Transgenic
TLR	Toll-like receptor
TNF-α	Tumor necrosis factor α
TP53	Tumor protein p53
TRAF	TNF receptor associated factor
Treg	Regulatory T cells
UCB	Umbilical cord blood
USA	United states of America
WT	Wildtype
WT1	Wilms' tumor 1

1. Introduction

1.1 Acute Myeloid Leukemia

Acute myeloid leukemia (AML) is a hematological malignancy that is characterized by the uncontrolled proliferation of abnormal myeloid progenitors, called blasts. These leukemic blasts fail to mature into functional blood cells, leading to the suppression of normal hematopoiesis in the bone marrow. As a result, patients develop cytopenia, including anemia, neutropenia, and thrombocytopenia, which contribute to a broad range of clinical symptoms. Anemia leads to fatigue and breathlessness, neutropenia increases susceptibility to recurrent infections and fever, and thrombocytopenia results in spontaneous bleeding and easy bruising. Additionally, AML blasts can infiltrate extramedullary organs, such as the liver and spleen, further impairing their function. Due to the non-specific and variable presentation of symptoms, AML can be challenging to diagnose early often leading to delayed initiation of treatment. According to the National Cancer Institute, 20,800 new cases of AML have been diagnosed in the United States of America (USA) in 2024, and the 5-year relative survival rate was 31.9% between 2014 and 2020 (National Cancer Institute, last accessed at 2nd of April 2025, available at: "https://seer.cancer.gov/statfacts/html/amyl.html"). AML is the most common leukemia in adults with a median age of onset of 68 years (1).

1.1.1 Pathogenesis

AML may develop in individuals with a pre-existing hematological condition or as a result of previous treatments, such as exposure to topoisomerase II inhibitors, alkylating agents or radiation (2). However, in most cases, AML emerges as a *de novo* malignancy in individuals with no severe prior health issues. While in general cancer develops from somatically acquired driver mutations, the enormous heterogeneity of AML makes it difficult to pinpoint the pathophysiology to one molecular mechanism. Next generation sequencing identified frequently mutated genes (> 5%) in patients with AML, including fms-like tyrosine kinase 3 (FLT3), neuroblastoma RAS viral oncogene homolog (NRAS), nucleophosmin 1 (NPM1), runt-related transcription factor 1 (RUNX1), CCAAT/enhancer binding protein alpha (CEBPA), DNA methyltransferase 3A (DNMT3A), isocitrate dehydrogenase 1 (IDH1), IDH2, tet methylcytosine dioxygenase 2 (TET2), tumor protein p53 (TP53), and wilms' tumor 1 (WT1), (3). These mutations cause functional changes that drive leukemogenesis through diverse mechanisms. Mutations in signaling genes, such as FLT3 and NRAS, promote uncontrolled proliferation by activating key pathways, including rat-sacroma (RAS) – rapidly accelerated fibrosarcoma (RAF), Janus-kinase-signal transducer and activator of transcription (JAK-STAT), and phosphatidylinositol 3-kinase/protein kinase B (PI3K-AKT) (4). Mutations in the NPM1 gene lead to aberrant cytoplasmic localization of NPM1 and its interacting proteins, affecting cellular homeostasis (4). Alterations in myeloid transcription factors (e.g.

RUNX1, CEBPA) and chromosomal translocations (e.g. RUNX1-RUNX1T1) disrupt transcriptional regulation and hinder normal hematopoietic differentiation (4). Mutations in DNMT3A, IDH1, IDH2, and TET2 lead to aberrant DNA methylation patterns via the accumulation of the oncometabolite 2-hydroxygluterate (4). Loss-of-function mutations in tumor suppressor genes, such as TP53, result in impaired transcriptional regulation and disrupted protein degradation via MDM2 and PTEN Döhner, Weisdorf (4). WT1 mutations affect a key transcriptional regulator involved in hematopoiesis and can interact with other genetic alterations such as FLT3- internal tandem duplication (ITD) (4). Additionally, disruptions in epigenetic regulators, including additional sex combs-like 1(ASXL1), enhancer of zeste 2 (EZH2), and lysine methyltransferase 2a (KMT2A) – mixed lineage leukemia translocated to 3 (MLLT3) fusions, alter chromatin modifications, such as histone methylation (4). Moreover, Spliceosome gene mutations (e.g. SRSF2, SF3B1, U2AF1, ZRSR2) contribute to defective RNA processing, while cohesion-complex mutations (e.g. STAG2, RAD21) impair chromosomal integrity and transcriptional control (4).

1.1.2 Treatment

The development of chemotherapy in the 1970s marked a breakthrough in the treatment of AML. The combination of anthracyclines, such as daunorubicin or idarubicin, with cytarabine (Ara-C) became the standard induction regimen due to its high efficacy in achieving complete remission (5, 6). This “7+3” regimen, consisting of seven days of continuous cytarabine infusion and three days of anthracycline administration, remains the cornerstone of AML induction therapy. However, the effectiveness varies depending on patient characteristics. Younger patients with favorable genetics achieve high remission rates while older patients and those with adverse genetics show lower remission rates and higher risk of relapse (7). Treatment response to chemotherapy is further stratified by the European LeukemiaNet (ELN) classification, including favorable, intermediate and adverse genetic risk groups (8). Better response rates compared to standard chemotherapy have been achieved with CPX-351, a liposomal formulation of cytarabine and daunorubicin designed to deliver a define drug ratio of 5 to 1, particularly in high-risk AML, e.g therapy-related AML (tAML) or secondary AML (sAML) (9). Moreover, leukemic-stem cells (LSCs) were identified to be resistant to chemotherapy due to their slow proliferation and pre-existing mutations and are considered as one of the main reasons for AML relapse (10).

Hematopoietic stem cell transplantation (HSCT) was initially introduced to restore hematopoiesis following intensive chemotherapy. However, it was discovered that allogenic HSCT also provides a potent anti-leukemic effect through the graft versus leukemia (GvL) response, where donor-derived immune cells eliminate residual leukemic cells (11). This immune-mediated mechanism has been critical in achieving long-term remission in patients. Despite of the GvL success in treatment of AML, HSCT comes with challenges, including risk of acute and chronic graft versus host disease (GvHD), in which donor T cells attack healthy recipient cells, leading to severe complications. Additionally, HSCT is not available to all patients due to the need for a suitable donor, and often not an option for older patients due to a limited tolerance to the procedure. One of the key

prognostic markers in AML treatment is measurable residual disease (MRD). The presence of MRD after induction therapy is associated with a high risk of relapse (12). Therefore, MRD assessment has become an essential tool for guiding post-remission strategies, including the decision to proceed with HSCT.

In recent years, progress has been made in developing novel therapeutic approaches for AML (**Fig. 1**). Hypomethylating agents (HMA), such as azacytidine and decitabine have been introduced as less intense treatment option for patients that are not eligible for intensive chemotherapy such as older or unfit patients. The B-cell lymphoma 2 (BCL-2) inhibitor venetoclax has shown promising data when used in combination with HMA by targeting the apoptotic pathways in leukemic cells (13). Targeted therapies that emerged, including FLT-3 tyrosine kinase inhibitors (midostaurin, gilteritib, quizartinib) for FLT3-mutated AML and IDH inhibitors (ivosidenib, enasidenib) for IDH-1/IDH-2-mutated AML (14-17). Despite an increase in response rates and improvement in overall survival, relapse and resistance to therapy is still a common scenario in AML, and the prognosis remains dismal, necessitating the development of novel treatment strategies.

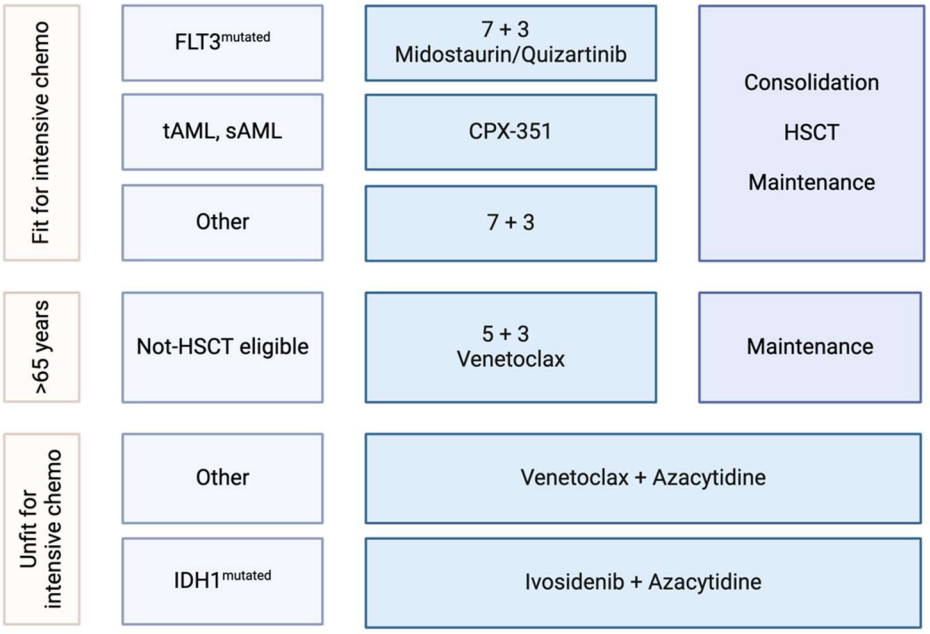

Figure 1: Overview of the main treatment strategies in AML
Treatment selection is based on age, comorbidities, and genetic factors. Patients eligible for intensive chemotherapy receive the 7+3 regimen (cytarabine + daunorubicin), which may be combined with FLT3 inhibtors (e.g. midostaurin, quizartinib) in FLT3-mutated AML. High-risk AML subtypes, such as tAML and sAML, may receive CPX-351, a liposomal formulation of cytarabine + daunorubicin. Those achieving remission may proceed to consolidation chemotherapy, HSCT, or maintenance therapy. Patients >65 years are those unable to tolerate intensive chemotherapy and receive a lower dose cytarabine (5+3) regimen combined with venetoclax. Patients unfit for chemotherapy are treated with HMA, such as azacytidine, in combination with venetoclax, with the addition of IDH inhibitor (e.g., ivosidenib) if IDH mutations are present. Figure adapted from (18), created with Biorender.

1.2 Immunotherapy

1.2.1 Platforms

The immune system has a crucial role in controlling malignancies, and the therapeutic potential of T cells has been demonstrated by the increase in long-term survival due to GvL after allogeneic HSCT. This proof of concept has inspired the development of immunotherapies (**Fig. 2**). To restore the endogenous anti-tumor immunity regulatory pathways are targeted with Immune checkpoint blockade. Blockade of inhibitory receptors such as programmed cell death protein 1 (PD-1), programmed cell death ligand 1 (PD-L1) and cytotoxic T-lymphocyte-associated protein 4 (CTLA-4) demonstrated enhanced T-cell activation and improved tumor recognition in multiple malignancies, including melanoma, lung cancer, and hematological malignancies (19). The concept of monoclonal antibodies (mAbs) recognizing defined structures, was translated to selectively target cancer cells. Antibody-drug-conjugates (ADCs) consist of mAbs linked to cytotoxic payload, allowing targeted binding to specific proteins and subsequent internalization, leading to tumor cell damage. Brentuximab vedotin (anti-CD30) has been approved by the U.S. food and drug administration (FDA) as second-line treatment of Hodgkin lymphoma and anaplastic large cell lymphoma due to it high response rates as single agent. Similar success was obtained with Trastuzumab emtansine (anti-HER2) that received global approval in metastatic breast cancer and showed improved survival in several clinical trials (20). In AML, gemtuzumab ozogamicin (Mylotarg), an ADC targeting CD33, was initially approved but later withdrawn due to toxicity concerns. However, with revised dosing schedules and better patient selection, it has been reintroduced and is now used with chemotherapy showing efficacy in newly diagnosed CD33-positive AML (21, 22). Another ADC in AML, Pivekimab sunirine, targets CD123. Results from a Phase I clinical study demonstrated a complete response (CR) rate of 17%, with a manageable safety profile, leading to its progression into Phase Ib/II trial (23).

In contrast to ADCs, ADCC is a fundamental mechanism to recruit immune cells, including macrophages and natural killer (NK) cells. NK cells expressing the activating receptor CD16 (FcγRIII) recognize the Fc region of antibodies opsonizing a tumor cell leading to NK cell-mediated killing of tumor cells. One of the most prominent ADCC-based antibodies is rituximab (anti-CD20) which is the standard-of-care for several B-cell malignancies (24). Other antibodies that achieved high response rates included Trastuzumab in breast cancer (anti-HER2; (25), and Daratumumab in multiple myeloma (anti-CD38; (26).

While mAbs naturally engage NK cells through Fc receptor interactions, bispecific antibodies are engineered molecules that can bind two different antigens simultaneously, enabling targeted T-cell activation independent of HLA. Blinatumomab is the most advanced bispecific T-cell engager (BiTE), targeting CD19 on B cells and CD3 on T cells. It is FDA approved for relapsed/refractory (r/r) B-cell acute lymphoblastic leukemia (ALL) and MRD-positive ALL, demonstrating high response rates but requiring continuous infusion and careful management of toxicities (27, 28). In

AML, a CD33xCD3 BiTE, AMG 330 demonstrated potent AML blast control at very low effector-to-target (E:T) ratios for up to 5 weeks *in vitro* (29). In a Phase I dose-escalating study in r/r AML, AMG 330 showed anti-leukemic activity; however, cytokine release syndrome (CRS) was observed frequently, and only eight out of 60 patients achieved a complete response (CR) (30, 31). The CD123-targeting, CD123xCD3 dual affinity retargeting antibody (DART), Flotetuzumab, is evaluated for treatment of AML in parallel and reported in a Phase I study a CR of 19% (5/27 patients) (32). While facing similar challenges with CRS, early use of interventions prevented high rates of CRS. One of the limiting factors of BiTE molecules is their short half-life. To achieve sufficient BiTE molecule levels in the patient's serum multiple injections are required leading to high costs.

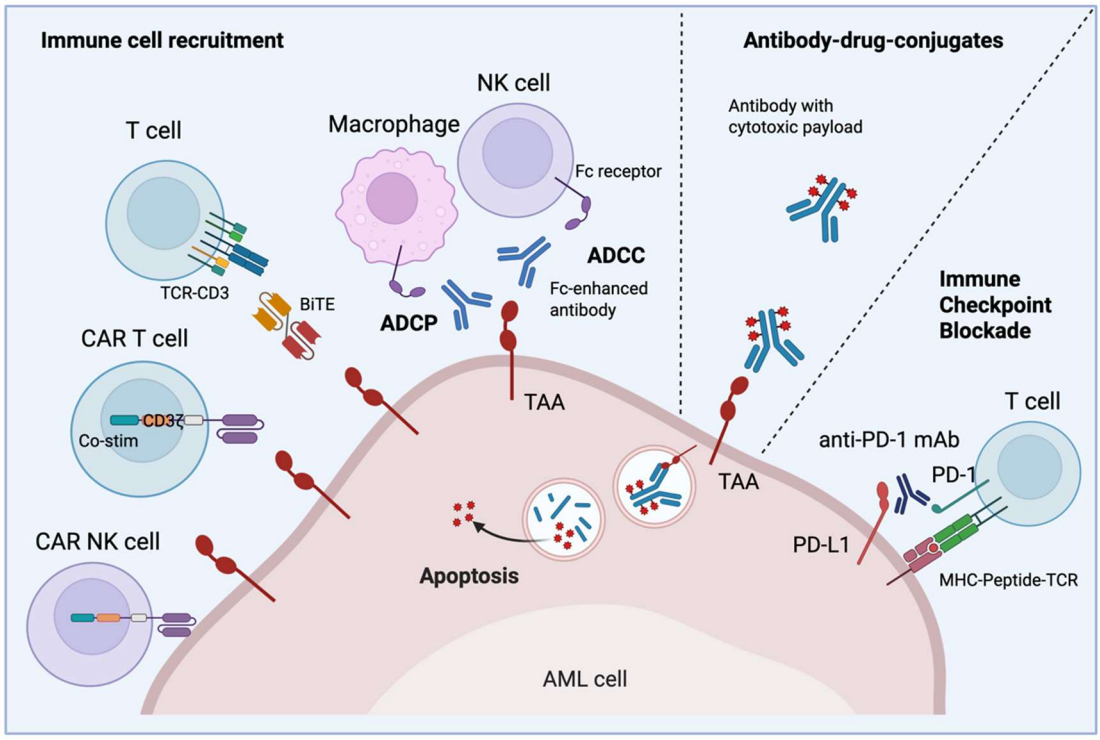

Figure 2: Selected immunotherapeutic strategies targeting AML
Immune checkpoint blockade: A mAb blocks the interaction between PD-L1 on AML cells and PD-1 on T cells, restoring T cell-mediated and HLA-restricted tumor immunity. Antibody-drug-conjugates: mAbs linked to cytotoxic payloads selectively bind tumor-associated antigens (TAAs), leading to internalization, and targeted tumor cell killing. Immune cell recruitment: NK cells and macrophages engage in ADCC or antibody-dependent cellular phagocytosis (ADCP), upon mAb binding to TAAs. Endogenous T cells can be recruited via bispecific molecules linking CD3 on T cells with TAAs. CAR T or NK cells are genetically engineered to recognize TAAs in an HLA-independent manner. Figure adapted from (33), created with Biorender.

This challenge supported the development of cell-based therapies that provide long-lasting immune responses. Chimeric antigen receptor (CAR) T cell therapy represents one of the most advanced forms of immunotherapy that has revolutionized the treatment of B-cell malignancies. CAR T cells are genetically modified to recognize tumor antigens in an HLA-independent manner, overcoming immune evasion of malignant cells. The evolution of CAR T cells has progressed through multiple generations: first generation CARs contained only a single activation domain

(CD3ζ), second generation CARs integrated co-stimulatory domains (CD28 or 4-1BB) to enhance persistence, and third generation CARs incorporated additional co-stimulation and cytokine secretion to improve expansion and efficacy. CD19-directed CAR T cells demonstrated remarkable clinical efficacy. In the ZUMA-1 trial CD19-CAR T cells axicabtagene ciloleucel (axi-cel) achieved a complete response rate of 57% in r/r diffuse large B cell lymphoma (DLBCL) (34). Similarly, the ELIANA trial evaluating tisagenlecleucel (tisa-cel) in pediatric and young adult patients with r/r B-ALL reported a CR rate of 81% (35). However, CAR T cell therapy is associated with severe toxicities including, CRS and immune effector cell-associated neurotoxicity (ICANs), which require close monitoring and clinical management. CRS is driven by excessive release of inflammatory cytokines, particular interleukin 6 (IL-6) and IL-1, leading to systemic symptoms such as fever, hypotension, and organ dysfunction. ICANs manifest as neurotoxicity with symptoms ranging from confusion and encephalopathy to cerebral edema in severe cases. To date, six different CAR-T cell therapies have received FDA approval including, tisa-cel (CD19, r/r B-ALL, r/r DLBCL), axi-cel (CD19, r/r DLBCL), lisocabtagene maraleucel (liso-cel, CD19, r/r large B cell lymphoma (LBCL)), brexucabtagene autoleucel (brexu-cel, CD19, r/r mantle cell lymphoma (MCL)), idecabtagene vicleucel (ide-cel, BCMA, r/r multiple myeloma (MM)), and ciltacabtagene autoleucel (cilta-cel, BCMA, in r/r MM). Looking ahead, next generation CAR T cell therapies are in clinical development including, CD22-targeting CAR-T cells for treatment of CD19-negative relapse in B-ALL, dual-targeting CAR-T cells (e.g. CD19/CD22 or CD19/CD20) to reduce antigen escape, and allogenic CAR T cells engineered to improve accessibility.

1.2.2 Challenges in selecting target antigens for AML immunotherapy

Selecting an optimal target antigen for immunotherapy in AML is particularly challenging due to the disease's inherent heterogeneity. Ideally, a target antigen should be exclusive expressed on malignant cells, including LSCs, while being absent from normal tissues. However, in AML, target antigen expression varies between patients (interindividual) and within different subclones of the same patient (intraindividual). A major limitation in AML immunotherapy is the expression of target antigens on healthy hematopoietic cells, which results in on-target, off-leukemia toxicity. Unlike B-cell depletion, which can be managed with immunoglobulin replacement therapy, the loss of healthy myeloid cells leads to cytopenia, increased risk for infection, and severe suppression of hematopoiesis. This toxicity restricts the use of lineage restricted therapies as a standalone approach, making them suitable as bridging therapy before HSCT. Moreover, the presence of target antigens in normal tissues can create an "antigen sink", were therapeutic agents bind to non-malignant cells, reducing their availability and diminishing therapeutic efficacy.

AML cells can evade immune targeting through several resistance mechanisms, including antigen escape. This involves the downregulation or alteration of surface antigen expression, allowing leukemic cells to become invisible to targeted therapies. This phenomenon has been observed in CD19-directed CAR T cell therapy, where approximately 30% of patients experience relapse due

to loss or mutation of CD19 (36). In addition to antigen escape, persistent antigen stimulation can lead to T-cell exhaustion, impairing their ability to sustain long-term cytotoxicity (37).

To date, no single AML target antigen with the same applicability as CD19 in B-ALL has been identified. However, several candidates have been explored, each with unique advantages and limitations (**Fig. 3**). CD33 and CD123 are among the most well-characterized myeloid lineage antigens, with CD33 expression detected in 85-90% of AML cases and CD123 in 60-80% (38-41). While their widespread expression makes them attractive targets, their presence on normal myeloid progenitors limits their clinical utility (42). FLT3 represents another promising target, its expression has been reported on AML bulk and precursor cells and a subset on HSCs (43, 44). C-type lectin-like molecule-1 (CLL-1) has also emerged as a potential target due to its expression on AML bulk and LSCs, while being expressed in myeloid lineage but largely absent on HSCs (45).

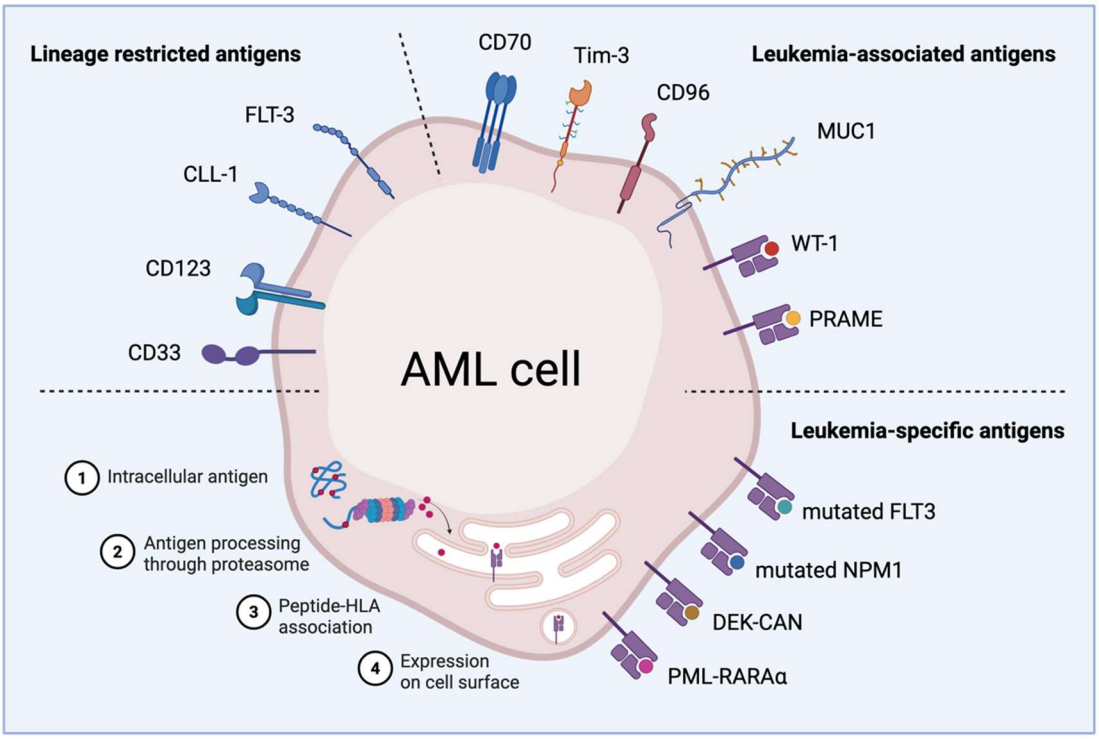

Figure 3: Target antigens considered for immunotherapy of AML
AML-associated target antigens can be categorized into three major groups: 1) lineage-restricted antigens, such as CD33, CD123, CLL-1, and FLT3, which are expressed in both leukemic and healthy hematopoietic cells; 2) leukemia-associated antigens, including CD70, TIM-3, CD96, MUC1, WT-1 and PRAME, which are aberrantly overexpressed in AML but may also be found at low levels in some normal tissue; and 3) leukemia-specific antigens, such as mutated FLT3, mutated NPM1, DEK-CAN, and PML-RARAα, which result from leukemia-specific genetic alterations and are presented via HLA molecules. Antigen processing and presentation of intracellular proteins involves initial degradation by the proteasome into short peptides that are transported into the endoplasmic reticulum, where they are loaded onto HLA class I molecules, and subsequently presented on the cell surface for recognition by T cells. Figure adapted from (46), created with Biorender.

Beside lineage-restricted antigens, several leukemia-associated antigens have been explored for immunotherapy, including CD70, TIM-3, CD96, MUC1, WT-1, and PRAME. These antigens are more selectively expressed on AML cells compared to normal hematopoietic cells, but heterogenous expression patterns and low antigen density pose challenges for uniform targeting. Additionally, tumor-specific neoantigens, such as mutated FLT3, mutated NPM1, DEK-CAN and PML-RARA fusion proteins, offer the potential for highly specific immunotherapy approaches, particularly in T cell receptor (TCR)-based or peptide vaccine strategies that rely on HLA presentation. The search for novel target antigens with restricted expression in healthy tissue is ongoing. By comparing transcriptomic datasets from malignant cells and healthy cells across multiple tissues, colony-stimulating factor 1 receptor (CSF1R) and CD86 have recently been identified as promising candidates (47).

Given the absence of a unique target in AML, overcoming these challenges requires innovative strategies. Dual-targeting approaches that combine multiple antigens, such as CD19/CD22 in B-ALL, are being investigated to minimize antigen escape. Moreover, advanced engineering of immune cells, such as enhanced CAR T cells with improved persistence, armored CARs that secrete cytokines to sustain activity, or allogenic CAR T cells to increase accessibility, are being explored to address the limitations of current antigen selection.

1.2.3 CD27-CD70 signaling axis

The CD27-CD70 signaling axis is one of many co-stimulatory pathways that support T-cell activation and shape memory T cell pools (**Fig. 4**). CD27 is constitutively expressed on naïve T cells, and unlike CD28, its downstream signaling is not mediated by direct phosphorylation but instead relies on the adapter proteins TNF receptor associated factor 2 (TRAF2) and TRAF5 (48). These molecules initiate a signaling cascade that activates NF-κB and c-Jun-N-terminal kinase (JNK) pathways promoting T-cell survival and clonal expansion (49). CD70 is the only known ligand for CD27, and its potent co-stimulatory function was demonstrated in studies utilizing CD70 transgenic (Tg) mice, where CD70 was overexpressed under the control of CD11c or CD19 promoters. T cells from these CD70 Tg mice showed a progressive loss of naïve T cells, detected by a reduction in the expression of the lymphoid homing receptor CD62L, leading to their conversion into effector/memory T cells (50, 51). In these experimental models, continuous T cell stimulation depletes the naïve T cell pool, rendering mice susceptible to opportunistic infections. These findings underscore the necessity of tight regulation in T-cell activation to prevent excessive immune responses. The interaction of CD27 with CD70 induces the cleavage of CD27 from the membrane by metalloproteases, leading to a reduction in CD27 expression following T-cell activation (52, 53). This mechanism contributes to T-cell homeostasis by limiting a prolonged stimulation. Moreover, the expression of CD70 is highly regulated and is typically transient, occurring only upon antigen encounter in activated dendritic cells (DCs), T-, NK- and B cells (54, 55). CD70 expression on DCs can be induced by toll-like receptor (TLR) and CD40 signaling (56). The expression of CD70 on T cells can be induced by CD28 signaling and is further upregulated by IL-1α, TNF-α,

IL-12, whereas IL-4 has been shown to negatively regulate CD70 expression (57, 58). These observations suggest that CD27-CD70 driven T-T cell interactions may play a role in immune regulation.

CD27-mediated co-stimulation promotes Th1 T-cell differentiation, resulting in an interferon-γ (IFN-γ) driven T-cell response that enhances CD4 T cell help to CD8 T cells and supports memory formation (59, 60). The CD27-CD70 axis has been implicated in T-cell memory formation, as demonstrated in an influenza virus infection mouse model (61). In this study, when CD27 wild-type (WT) and CD27 knock-out (KO) mice were challenged with primary influenza virus infection, CD27 KO mice showed a reduced absolute T cell count at the site of infection. However, the infection clearance rate remained comparable, suggesting that CD27 signaling is not essential for the initial T-cell response. In contrast, during secondary influenza virus infection, CD27 KO mice showed delayed expansion of CD4 and CD8 T cells and a lower frequency of influenza virus-specific T cells in both the lungs and spleen, indicating a key role of CD27 signaling in memory T-cell formation.

In healthy individuals, CD70 expression is restricted to medullary thymic epithelial cells (mTECs), dendritic cells (DCs) in the thymic medulla (54, 62) and antigen presenting cells (APCs) in the lamina propria (63). CD70 expression in the thymus has been associated with the development of regulatory T-cells (Tregs). In addition to its role as a co-stimulatory ligand for CD27, the full spectrum of CD70's function remains poorly characterized. However, germline biallelic loss-of-function mutations in CD27 or CD70 have been linked to recurrent Epstein-Barr virus (EBV) infections and severe cases of hemophagocytic lymphohistocytosis (HLH), lymphoproliferative malignancies, and altered T and B cell memory formation, indicating its importance in immune homeostasis (64). Functional analyses of patient-derived T cells revealed that CD27/CD70 mutations lead to altered CD4/CD8 T cell ratios, reduced cytotoxicity and impaired cytokine production.

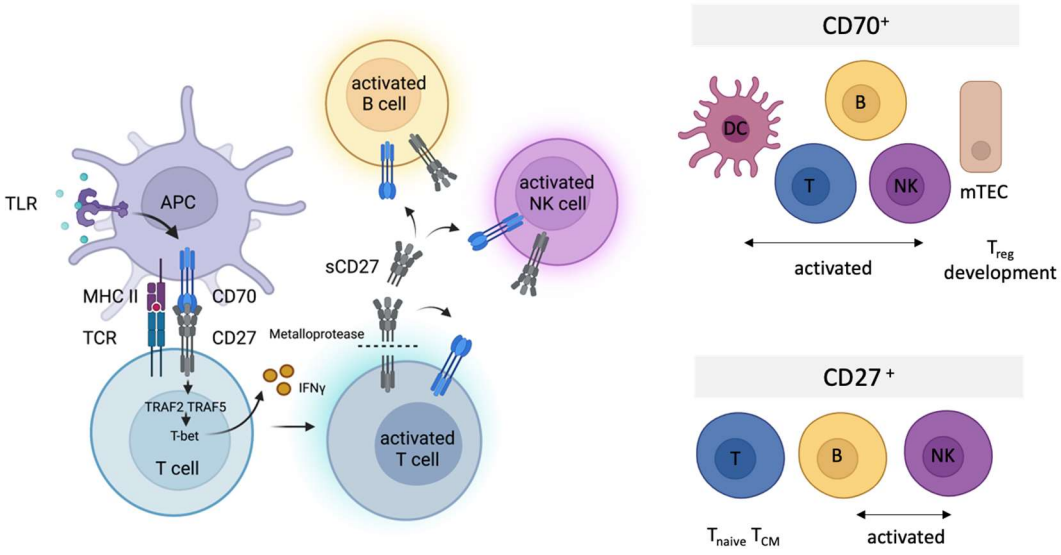

Figure 4: CD70-CD27 signalling axis
Left: Antigen encounter, such as TLR signaling, induces CD70 expression on APCs. CD70 is the natural ligand for CD27, which is constitutively expressed on naïve T cells. CD27 signals via the adapter proteins TRAF2 and TRAF5, leading to

increased expression of the transcription factor T-bet, which promotes differentiation into Th1 T cells and secretion of IFN-γ. Following CD70-CD27 interaction, CD27 is cleaved from the cell membrane by metalloproteinases. Notably, CD70 expression is also induced after TCR and BCR signaling, as well as NK cell activation, suggesting its role in immune homeostasis. **Right:** Expression profile of CD70 and CD27 in humans. Figure adapted from (65), created with Biorender.

Interestingly, aberrant CD70 expression has been reported in several hematological and sloid malignancies, including AML. CD70 has been detected in both acute and chronic leukemias (58, 66), as well as in various lymphomas including non-Hodkin lymphoma (NHL), DLBCL, and MCL (67). Additionally, CD70 expression has been identified in solid tumors such as renal cell carcinoma (RCC), glioblastoma, melanoma, ovarian, lung, colon, and breast cancer (68). In AML, CD70 is variably expressed on both leukemic bulk and LSCs but not on normal HSCs (69-71). Moreover, elevated levels of soluble CD27 (sCD27) have been detected in patients with autoimmune disease (72), and hematological malignancies (70, 73), where its presence is associated with poor prognosis (74). This further underscores the relevance of the CD27/CD70 axis in tumor biology, highlighting sCD27 as a potential biomarker. The transient expression of CD70 in healthy immune cells, including activated T cells, B cells, NK cells, and DCs, makes CD70 an attractive target for immunotherapy of AML.

1.2.4 CD70 in clinics

To date, several clinical studies have investigated CD70-trageted approaches in both hematological and solid tumors. Early trials, focused on ADCs developed from Seattle Genetics, Bristol-Myers-Squibb and Amgen in NHL and RCC (75-78). However, the development of AMG172 and MDX-1203 was discontinued, and clinical trials for SGN-75 and SGN-CD70A terminated early due to toxicity concerns. Although ADCs represent a promising therapeutic strategy, their efficacy depends on receptor internalization, which varies among tumor types, and the effectiveness of their cytotoxic payload, is depending on the linker chemistry.

Encouraging results were later achieved with the anti-CD70 mAb, cusatuzumab, in AML. Interestingly, azacytidine was shown to demethylate the CD70 promoter, leading to increased CD70 expression (79). The combination of azacytidine with CD70-targeted therapy demonstrated a complete remission rate of 67% (8/12 patients) with no dose-limiting toxicities in a Phase I trial (NCT03030612, (80)). Currently, the safety and efficacy of SEA-CD70, a mAb from Seattle Genetics that shares the conserved CD70 epitope binder with the anti-CD70 ADC, are studied in a Phase I clinical trial as monotherapy or in combination with azacytidine for patients with MDS and AML (NCT04227847). Initial results indicate good tolerability with manageable adverse events (81). The safety profile of cusatuzumab led to a Phase II clinical trial investigating its combination with azacytidine in AML patients unfit for intensive chemotherapy (NCT04023526, (82)). However, ADCC-based therapies rely on the patient's endogenous NK cell pool, which is often altered in AML. Studies have reported lower absolute NK cell numbers, impaired maturation of NK cells, reduced expression of natural cytotoxicity receptors (NCRs), and higher expression of inhibitory receptors, including checkpoint inhibitors have been described (83).

To improve selectivity for AML cells over healthy HSCs, a tri-specific CD33xCD123xCD70xCD3 DARPin engager developed by Molecular Partners is currently under evaluation in a Phase I clinical trial (NCT05673057, (84)). In the field of CAR-T cell therapy, early clinical trials in B-cell malignancies explored dual-targeting CD19 and CD70 to overcome antigen escape (85). However, a major challenge in CD70-CAR development has been fratricide because CD70 is transiently expressed on activated T and NK cells. In a preclinical AML study, CD70 single chain variable fragments (scFv) and CD27-based CAR T cells were compared, with the latter demonstrating superior activity to control leukemia, higher CAR T cell expansion, and enhanced persistence (71). The use of CD27, the natural ligand of CD70, enhanced specificity while reducing fratricide. Another approach to overcome fratricide involved CRISPR-Cas9 edited CD70 and MHC knockout allogenic CAR T cells, reducing self-targeting (86). CD70-targeting CAR-T cell and NK cell therapies are currently evaluated in multiple entities including, renal cell carcinoma (NCT04696731, NCT05795595), glioblastoma (NCT05353530), ovarian carcinoma (NCT02830724), B-cell lymphoma (NCT06345027) and AML (NCT06492304). Among all ongoing recruiting CD70-based clinical studies, 29 are in phase I while 13 have progressed to Phase II (ClinicalTrial.gov last accessed on 31st of March, 2025 available at: "https://clinicaltrials.gov/search?intr=CD70&aggFilters=phase:2%201,status:rec").

Of note, CD27 agonistic antibodies such as Varlilumab (anti-CD27) are under clinical evaluation, aiming to enhance T-cell activation and function by delivering co-stimulatory signals, thereby boosting anti- tumor immune responses (87).

1.3 NK cell as effector cells in AML immunotherapy

NK cells are innate lymphoid cells important for immune surveillance by controlling infections and recognizing transformed cells. Based on their phenotype, NK cells can be categorized into two major subsets: $CD56^{bright}CD16^{-}$ NK cells are tissue resident and secrete cytokines, and $CD56^{dim}CD16^{+}$ NK cells, which circulate in peripheral blood and contain pre-assembled cytolytic granules, allowing them to respond rapidly to infected or malignant cells (88). The persistence of NK cells is dependent on cytokine signaling, particularly through IL-2 and IL-15. IL-15 is a key mediator of STAT5 activation, which enhances survival, proliferation, and toxicity of NK cells (89). Unlike T and B cells, NK cells do not require somatic rearrangement of antigen receptors. Instead, NK cell activation is regulated by a balance of activating and inhibitory receptor signaling (**Fig. 5**).

1.3.1 NK cell activation and inhibition

NK cell activation is mediated by crosslinking of activating receptors, which leads to phosphorylation of immunoreceptor tyrosine-based activation motifs (ITAMs). This phosphorylation initiates intracellular signaling cascades that trigger the release of cytolytic granules containing perforin and granzymes. Among the activating receptors, natural cytotoxicity receptors (NCRs), such as NKp30, NKp40, NKp44, and NKp46 are involved in recognizing viral, bacterial and/or cancer-

associated molecules. The Fc receptor CD16, (FcγRIIIa) is a potent activating receptor on NK cells essential for ADCC. By binding to the Fc region of antibodies, CD16 enables NK cells to recognize antibody-opsonized target cells. Notably, CD16 is the only activating receptor capable of inducing NK cell cytotoxicity without requiring additional stimulatory signals (90). Another key activating receptor, NKG2D, signals through DAP-10 and recognizes stress-induced ligands, including the MHC class I polypeptide-related sequence A (MICA), MICB, and the UL16 binding-proteins (ULBPs). These ligands are upregulated in response to DNA damage, oncogenic transformation, and viral infection, serving as danger signals that promote NK cell-mediated cytotoxicity (91). In addition to direct cytotoxicity, NK cells can also induce apoptosis in tumor cells through death receptor signaling pathways, such as Fas ligand (FasL) and TNF-related apoptosis inducing ligand (TRAIL).

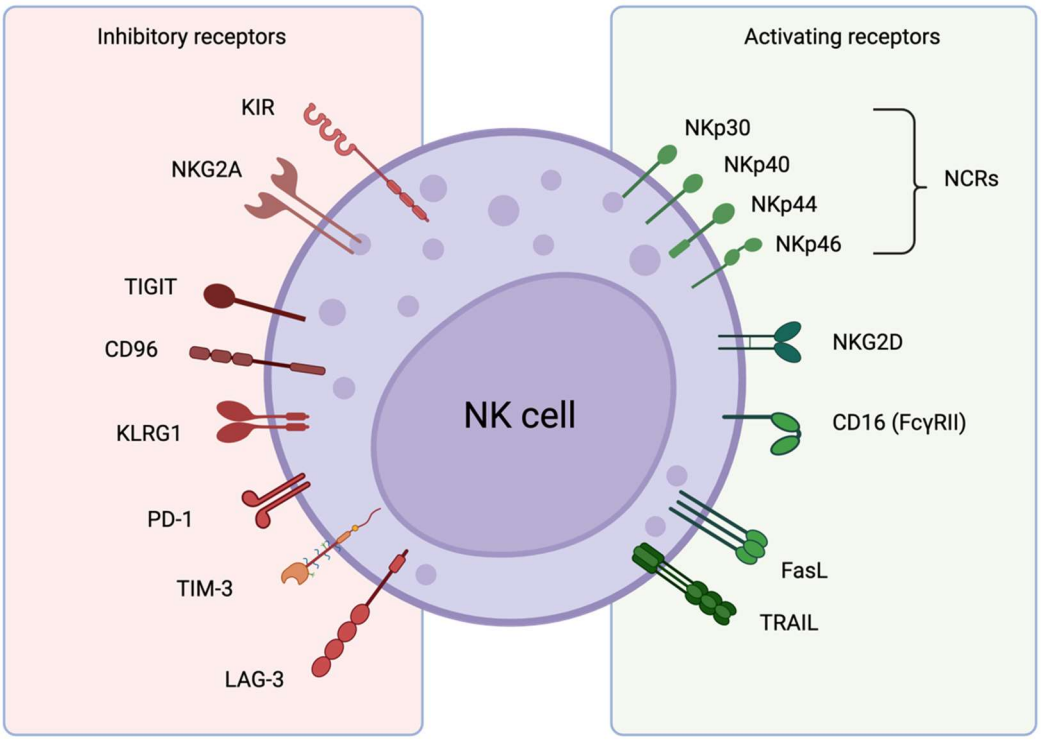

Figure 5: NK cell receptor repertoire
This schematic illustrates the balance of signals that regulate NK cell activity. On the left, inhibitory receptors include KIR and NKG2A, which recognize HLA class I molecules and help to prevent autoreactivity. In addition, immune checkpoint receptors such as TIGIT, CD96, KLRG1, PD-1, TIM-3, and LAG-3 mediate suppression of NK cell activation, particular within the tumor microenvironment. On the right, activating receptors include the NCRs (NKp30, NKp40, NKp44, NKp46), as well as NKG2D and CD16 (FcγRIII), which facilitates ADCC. NK cell also express apoptosis-inducing ligands, such as FasL and TRAIL, which contribute to the elimination of target cells through death receptor pathways. Figure adapted from (92), created with Biorender.

Given the cytotoxic potency of NK cells, their activation must be tightly regulated to prevent unintended immune responses. This is achieved through inhibitory receptors, including killer immunoglobulin-like receptors (KIRs) and NKG2A. These receptors recognize self-HLA class I molecules (HLA-A, HLA-B, and HLA-C for KIRs; HLA-E and HLA-G for NKG2A) and suppress NK cell activation through immunoreceptor tyrosine inhibiting motifs (ITIMs). Upon phosphorylation, ITIMs

recruit the tyrosine phosphatases SH-1 and SH-2, which inhibit activating receptor signaling cascades, thereby maintaining tolerance to self-tissue (93). A common immune evasion strategy by tumors, is the downregulation or loss of HLA class I expression. While this allows tumor cells to evade T cell-mediated killing, it simultaneously induces “missing self” which disrupts inhibitory receptor signaling in NK cells (94). Analogous to T cells, the activation and effector functions of NK cells can be tightly regulated by immune checkpoint molecules, such as TIGIT, CD96, KLRG1, PD-1, TIM-3, and LAG-3 (95).

1.3.2 Current NK cell-based immunotherapeutic approaches

Autologous NK cells, derived from the patient’s own peripheral blood, have been investigated in early immunotherapy trials. However, their clinical utility is limited by several factors, including impaired cytotoxicity and limited *in vivo* expansion and persistence (96). Due these limitations, the focus has shifted toward allogenic NK cell sources.

NK cells for immunotherapy can be derived from multiple sources, including peripheral blood mononuclear cells (PBMCs), umbilical cord blood (UCB), hematopoietic stem cells, and induced pluripotent stem cells (iPSCs) (97). The use of allogenic NK cells holds several advantages over allogenic T cell-based therapies, particular a lower risk of GvHD, making them suitable for off-the-shelf approaches (98). PBMC-derived NK cells can be efficiently expanded ex vivo using feeder cell lines, such as K562 cells engineered to express 4-1BBL and membrane-bound IL-21 (99). UCB-derived NK cells, which are less mature immunologically, also offer a promising alternative. Notably, CD19-CAR NK cells derived from UCB and engineered to secret IL-15 have shown potent antitumor activity in preclinical models and favorable safety in clinical settings (100). A Phase I study demonstrated that these HLA-mismatched CAR NK cells were well tolerated, with no evidence of GvHD, CRS, or ICANs (101). This favorable toxicity profile represents an advantage over allogenic CAR T cell therapies. Among novel NK-based therapies, CD70-directed CAR NK cells engineered to secret IL-15 are currently under clinical evaluation for r/r hematological malignancies (NCT05092451), and advanced RCC (NCT05703854).

In addition to PBMC- and UCB-derived sources, the generation of NK cells from stem or progenitor cells has been explored as a therapeutic source. However, these strategies face challenges related to incomplete NK cell differentiation, resulting in phenotypic variations that may impact their clinical efficacy.

Furthermore, adoptive NK cell transfer is evaluated in combination with mAbs to enhance ADCC. For example, a Phase I trial is evaluating the use of allogenic NK cells in combination with trastuzumab and pertuzumab (anti-HER2 mAbs) in patients with advanced HER-2-positive breast cancer (NCT05385705). This strategy leverages the ability of NK cells to mediate ADCC via CD16 and highlights the flexibility of antibody-based approaches. Importantly, in heterogenous diseases like AML, where antigen expression is highly variable, such flexibility enables the targeting of multiple antigens or the adaption to antigen escape variants. Taken together, these approaches

underscore the therapeutic potential of NK cells as both engineered cellular products and effector cells in combination therapies.

1.4 Aim

Novel T- and NK cell-based immunotherapies are rapidly evolving as promising treatment strategies for patients with AML. However, the identification of an ideal target antigen, one with restricted expression on healthy tissues and LSCs, remains a critical challenge and a key perquisite for therapeutic success.

CD70 has been reported to be aberrantly expressed on AML cells and LSCs, while its physiological expression is largely limited to transient activation states of T cells, B cells, and NK cells. Despite this favorable expression profile, the mechanism driving CD70 expression in AML remain poorly understood. Nevertheless, its limited expression in normal tissue makes CD70 an attractive candidate for targeted immunotherapy, with the potential to minimize on-target, off-tumor toxicity.

In this preclinical study, we investigate CD70 as a potential target for immunotherapy in AML and to investigate mechanisms influencing the efficacy of CD70-directed immunotherapy. The specific objects were:

1. To characterize CD70 expression as target antigen in AML through in-depth characterization of its expression across molecular subtypes, disease stages and cellular compartments.
2. To evaluate the therapeutic potential of an Fc-enhanced, non-fucosylated mAb targeting CD70 (PF-84 08046040, SEA-CD70) for NK cell-mediated immunotherapy in both *in vitro* and *in vivo* models.
3. To investigate resistance and immunomodulatory mechanisms driven by CD70 or inflammatory signalling, particular those impairing NK or T cell function and to explore strategies to overcome them, with the goal of improving the clinical translation of CD70-directed immunotherapies.

2. Material and Methods

2.1 Materials

2.1.1 AML cell lines

The human AML cell lines MOLM-13, OCI-AML-3, MV4-11 and the lymphoma cell line OCI-Ly1 were purchased from the German Collection of Microorganisms and Cell Cultures (Leibniz-Institut DSMZ, Braunschweig, Germany). Cells were cultivated with RPMI 1640 (PAN-Biotech, Aidenbach, Germany) supplemented with 10–20% fetal bovine serum (FBS) and 0.5 mg/ml penicillin–streptomycin–glutamine (PSG, Thermo Fisher Scientific, Waltham, MA, USA). Where indicated, cells were exposed to 2.5 ng/ml IFN-γ and/or 5 ng/ml TNF-α (Peprotech, Hamburg, Germany) for 72 h. After cytokine stimulation, cells were thoroughly washed in fresh culture medium prior to co-culture experiments with NK cells to ensure removal of residual cytokines.

2.1.2 Patients

Bone marrow samples were obtained from AML patients at initial diagnosis, remission or relapse, as well as from healthy donors (HDs). All participants provided written informed consent, and the study protocols were approved by the Ethics Committee of the Ludwig-Maximilians-University (LMU, Munich, Germany, reference number: 216-08), in accordance with Declaration of Helsinki. Mononuclear cells were isolated from bone marrow samples by gradient centrifugation using Ficoll (Biochrom, Berlin, Germany), followed by cryopreservation in liquid nitrogen. The freezing medium consisted of 80% FBS and 20% dimethyl sulfoxide (Serva Electrophoresis, Heidelberg, Germany). At the time of diagnosis, each patient sample underwent a standardized diagnostic analysis at the LMU's Laboratory for Leukemia Diagnostics. This included cytomorphologic assessment, classical cytogenetics, fluorescence *in situ* hybridization, and molecular genetic testing. Cytogenetic risk was classified according to refined Medical Research Council (UK) guidelines. Integrated risk categorization was conducted based on the with ELN 2017 recommendations.

2.1.3 Healthy donor material and NK cell isolation

Peripheral blood or leukoreduction chambers from single-donor platelet apheresis collections were obtained from healthy volunteers at the LMU Munich's division of Transfusion Medicine, Cell Therapeutics and Hemostasis. All donors gave informed consent, and the study was approved by the LMU Institutional Review Board (reference number: 23-0283). Peripheral blood mononuclear cells (PBMCs) were isolated by density gradient centrifugation using Pancoll (PAN-Biotech, Aidenbach, Germany). Following centrifugation, PBMCs were harvested from the interphase layer.

NK cells were purified via negative selection using the NK Cell Isolation Kit (Miltenyi Biotec, Bergisch Gladbach, Germany) following the manufacturer's recommended instructions.

2.1.4 Antibodies for multi-parameter flow cytometry (MPFC)

Expression was determined either as % positive cells or as mean fluorescence intensity (MFI) ratio, and gating was based on the corresponding isotype control. Anti-human CD45-AF700, clone: 2D1; CD34-BV421, clone 561; CD38-PE, clone HB-7; CD3-PerCP-Cy5.5, clone: HIT3a; Galetin-9-BV421, clone 9M1-3; HLA-G-AF488, clone 87G; HLA-E-PE, clone 3D12; HLA-ABC-APC, clone W6/32; PD-L1-BV421, clone MIH3; HLA-DR-FITC, clone L243; PD-1-FITC, clone EH12.2H7; CD158b-PE, clone DX27; NKG2A-BV421, clone S19004C; CD155-APC, clone SKII.4; CD112-PE, clone TX31; MIC A/B-PE, clone 6D4 (BioLegend, San Diego, CA, USA); CD33-PE-Cy7, clone WM53 (eBioscience by Thermo Fisher Scientific, Waltham, MA, USA); CD27-FITC, clone L128 (BD Bioscience, Franklin Lakes, NJ, USA); CD14-APC-Vio®770, clone REA599; CD70-APC, clone REA292 (Miltenyi Biotech, Bergisch Gladbach, Germany); CD70-APC, clone h1F6 (Seattle Genetics, Bothell, WA, USA).

2.1.5 Antibodies for preclinical testing

Monoclonal Fc enhances antibodies (IgG control, SEA-CD70 and SEA-CD33) and SEA-CD70 conjugated to APC fluorophore were obtained through a material transfer agreement with Seattle Genetics/Pfizer.

2.2 Methods

2.2.1 Bioinformatical analysis of the TCGA-AML cohort

Data acquisition and preprocessing

Transcriptome and clinical datasets for AML patients (n = 173) were retrieved from The Cancer Genome Atlas (TCGA-AML) via the National Cancer Institute Genomic Data Commons (GDC) data portal. Raw count RNA-seq data were imported, and redundant gene entries were filtered. Using the DESeqDataSet function in R, data were formatted into a matrix of non-negative integer values. Ensembl gene identifiers were converted to gene symbols (102). Genes with low expression (row sums < 10) were excluded. Normalization was performed using variance-stabilizing transformations (VST). Patient samples were clustered based on CD70 expression using the PAM algorithm from the cluster (cluster R package version 2.0.3).

Differential gene expression (DEG) and gene ontology (GO) analysis

DEG was assessed by stratifying samples into $CD70^{high}$ and $CD70^{low}$ groups. The DESeq function from the DESeq2 package in R was applied for statistical analysis. Genes with a p-value < 0.01

and log2(foldchange) > 1 were assigned as significantly upregulated, while downregulated genes met the same p-value threshold with log2(foldchange) < -1. Volcano plots were generated using the EnhancedVolcano R package. Gene lists were submitted to EnrichR (https://maayan-lab.cloud/Enrichr), and pathway enrichment was conducted based on the Bioplanet 2019 database, selecting the top 10 enriched terms.

2.2.2 *Ex vivo* cultures using primary AML samples

Assays with primary AML cells were carried out as previously established in our laboratory (103, 104). Following a 72 h pre-incubation period, T cells were selectively removed using the CD3 Positive Selection Kit II (StemCell Technologies, Vancouver, Canada), following the supplier's protocol. In certain experiments, AML cells underwent additional cytokine exposure with 25 ng/ml IFN-γ and 50 ng/ml TNF-α (Peprotech, Hamburg, Germany) for a further 72 h. Prior to co-culture with NK cells, cytokine-exposed cells were washed thoroughly with fresh medium to eliminate residual cytokines.

2.2.3 Detection of CD70 isoforms by qPCR

Total RNA was extracted using the RNeasy Mini kit (Qiagen, Hilden, Germany), and cDNA synthesis was carried out with the RevertAid First Strand cDNA Synthesis Kit (Thermo Fisher Scientific). Gene expression was quantified using iTaq universal SYBR® Green Supermix (BioRad, Hercules, CA). Primer sequences were as follow:

CD70 isoform 1: forward: 5'-*GGGCAGCTACGTATCCATCG*; reverse: 5'-*AGGTTGGTGCAGAGTGTGTC*

CD70 isoform 2: forward: 5'-*GGGCAGCTACGTATCCATCG*; reverse: 5'-*GACTTTGAGTCCCCAGTTCCA*

ABL-1 (BioRad) served as the reference gene.

2.2.4 Antibody-fluorochrome staining for MPFC

For flow cytometric staining, 1-3 x 10^5 cells per well were transferred to 96-well plates and centrifuges at 550 x g for 5 minutes. After removing the supernatant, cells were washed with PBS containing 0.5% BSA and 0.2% EDTA. Subsequently, cells were incubated in the staining mix containing pre-determined dilutions of fluorochrome-conjugated antibodies and 0.25 µl of viability dye LIVE/DEAD™ Fixable Aqua Dead Cell Stain Kit (Thermo Fisher Scientific) per well. Staining was performed in the dark at 4 °C for 15-20 minutes. After staining, cells were washed again and finally resuspended to achieve a concentration of 1 x 10^6 cells/ml. Cells were stored protected from light at 4 °C until flow cytometric analysis, which was conducted the same day.

For primary AML expression studies, where LSCs occur at low frequencies, the staining protocol was adapted by increasing the cell number to 2 x 10^6 cells per condition, scaling all reagents, and acquiring 1x10^6 events per sample (**Fig. 6**).

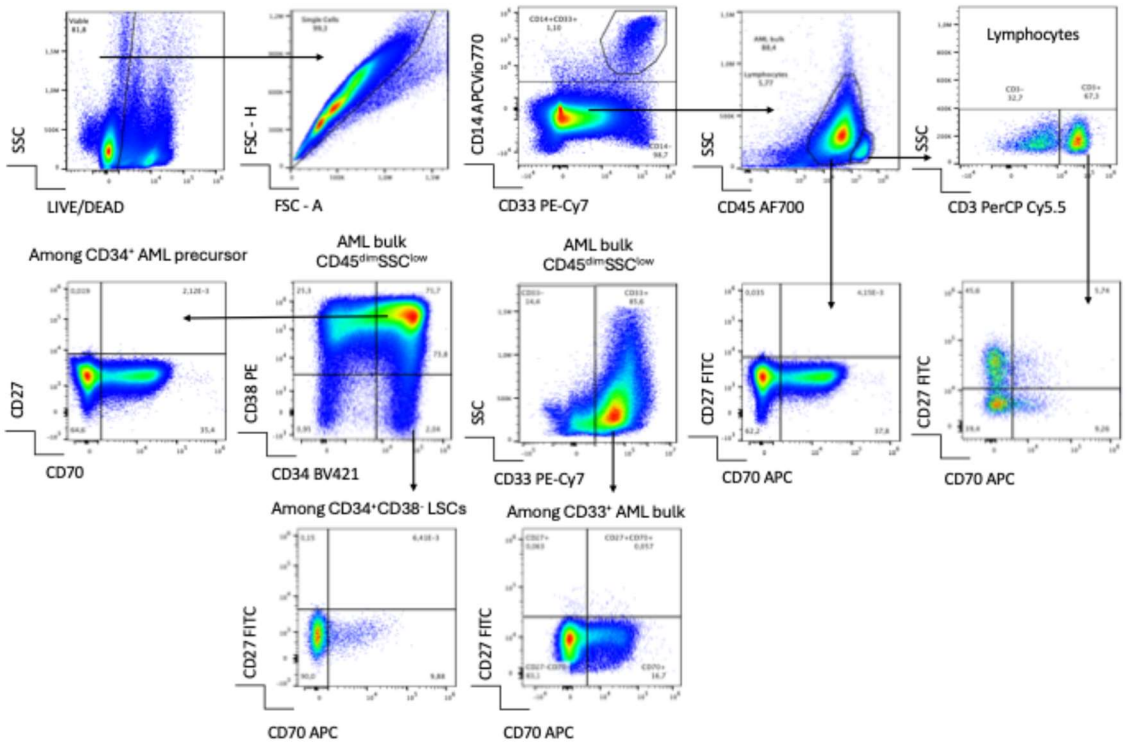

Figure 6: Gating strategy for flow cytometry-based analysis of CD27 and CD70 expression in primary AML
Cells were first gated based on viability, excluding dead cells with LIVE/DEAD™ Fixable Aqua viability dye. Doublets were then excluded using FSC-Area versus FSC-Height parameters. To remove mature myeloid cells, $CD14^+CD33^+$ monocytes were excluded. Subsequently, CD45 expression and SSC characteristics were used to identify the leukemic population ($CD45^{dim}SSC^{low}$) and lymphocytes ($CD45^{bright}SSC^{low}$). Within the lymphocytes gate, $CD3^+$ T cells were identified, and CD27 and CD70 expression was assessed on this subset based on an isotype control. In the AML gate, CD27 and CD70 expression were analyzed on the bulk $CD45^{dim}SSC^{low}$ population, and further evaluated on $CD33^+$ cells, $CD34^+$ progenitor cells, and the $CD34^+CD38^-$ compartment enriched for LSCs.

2.2.5 Immunohistochemistry

IHC staining was performed in collaboration with the Pathology department of the University Hospital LMU (Prof. Dr. Martina Rudelius). Bone marrow biopsies were decalcified, fixed in 4% paraformaldehyde, and paraffin-embedded. Sections underwent heat-induced epitope retrieval using AR9 buffer (pH = 9; Akoya Bioscience; Marlborough, MA USA) and were stained with an anti-CD70 antibody (1:50 dilution, Cell Signalin Technology). Signal detection was performed with the ImmPRESS Polymer Kit (Vector Laboratories, Newark, CA, USA) according to the manufacturer's instructions.

2.2.6 Patient azacytidine treatment

Patients received azacitidine in accordance with the approved prescribing information and guidelines issued by the relevant regulatory authorities.

2.2.7 Detection of sCD27 by ELISA

Levels of sCD27 in serum or bone marrow aspirated were assessed in HDs and AML patients at diagnosis, remission, and relapse using the Instant ELISA Kit (Invitrogen by Thermo Fisher Scientific) follwoing the manufacturer's protocol.

2.2.8 *Ex vivo* ADCC assays

NK cells were co-cultured with AML cell lines or primary AML cells at an E:T ratio of 5:1 in culture medium. Co-cultures were treated with either anti-CD70 mAb (clone h1F6, SEA-CD70), anti-CD33 mAb (clone h2H12, SEA-CD33), or a non-binding isotype (IgG) control (clone h00), all afucosylated to enhance Fc receptor binding. Antibodies were applied at 0.01 – 5 µg/ml for 16 to 24 h.

Effector and target cells were distinguished using the CellTrace Far Red or CFSE dyes (Thermo Fisher Scientific). Cell death was evaluated using the LIVE/DEAD™ Fixable Aqua Dead Cell Stain Kit (ThermoFisher Scientific; **Fig. 7**), and cytotoxicity was assessed by flow cytometry (Cytoflex S, Beckman Coulter, Brea, CA, USA). NK-cell activation was determined by CD69 expression (Vioblue, clone REA824; Miltenyi Biotec; **Fig. 7**). Specific lysis was calculated as:

$$specific\ lysis\ (\%) = 100 - \left(\frac{viable\ target\ cells\ in\ mAb\ condition}{viable\ target\ cells\ in\ control}\right) * 100$$

For some ADCC assays, blocking antibodies against KIR with lirilumab (anti-human CD158a, IchorBio, Oxford, UK) or NKG2A with monalizumab (anti-human CD159a, IchorBio) were used at a concentration of 10 µg/ml in selected conditions.

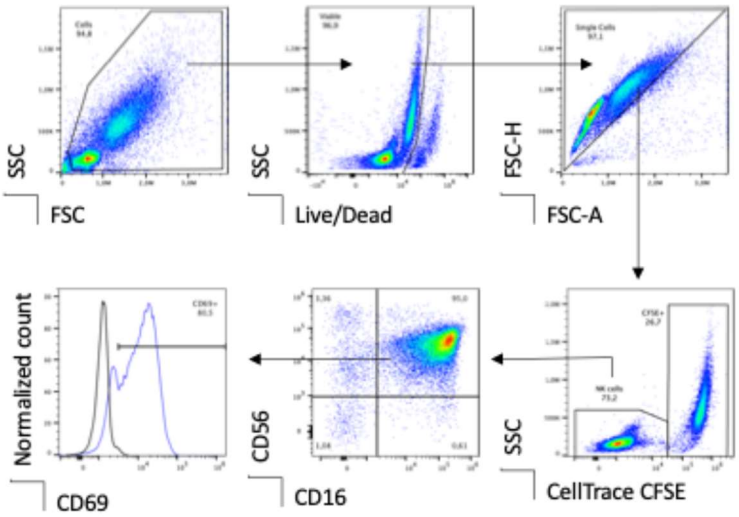

Figure 7: Gating strategy for flow cytometry-based ADCC assays
Cell debris were excluded based on FSC and SSC characteristics. Dead cells were identified using the LIVE/DEAD™ Fixable Aqua Dead Cell Stain Kit and excluded from the analysis. Doublets were removed by comparing FSC-Area and FSC-Height signals. AML cells were distinguished from NK cells using the cell tracer CFSE. NK cells were further identified

by expression of CD56 and CD16. $CD56^+CD16^+$ double positive cells were analyzed for expression of CD69, with an isotype control (grey) used to define the gating threshold.

2.2.9 *In vivo* mouse experiment with SEA-CD70 and MV4-11

Animal experiments were conducted by Pfizer, which provided the therapeutic mAbs used in this study. The experimental design was developed in collaboration with the company and the data provided for analysis. Experiments were ethically approved and followed institutional guidelines. MV4-11 cells were maintained in IMDM or RPMI with 10% FBS, and >90% viability was confirmed prior to injection. A total of 5 x 10^6 cells mixed with 25% Matrigel HC (Corning) were injected subcutaneously into SCID mice. Once tumors reached approximately 50 mm^3, mice were randomized into treatment groups of nine mice per group. SEA-CD70 (clone h1F6) and the G1V1 variant (contains the mutations: E233P, F234V and L235A) was administered intraperitoneally every four days for five doses.

Tumor dimensions were measured biweekly, and volume was calculated as:

$$volume = \left(\frac{1}{2} length\right)(width)(width)$$

Mice were sacrificed at endpoint or if tumor burden exceeded 1000 mm^3. Tumor growth inhibition (%TGI) was calculated at day 29 using the Jackson Lab formula:

$$\%TGI\ (Jax) = 100\ \times (1 - \frac{mean\ vol_{treated}}{mean\ vol_{control}})$$

Statistical comparison of tumor progression was performed using two-way ANOVA with Tukey's multiple comparisons test (GraphPad Prism 9; (105)).

2.2.10 T cell-mediated cytotoxicity assays with CD70 blockade

Pan T cells from healthy donor PBMCs were isolated using the Human T cell Isolation Kit (StemCell Technologies), and co-cultured with MOLM-13 cells (E:T ratio 1:5) in the presence of CD33xCD3 bispecific antibody (BsAb; (106)) at a concentration of 5 ng/ml with or without anti-CD70 mAb (10 µg/ml; clone: h1F6 SEA). After 72h, cytotoxicity, T-cell proliferation, and expression of CD27/CD70 were assesed by MPFC. T cells and targets were labeled with CD2-BV421 (clone TS1/8) and CD33-PE (clone WM53). Live/dead discrimination was done using LIVE/DEAD™ Fixable Aqua Dead Cell Stain Kit (ThermoFisher Scientific). Specific lysis was calculated as:

$$specific\ lysis\ (\%) = 100 - \left(\frac{viable\ CD33^+ cells\ in\ BsAb\ condition}{viable\ CD33^+\ cells\ in\ control}\right) * 100$$

T-cell proliferation was determined by comparing $CD2^+$ cell counts on days zero and three.

Long-term co-cultures with blinatumomab (CD19xCD3 BsAb) were performed as previously described (37). Supernatants were collected on days 3, 10, 17, and 24. T cells were restimulated with OCI-Ly1 cells and supplied with culture medium every three – four days. At weekly intervals (day 7, 14, 21, and 28), T cells were harvested from the culture using the human T cell isolation kit (StemCell Technologies) and used in short-term co-cultures with Ba/F3 cells, transduced with human CD19, to assess functional capacity.

2.2.11 Metabolic analysis of T cells

T cells were activated for 48 h using CD3/CD28 Dynabeads (Thermo Fisher Scientific). Following magnetic removal of the beads 2.5 x 10^5 T cells were seeded per well in poly-D-lysine-coated 96-wellplates. Metabolic profiling, including mitochondrial respiration and glycolytic capacity, was carried out on a Seahorse XFe96 Analyzer (Aglient Technologies, Santa Clara, CA, USA) using manufacturer-supplied stress test kits. Cellular metabolic activity was normalized to cell number, which was quantified with a Cytation 1 imaging reader (BioTek Instruments, Winooski, VT, USA).

2.2.12 Conditioned media from BsAb-activated T cells

Pan T cells from healthy donor PBMCs were isolated using the human T cell Isolation Kit (Stem Cell Technologies) according to the manufacturer's instructions. T cells were co-cultured with MOLM-13 cells at an E:T ratio of 1:1 in the presence of a CD33xCD3 bispecific antibody (106) at a concentration of 5 ng/ml. After 72 h, cells were spun down, and supernatants harvested. AML cells (MOLM-13, OCI-AML-3, and MV4-11) were incubated for 72 h in culture media mixed 1:1 with conditioned supernatant. Cytokine were quantified using LEGENDplex™ Human Inflammation Panel 1 (BioLegend), following the manufacturer's instructions. In some assays, IFN-γ neutralization was performed by adding anti-IFN-γ mAb (clone: B133.5, 10 µg/ml; Bio X Cell, Lebanon, NH, USA).

2.2.13 CRISPR-Cas9 knockout of TNFRSF1A and IFNGR1

CRISPR-Cas9 gene editing was performed in collaboration with the department of biochemistry (Prof. Dr. Veit Hornung). Knockouts were generated using ribonucleoproteins (RNPs) formed by annealing 100 pmol of crRNA and tracrRNA (Integrated DNA Technologies).

IFNGR1: 5'-*ACGGTAAAAACAGGGACCTG*-3'

TNFRSF1A: 5'-*GACCAGTCCAATAACCCCTGAGG*-3'

RNPs were complexed with 40 pmol of recombinant S.p. Cas9 nuclease V3 (Integrated DNA Technologies) and delivered into MOLM-13 cells (0.5 - 1 x 10^6 cells) via nucleofection using the X-unit of a 4D nucleofector (Program EH-100, Lonza, Basel, Switzerland). After recovery and expansion, clones were sequenced to confirm bi-allelic knockouts for the gene of interest as described before (107) and knock out efficacy confirmed by MPFC.

2.2.14 Bulk RNA sequencing analysis

Bulk RNA sequencing was performed at the Laboratory for Functional Genome Analysis (LAFUGA) in collaboration with the Faculty of Biology, Anthropology and Human Genomics (Prof. Dr. Wolfgang Enard), LMU and data were processed by the Bioinformatics Unit at LMU (Dr. Tobias Straub). MOLM-13 cells were exposed to IFN-γ (2.5 ng/ml), TNF-α (5 ng/ml), or both for 72 h. 1 x 10^4 cells were lysed in Buffer RLT Plus (Qiagen, Venlo, Netherlands) containing 1% β-mercaptoethanol and stored at −80 °C. RNAseq was performed using the Prime-seq workflow (see protocol: https://doi.org/10.17504/protocols.io.s9veh66).

In short, cell lysates were treated with proteinase K and DNase I. First strand cDNA was synthesized using Maxima H Minus Reverse Transcriptase (Thermo Fisher Scientific, EP0753) with barcoded oligo-dT primers (E3V7NEXT) and a custom template-switching oligo. cDNAs of samples were pooled and treated with exonuclease I (Thermo Fisher Scientific, EN0581) to remove unreacted primers. PCR amplification of cDNAs was carried out using KAPA HiFi HotStart ReadyMix (Roche, 07958935001) and SINGV6 primers. Libraries were prepared from 30 ng of the pooled cDNA were subjected to library preparation using the NEBNext Ultra II FS DNA Library Prep Kit for Illumina (New England Biolabs, E7805S) using a prime-seq specific custom ligation-adapter and dual-indexing with TruSeq i5 and Nextera i7 primers via PCR. Libraries were sequenced on an Illumina Nextseq 2000 system utilizing 28 cycles for the forward read, 8 cycles for each of both index reads and 93 cycles for the reverse read. Quality assessment of the fastq data files was conducted using fastqc (v0.11.5) (108), followed by polyA trimming using cutadapt (v 4.1) (109). Subsequent read filtering, mapping, and counting were performed using the zUMIs pipeline (v 2.9.7) (110), with reads mapped to the human genome (hg38). Fastq files were sample-demultiplexed using deML (111).

The RNA-seq data generated and analyzed during this study have been submitted to the Gene Expression Omnibus (GEO) and are available under the accession number GSE286349.

2.2.15 Imaging of conjugates between AML and NK cells

Imaging experiments were performed in collaboration with the Faculty of Biology and Center for Molecular Biosystems, Human Biology and Bioimaging at LMU (Prof. Dr. Heinrich Leonhardt). Images were acquired on a Nikon TiE microscope equipped with a Yokogawa CSU-W1 spinning-disk confocal unit (50 µm pinhole size), an Andor Borealis illumination unit, an Acal BFi laser beam combiner (405 nm/488 nm/561 nm/640 nm), and an Andor IXON 888 Ultra EMCCD camera. The microscope was controlled by Nikon software (NIS Elements, ver. 5.02.00). Cells were imaged in an environmental chamber maintained at 37 °C with 5% CO_2 (Oko Labs), using a Nikon PlanApo 100x/1.45 NA oil immersion objective and a Perfect Focus System (Nikon). Image stacks were recorded with a step size of 1.0 µm and a pixel size of 130 nm. HLA-E BV421, CFSE cell tracer, HLA-ABC PE and FarRed cell tracer were excited using the 405, 488, 561 and 640 nm laser lines, respectively. Image analysis was done in Fiji software.

3. Results

3.1 CD70/CD27 expression profile in AML

3.1.1 CD70 expression on RNA level

To investigate CD70 expression patterns in AML, transcriptomic data from the TCGA-AML cohort was analyzed using an unsupervised clustering approach. Specifically, partitioning around medoids (PAM) clustering was used to group patient samples based on CD70 mRNA expression profiles. This analysis revealed two distinct subgroups: $CD70^{High}$ (37%) and $CD70^{Low}$ (63%) as determined by silhouette statistic methods and principal component analysis (**Fig. 8 A**).

Moreover, the expression of CD70 transcript isoforms (CD70.1, CD70.2) was analyzed in AML cell lines (OCI-AML-3, MOLM-13, and MV4-11) and a cohort of primary AML samples (n =19). This analysis revealed higher levels of isoform 1 compared to isoform 2 (**Fig. 8 B** and **Tab. Suppl. 1**).

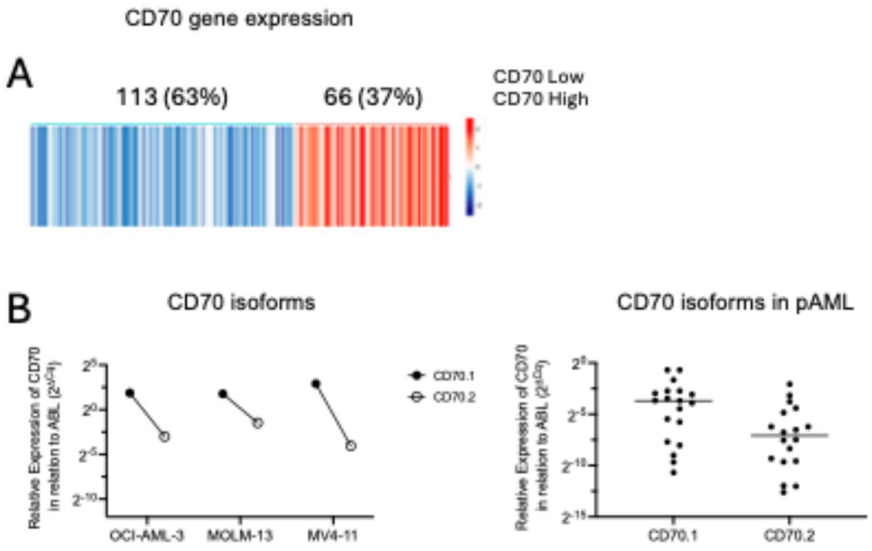

Figure 8: Characterization of CD70 expression on RNA level in AML
A: CD70 gene expression analysis in the TCGA AML cohort (n = 179). **B:** Relative expression of CD70 isoform 1 and 2 in relation to ABL in AML cell lines: OCI-AML-3, MOLM-13 and MV4-11 (n = 1–3; left), and in primary AML cells (n = 19; right) detected by quantitative PCR.

3.1.2 CD70 expression on protein level

Subsequently, we evaluated surface expression of CD70 protein in AML patient samples using MPFC. AML bulk cells, defined by $CD45^{dim}SSC^{low}$ characteristics, were analyzed at both the time of initial diagnosis and relapse. A broad inter-patient variability in CD70 surface expression was

observed, ranging from 0.2 to 89.6%, with a median value of 7.0% across the cohort (n = 86; **Fig. 9 A**, **B** and **Tab. Suppl. 2**). When comparing initial diagnosis and relapse samples (n = 14), no differences in CD70 expression were detected, with percentages ranging from 0.3 to 90.3% and a median of 3.9% (**Fig. 9 A** and **Tab. Suppl. 2**). Analysis of the relationship of CD70-positive cells and the MFI ratio showed a positive correlation (**Fig. 9 B**). Further stratification of the data based on genetic risk categories did not reveal any correlation between CD70 expression and cytogenetic or molecular risk classification (**Fig. 9 C**). To assess the consistency of CD70 detection across platforms, we compared MPFC with IHC. Despite the use of a different antibody clone for IHC, the expression patterns were concordant, and a moderate correlation between the two methods was observed (r = 0.4502; **Fig. 9 D**).

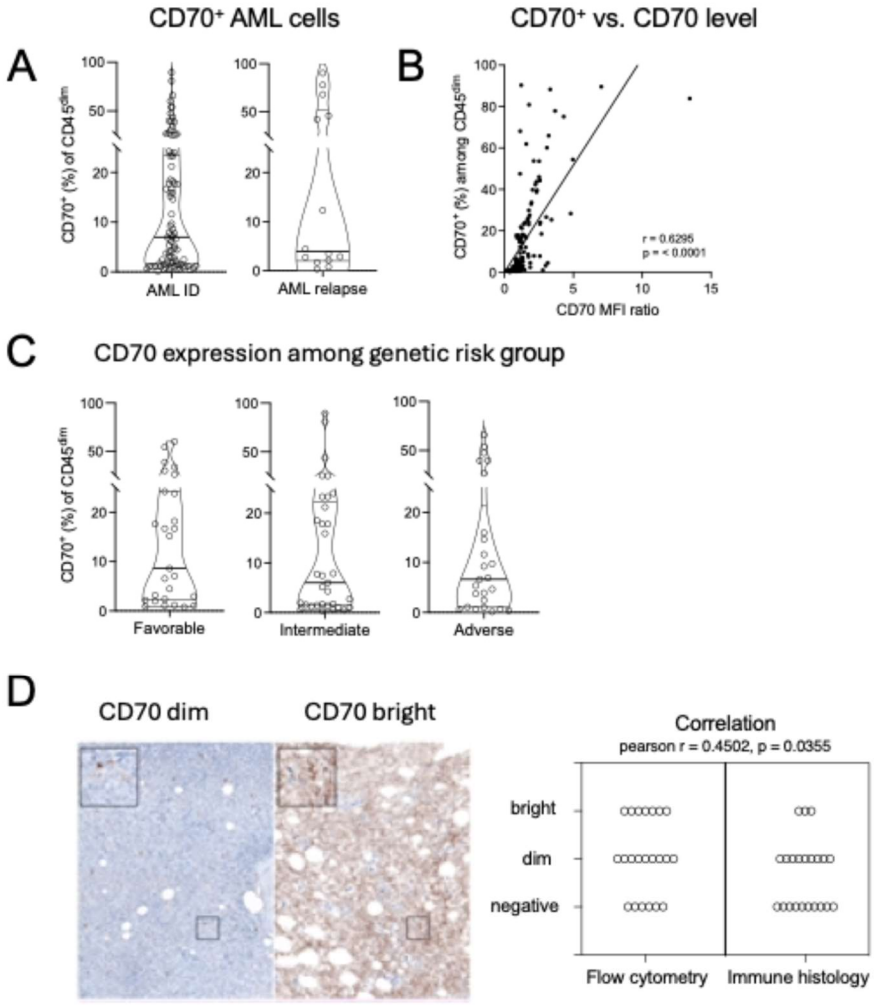

Figure 9: Characterization of CD70 expression on protein level

A: Expression of CD70 (Ab clone REA-292) on $CD45^{dim}SSC^{low}$ cells from AML patients at the time point of initial diagnosis (ID; n = 86), and at time point of relapse (n = 14) detected by multi-parameter flow cytometry (MPFC). **B:** Correlation of CD70 expression and expression level (CD70 % positive vs. MFI ratio) of AML patients from initial diagnosis detected by multi-parameter flow cytometry (MPFC), (n = 86). **C:** Expression of CD70 on $CD45^{dim}SSC^{low}$ cells detected by MPFC from AML patients at time point of initial diagnosis among genetic risk groups: favorable (n = 29), intermediate (n = 22) and adverse (n = 28). **D** left: representative immunohistochemistry (IHC) images showing dim CD70 staining (left) and bright CD70 staining (right) in AML patient bone marrow biopsy FFPE samples. Right: correlation of CD70 expression between MPFC and IHC (n = 22).

To further characterize CD70 expression across different AML cell differentiation stages, we compared $CD34^+$ progenitor cells, $CD34^+CD38^-$ LSCs and the $CD33^+$ AML bulk population. This analysis revealed similar expression of CD70, with a median of 8.5% CD70 positive cells among $CD34^+$ cells (n = 15) and 7.6% among $CD33^+$ bulk cells (n = 28; **Fig. 10 A** and **Tab. Suppl. 3**).

Because of recent clinical trials of anti-CD70 mAb therapies in combination with HMA such as azacytidine and in some alongside venetoclax, we aimed to analyze whether azacitidine treatment modulated CD70 expression in AML (112). While previous reports, including findings by Riether et al., described upregulation of CD70 on leukemic stem and progenitor cells following HMA treatment, our analysis did not reproduce this observation (113). CD70 expression was analyzed in both $CD45^{dim}SSC^{low}$ AML bulk cells and $CD34^+$ precursor population at baseline (days 0-1) and after exposure to azacytidine (days 4-6). No changes in CD70 expression were detected over this period in $CD45^{dim}SSC^{low}$ cells, the percentage of CD70-positive cells was 3.1% at baseline and 3.5% post treatment; in $CD34^+$ cells, expression showed a similar variation from a mean of 4.6% to 4.0% (n = 4; **Fig. 10 B** and **Tab. Suppl. 4**).

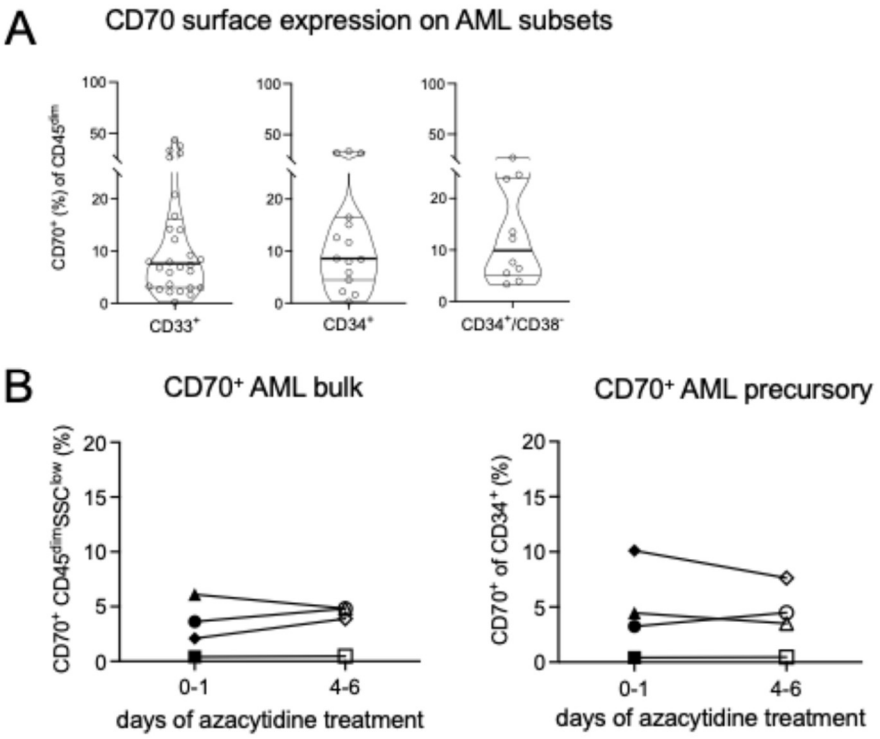

Figure 10: Comparison of CD70 expression between AML bulk and precursor cells
A: Expression of CD70 (Ab clone h1F6) on AML subpopulations: $CD33^+$ AML bulk (n = 28), $CD34^+$ AML precursors (n = 15), $CD34^+CD38^-$ leukemic stem cells (LSCs; n = 10). **B:** Expression of CD70 on AML bulk ($CD45^{dim}SSC^{low}$) and precursor ($CD34^+$) cells from patient samples pre and post azacytidine treatment (n = 4).

3.1.3 CD27 protein expression in AML

We assessed the expression of CD27, the ligand for CD70, on both AML cells and the patients T cell population. MPFC showed no CD27 expression on $CD45^{dim}SSC^{low}$ AML cells but CD27 was variably expressed on $CD3^+$ T cells (**Fig. 11 A**). The proportion of CD27-positive $CD3^+$ T cells ranged widely between patients, from 9.7 to 91.6%, with a mean of 63.3% (n = 28; **Fig. 11 A**). However, no correlation was found between CD70 expression on AML cells and CD27 expression on T cells (r = –0.200; **Fig. 11 B)**.

As CD27 can be proteolytically cleaved from the cell surface and subsequently released as a soluble molecule, we further evaluated sCD27 concentration in the serum of AML patients. Using ELISA, we detected increased concentration of sCD27 in the serum of AML patients compared to HDs (HDs = 33.0 U/ml, n = 9; AML = 109.7 U/ml, n = 11, Mann Whitney test $p = 0.0003$; **Fig. 11 C** and **Tab. Suppl. 5**). However, when comparing bone marrow plasma samples from AML patients and HDs, no significant differences in sCD27 levels were observed, regardless of disease stage or treatment status (**Fig. 11 C, Tab. Suppl. 6**).

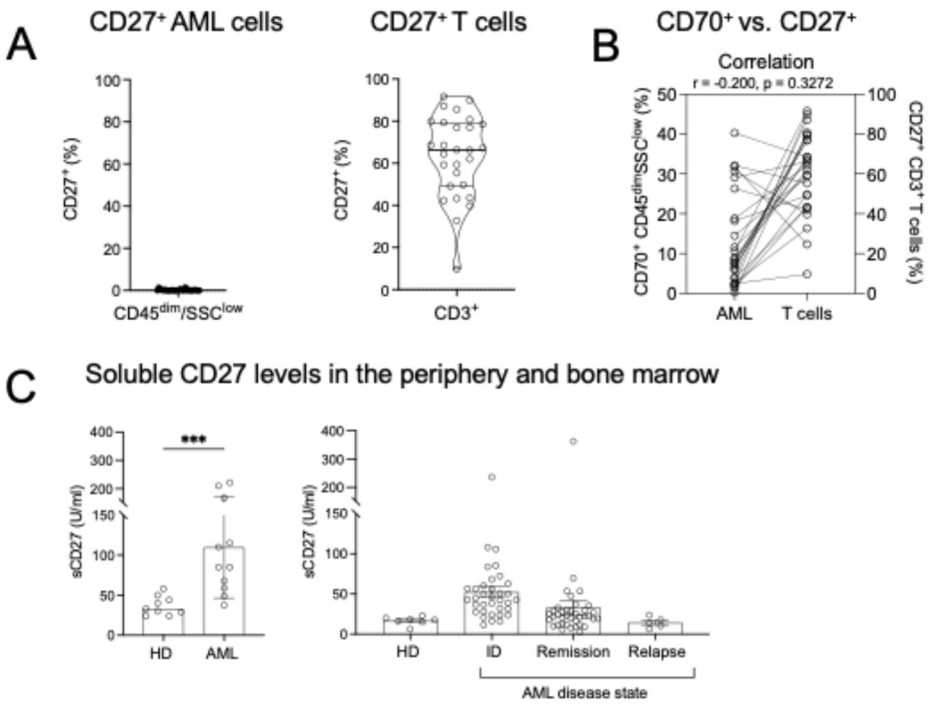

Figure 11: Characterization of CD27 protein expression in AML
A: Expression of CD27 on AML bulk ($CD45^{dim}SSC^{low}$) and $CD3^+$ T cells of AML patients (n = 28). **B:** Correlation of $CD70^+$ cells on $CD45^{dim}SSC^{low}$ cells and $CD27^+$ $CD3^+$ T cells (n = 28). Statistical analysis: Pearson correlation. **C:** Comparison of soluble CD27 levels detected by ELISA, left: in peripheral serum between healthy donors (HDs; n = 9) and AML patients (n = 11); right: in bone marrow fluid of HDs (n = 7), and AML patients at timepoint of initial diagnosis (ID; n = 35), remission (n = 38) and relapse (n = 5). All graphs show the mean ± SEM; Statistical analysis: Mann–Whitney test; ns $p > 0.05$; *$p < 0.05$; **$p < 0.01$; ***$p < 0.001$; ****$p < 0.0001$.

3.2 SEA-CD70-mediated ADCC

3.2.1 Cytotoxicity against AML cell lines

To investigate the therapeutic potential of CD70-targeted ADCC, we did preclinical evaluations using SEA-CD70 (clone h1F6), a sugar engineered mAb with a non-fucosylated Fc region to enhance interaction with FcγRIII (CD16) on NK cells thereby improving ADCC. SEA-CD33, an Fc enhanced mAb targeting CD33 (clone h2H12), was used as a positive control while a non-binding IgG isotype antibody served as a negative control (clone h00). Prior to assessing functional capacity, we characterized surface expression of CD70 and CD33 across AML cell lines, OCI-AML-3, MOLM-13, and MV4-11 (**Fig. 12 A**). OCI-AML-3 expressed CD70 stronger than CD33 (CD70 MFI ratio = 19.7; CD33 MFI ratio = 7.7), MOLM-13 showed high CD33 expression and moderate CD70 expression (CD70 MFI ratio = 14.2; CD33 MFI ratio = 138.1), while MV4-11 showed low CD70 expression and moderate CD33 expression (CD70 MFI ratio = 4.9, CD33 MFI ratio = 59.3). Notably, CD70 surface levels on these cell lines were within the expression range observed in primary AML patient samples (**Fig. 9 B**), supporting the relevance of these *in vitro* models.

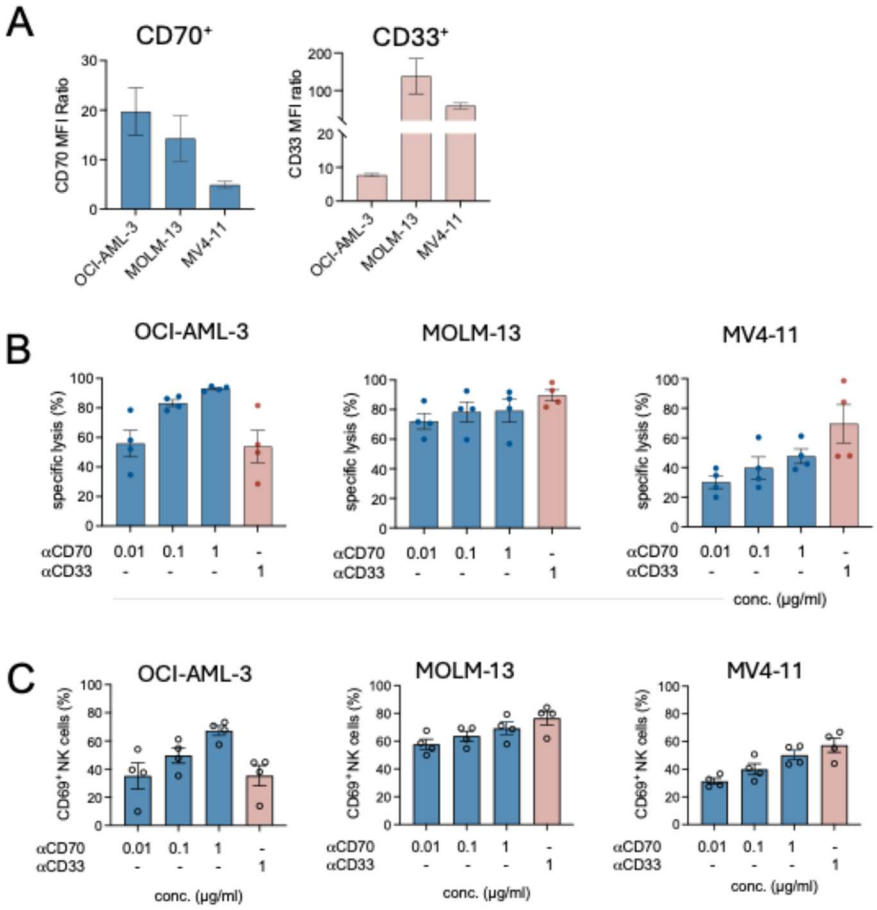

Figure 12: NK cell-mediated ADCC against AML cell lines *in vitro*
A: Expression levels of CD70 (left) and CD33 (right) determined by multi-parameter flow cytometry (MPFC) in AML cell lines (OCI-AML-3, MOLM-13, MV4-11; n = 2). **B:** Antibody-dependent cellular cytotoxicity (ADCC) mediated by anti-CD70 Ab (0.01–1 µg/ml) and anti-CD33 Ab (1 µg/ml) mediated ADCC against AML cell lines (OCI-AML-3, MOLM-13, MV4-11)

at an E: T ratio of 5:1 (n = 4). Specific lysis was calculated based on the anti-IgG Ab (1 µg/ml) control condition. **C:** Expression of activation marker CD69 on NK cells after co-culture with AML cell line OCI-AML-3, MOLM-13 and MV4-11. All graphs show the mean ± SEM.

To assess the cytotoxic potential of SEA-CD70, NK cell-mediated ADCC assays were performed at an E:T ratio of 5:1 using the characterized AML cell lines as targets. Specific lysis of AML cells and NK-cell activation were both dependent on the level of target antigen expression as well as antibody concentration (**Fig. 12 B, C**)

3.2.2 Cytotoxicity against primary AML samples

Building on the results obtained from AML cell lines, we next evaluated the efficacy of SEA-CD70-mediated ADCC in primary AML samples. The percentage of CD70-positive cells in this cohort ranged from 1.4 to 65.7% with a mean of 22.0% (n = 18; **Fig. 13 A** and **Tab. Suppl. 7**). For comparison, CD33 expression within the sample patient samples was consistently higher ranging from 31.1% to 99.6% (mean = 87.4%, n = 18; **Fig. 13 B**). In line with our findings in AML cell lines, SEA-CD70 triggered NK cell-mediated cytotoxicity in a target antigen-dependent manner. Specific lysis ranged from 4.6% to 66.9% with a mean of 20.3% (n = 18), and a correlation between CD70 expression and target cell lysis was observed (r = 0.6961; **Fig. 13 C**, **D** and **Tab. Suppl. 7**). Although direct comparisons between CD70- and CD33-mediated ADCC are influenced by differences in antibody characteristics (e.g. binding affinity and epitope accessibility), SEA-CD33 served as a function control in these experiments. Anti-CD33-mediated lysis of the same samples ranged from 3.4% to 79.5% with a higher mean specific lysis of 35.5% (n = 18), but a lower correlation with antigen expression levels (r = 0.3505; **Fig. 13 E**, **F**)

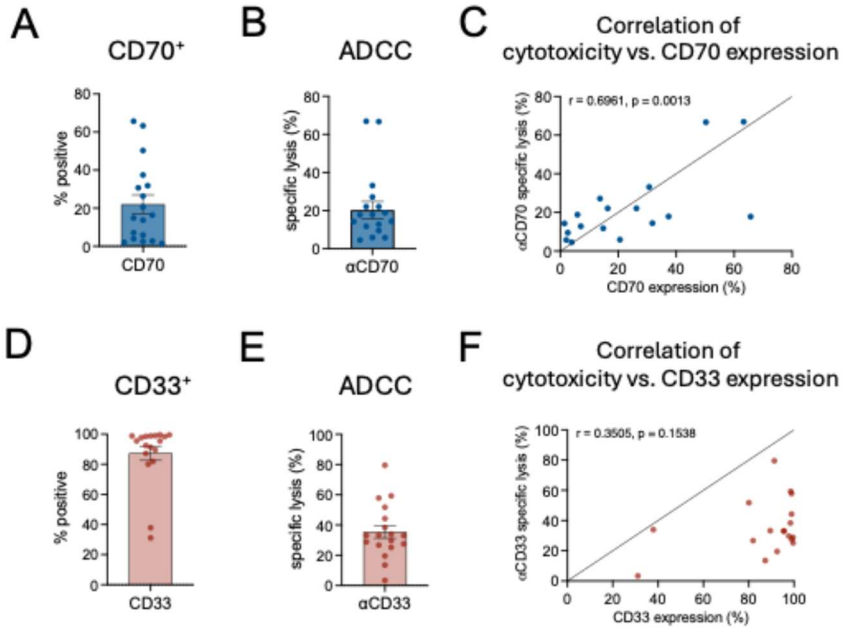

Figure 13: NK cell-mediated ADCC against primary AML cells *in vitro*

A: Expression of CD70 in tested primary AML samples (left, n = 18) and **B:** anti-CD70 Ab mediated ADCC (right, αCD70 Ab = 1 µg/ml, E:T ratio = 5:1, n = 18). **C:** Pearson correlation of SEA-CD70-mediated cytotoxicity and CD70 expression

(n = 18). **D:** Expression of CD33 in tested primary AML samples (left, n = 18) and **E:** anti-CD33 Ab mediated ADCC (right, αCD33 Ab = 1 µg/ml, E:T ratio = 5:1, n = 18). **F:** Pearson correlation of SEA-CD33-mediated cytotoxicity and CD33 expression of tested primary AML cells (n = 18). All graphs show the mean ± SEM.

3.2.3 SEA-CD70-mediated tumor control in an *in vivo* mouse model

To assess the therapeutic potential of SEA-CD70 *in vivo*, we used a xenograft model using MV4-11 cells in severe combined immunodeficiency (SCID) mice. Two antibody variants were tested: SEA-CD70, and SEA-CD70_G1V1, a functionally inert variant with reduced Fcγ receptor binding. Treatment with SEA-CD70 (10 mg/kg) led to a reduction in tumor growth compared to untreated control, resulting in a tumor growth inhibition (TGI) of 54.7% ($p = 0.0002$). In contrast, administration of SEA-CD70_G1V1 had no significant effect on tumor progression (TGI = 20.1%, $p = 0.1457$; **Fig. 14**).

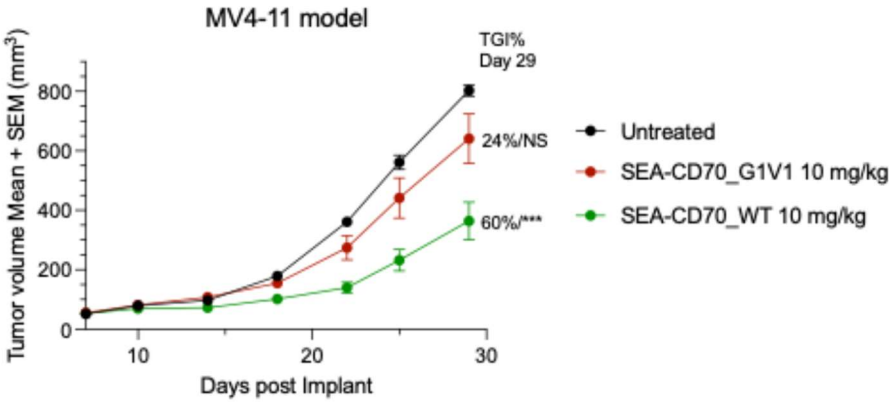

Figure 14: SEA-CD70-mediated cytotoxicity in a MV4-11 model *in vivo*
Tumor volume in MV4-11 tumor-bearing mice plotted against time. Mice were treated with either anti-CD70 Ab (SEA-CD70_WT) or a variant with reduced Fc binding (SEA-CD70_G1V1); n = 9 per group. Statistical analysis: two-way ANOVA followed by Tukey's multiple comparison test; ns $p > 0.05$; *$p < 0.05$; **$p < 0.01$; ***$p < 0.001$; ****$p < 0.0001$.

3.3 Immunomodulation of the anti-CD70 antibody

3.3.1 CD70 blockade has no impact on bispecific antibody-activated T–AML cell crosstalk

Considering the high expression of CD27 on T cells in AML and the potential immunomodulatory role of CD70, we analyzed whether CD70 blockade might interfere with T-cell-mediated antitumor responses. To this end, we established co-culture assays using HD T cells and MOLM-13 cells in the presence or absence of SEA-CD70.

T cells were activated via a CD33xCD3 BsAb, and cytotoxic responses were monitored (106). No significant differences were observed in BsAb-mediated cytotoxicity or T-cell proliferation upon CD70 blockade with SEA-CD70 (**Fig. 15 A**).

Interestingly, while it is known that activated T cells express CD70 (**Fig. 15 B**; (114)), we observed that CD70 expression on MOLM-13 cells was upregulated in the presence of BsAb-activated T cells. The mean CD70 MFI ratio increased from 11.4 at baseline to 38.6 following exposure to activated T cells (72 h, n = 8, *p* = < 0.0001; **Fig. 15 C**).

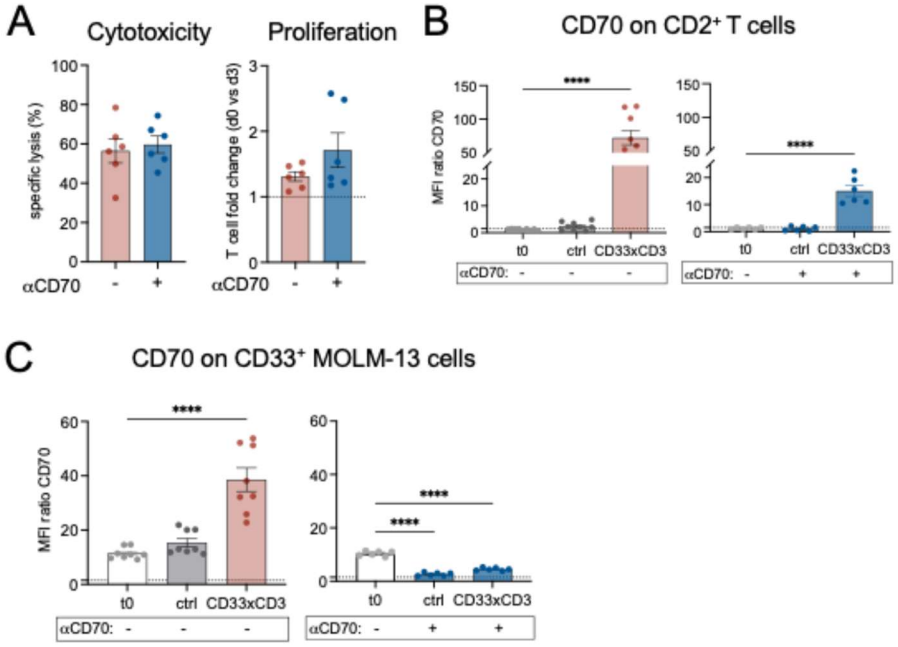

Figure 15: Immunomodulation of SEA-CD70 to bispecific antibody-activated T cells
Pan T cells were isolated and co-cultured with the AML cell line MOLM-13 in the presence of an anti-CD70 Ab (10 µg/ml) together with a CD33xCD3 bispecific antibody (5 ng/ml) at an E:T ratio of 1:5. **A:** CD33xCD3-mediated cytotoxicity against MOLM-13 cells (left) and T-cell proliferation (right) with (blue) and without (red) CD70 blockade (n = 6). **B:** CD70 expression on CD2+ T cells without (left) and with (right) CD70 blockade at timepoint zero (t0), or after co-culture with or without CD33xCD3 BsAb (n = 6). **C:** Expression of CD70 on CD33+ MOLM-13 cells without (left) and with (right) CD70 blockade, at timepoint zero (t0), or after co-culture with or without CD33xCD3 BsAb (n = 6-8). All graphs show the mean ± SEM; statistical analysis: one-way-ANOVA, Bonferroni's multiple comparison; ns p > 0.05; *p < 0.05; **p < 0.01; ***p < 0.001; ****p < 0.0001

3.3.2 CD70 blockade has no impact on bispecific-mediated T-cell exhaustion

We were interested if CD70 blockade has a biological role in regard of T-cell exhaustion. To analyze this, we followed a robust *in vitro* model for T-cell exhaustion that was established in our group earlier (37). Our experimental set up involved a 28-day blockade of CD70 and continuous stimulation of T cells with blinatumomab in co-culture with the lymphoma cell line OCI-Ly1.

Interestingly, CD27 expression was sustained throughout the co-culture with CD70 blockade on $CD4^+$ and $CD8^+$ T cells (**Fig. 16 A**). Despite this sustained CD27 expression, we observed no alteration in T-cell cytotoxicity or proliferation at time point 7, 14, 21 and 28 days (**Fig. 16 B)**. However, cytokine secretion (IL-2, TNF and IFNγ) was slightly compromised in the presence of CD70 blockade at timepoint 3, 10, 17 and 24 days (**Fig. 16 C)**. At day 28, we compared metabolic

profiles of T cells that received continuously blinatumomab with T cells that additionally underwent CD70 blockade. Indeed, sustained CD27 expression was accompanied by higher metabolic fitness and showed elevated extracellular acidification rate (ECAR) and enhanced oxygen consumption rate (OCR) during glycolytic and mitochondrial stress tests, respectively (**Fig 16 D**).

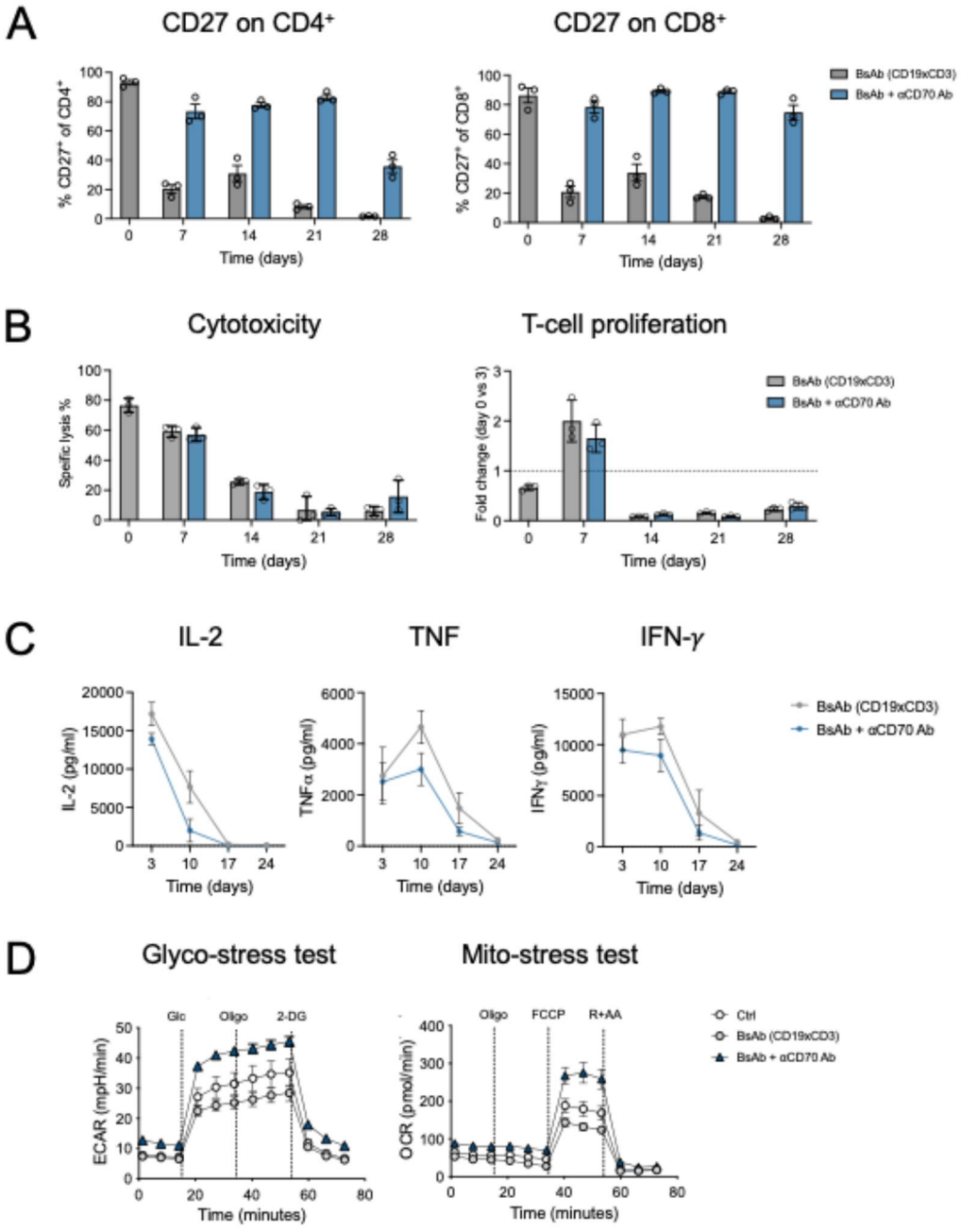

Figure 16: CD70 blockade sustains CD27 expression on continuously BsAb-activated T cells
Pan T cells were isolated and co-cultured with the B cell lymphoma cell line OCI-Ly1 in the presence of an anti-CD70 Ab, together with a BsAb (blinatumomab, CD19xCD3, 5 ng/ml) at an E:T ratio of 1:5. **A:** CD27 expression on CD4+ and CD8+ T cells continuously stimulated with BsAb (grey) without or with CD70 blockade (blue, anti-CD70 Ab = 10 µg/ml) at timepoint 0, 7, 14, 21 and 28 of co-culture (n = 3). **B:** BsAb-mediated cytotoxicity against hCD19+ Ba/F3 cells (left) and T-cell proliferation (right) without (grey) or with (blue) CD70 blockade tested at timepoint 0, 7, 14, 21 and 28 of co-culture (n = 3). **C:** Cytometric bead array analysis of IL-2, TNF and IFN-γ from supernatant of co-cultures collected at day 3, 10,

17 and 24 (n = 3). **D:** Metabolic fitness analysis of T cells without (grey) or with CD70 blockade (blue) isolated after 28 days of co-culture or unstimulated T cells (white, ctrl, n = 3).

3.3.3 TNF-α enhances CD70 expression in AML cells

Given the increased CD70 levels observed in AML cells following exposure to BsAb-activated T cells, we hypothesized that secreted inflammatory mediators could be responsible for this effect. To test this, we quantified cytokines in the supernatant of CD33xCD3 BsAb-activated T-cell co-cultures with MOLM-13 cells using a cytometric bead array. As expected, the cytokine milieu was rich in TNF-α, IFN-γ, MCP-1, IL-6, IL-8 and IL-10 (TNF-α = 1.7 ng/ml and IFN-γ = > 9 ng/ml, n = 6, **Fig. 17 A**).

To dissect the contribution of these cytokines, AML cell lines were either exposed to this conditioned medium (CM) or directly exposed to TNF-α and IFN-γ. Both CM and the cytokine cocktail induced an increase in CD70 surface expression (e.g. MOLM-13 MFI ratio: unstimulated = 9.9 vs. CM = 23.6, p = 0.0064; vs. TNFα + IFN-γ = 33.9, p < 0.0001; n = 5; **Fig. 17 B**). This effect was not unique to MOLM-13 cells, as similar CD70 upregulation was observed in OCI-AML-3 and MV4-11 cells (**Fig. 17 B**).

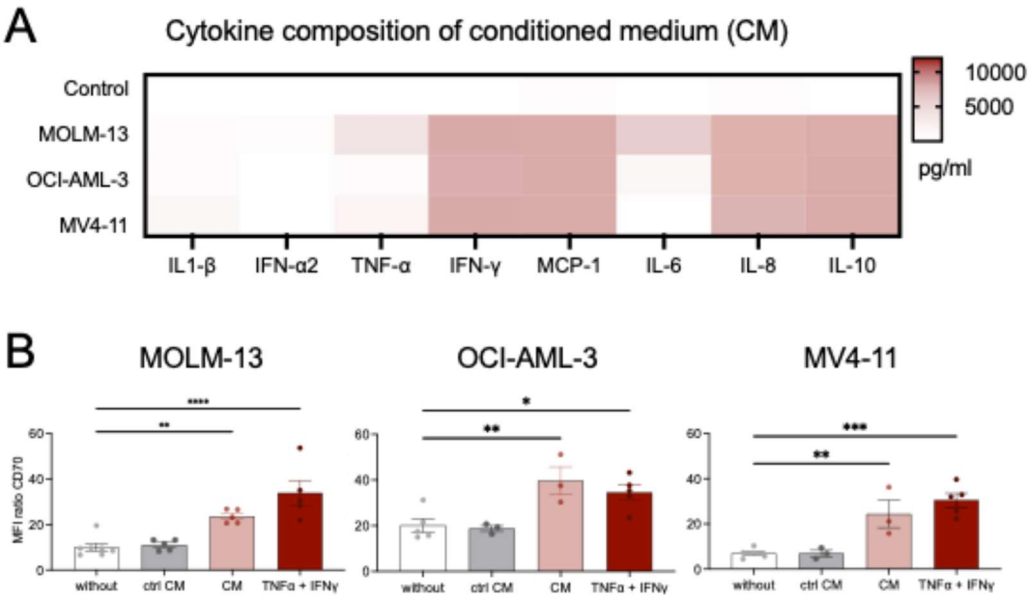

Figure 17: Pro-inflammatory cytokines increase the expression of CD70 on AML cell lines
A: Heatmap of cytokine analysis by bead array (LegendPlex, human inflammation panel) of supernatant from co-cultures of T cells and MOLM-13, OCI-AML-3, and MV4-11 cells with or without an CD33xCD3 bispecific antibody after 72 h (n =3). **B:** Expression of CD70 on MOLM-13, OCI-AML-3, and MV4-11 cells conditioned with supernatant from co-cultures of T cells and MOLM-13 cells containing CD33xCD3 bispecific antibody (conditioned medium, CM) after 72 h (1:1 ratio with culture medium), and TNF-α (5 ng/ml) + IFN-γ (2.5 ng/ml) for 72 h (n = 3-7). All graphs show the mean ± SEM; statistical analysis: one-way-ANOVA, Bonferroni's multiple comparison; ns p > 0.05; *p < 0.05; **p < 0.01; ***p < 0.001; ****p < 0.0001.

Further analysis revealed that CD70 upregulation was specifically dependent on TNF-α signaling. MOLM-13 cells responded to TNF-α in a dose-dependent manner (**Fig. 18 A**), and this upregulation was abrogated in TNFRSF1A knockout clones (**Fig. 18 B**). Likewise, in primary AML samples, TNF-α exposure increased both the frequency and surface levels of CD70 (mean percentage of CD70⁺ cells in unstimulated group = 18.6% vs. TNF-α group = 31.9%, n = 19, $p = 0.0007$; **Fig. 18 C** and **Tab. Suppl. 7**).

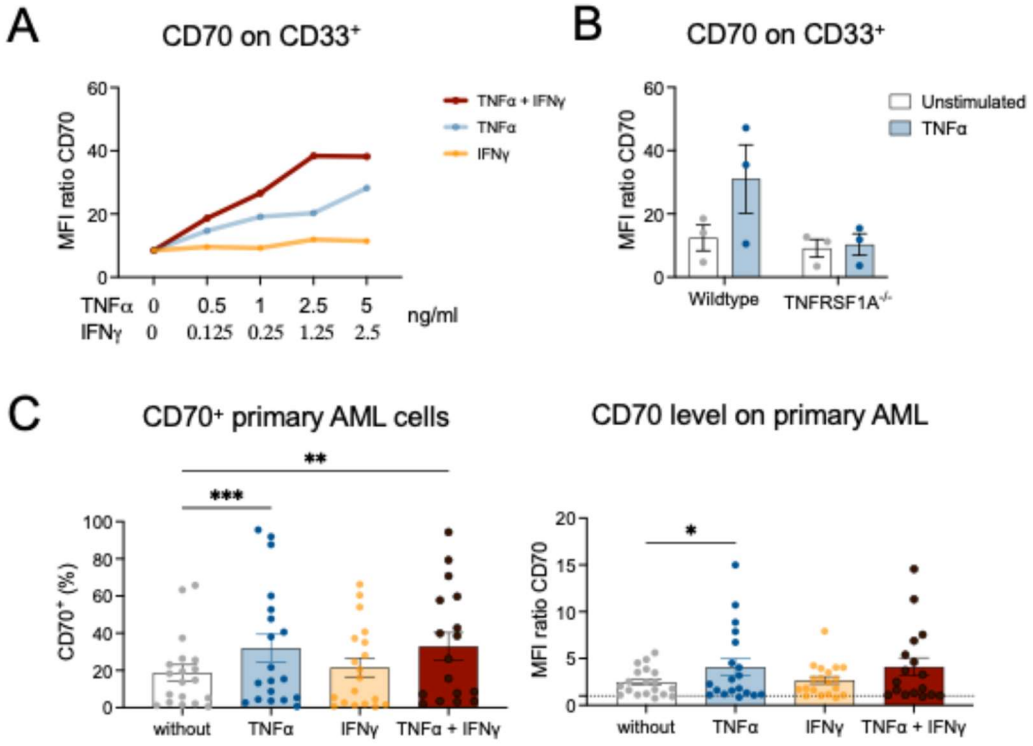

Figure 18: TNF-α increases the expression of CD70 on AML cells

A: Expression of CD70 on MOLM-13 cells in response to different doses of TNF-α (0–5 ng/ml) and IFN-γ (0–2.5 ng/ml) exposed for 72 h. **B:** Expression of CD70 in wildtype and CRISPR–Cas9-based TNFRSF1A MOLM-13 knock out clones with or without exposure to TNF-α (5 ng/ml) for 72 h (n = 3). **C** Left: Expression of CD70 on primary AML cells without (n = 19) or after exposure to TNF-α (50 ng/ml, n = 19) and IFN-γ (25 ng/ml, n = 19) or both (n = 16) for 72 h. Right: Expression level of CD70 on primary AML cells without (n = 19) or after exposure to either TNF-α (50 ng/ml, n = 19), IFN-γ (25 ng/ml, n = 19), or both (n = 16) for 72 h. All graphs show the mean ± SEM; statistical analysis: one-way-ANOVA, Bonferroni's multiple comparison; ns $p > 0.05$; *$p < 0.05$; **$p < 0.01$; ***$p < 0.001$; ****$p < 0.0001$.

Of note, this regulatory effect appeared specific to CD70, as CD33 expression remained unchanged after exposure to TNF-α or IFN-γ (**Fig. 19 A-C**). Importantly, TNF-α did not induce CD70 on healthy HSCs, which lacked CD70 both at baseline and following exposure (**Fig. 19 D**), underscoring the therapeutic relevance of this finding.

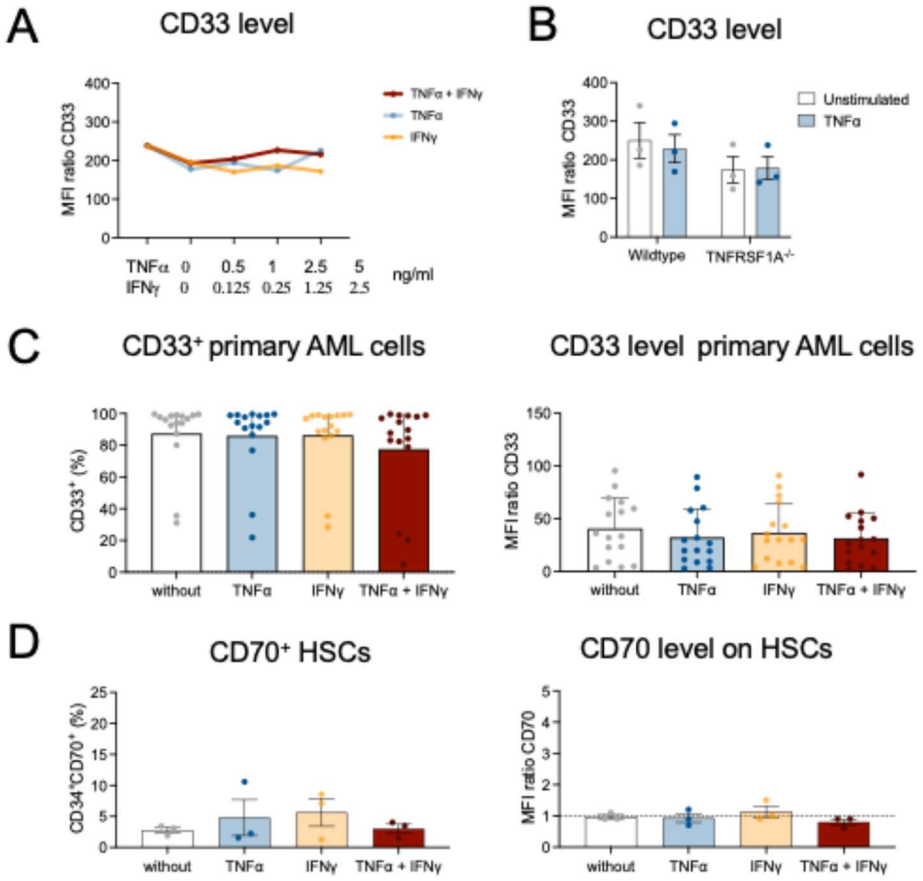

Figure 19: TNF-α and/or IFN-γ does not change expression of CD33 or induce CD70 on HSCs
A: Expression of CD33 on MOLM-13 cells in response to different doses of TNF-α (0 - 5 ng/ml) and IFN-γ (0–2.5 ng/ml). **B:** Expression of CD33 in wildtype MOLM-13 cells and CRISPR–Cas9 based TNFRSF1A knock out clones with or without exposure to TNF-α (5 ng/ml) for 72 h (n = 3). **C**: Expression of CD33 on primary AML cells after exposure to TNF-α (50 ng/ml) and/or IFN-γ (25 ng/ml) for 72 h (n = 16). **D:** Expression of CD70 on hematopoietic stem cells (HSCs) isolated from healthy donor bone marrow after exposure to TNF-α (50 ng/ml) and/or IFN-γ (25 ng/ml) for 72 h (n = 3). All graphs show the mean ± SEM.

3.4 TNF-α increases while IFN-γ decreases anti-CD70 Ab-mediated ADCC

After observing that TNF-α increase CD70 expression, we next analyzed whether this translates into enhanced susceptibility to ADCC. Surprisingly, exposure to either CM or the TNF-α and IFN-γ combination resulted in a consistent decrease in ADCC against AML cell lines (MOLM-13, OCI-AML-3, and MV4-11), regardless of whether CD70 or CD33 was targeted (**Fig. 20 A-C**).

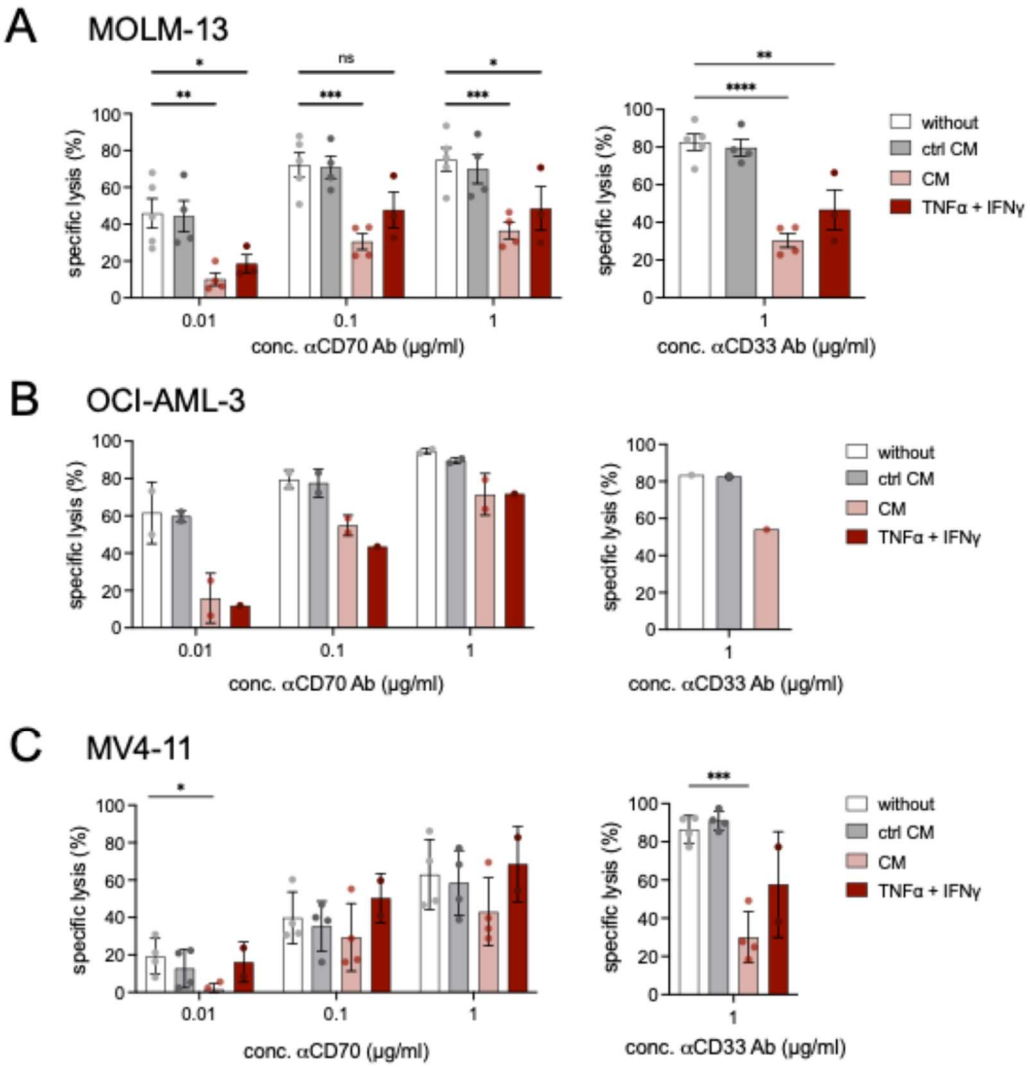

Figure 20: Exposure to CM or TNF-α and IFN-γ reduces ADCC against AML cell lines independent of the target
NK cells were co-cultured with conditioned **A:** MOLM-13 cells **B:** OCI-AML-3 cells, and **C:** MV4-11 cells (supernatant of CD33xCD3 bispecific Ab co-cultures or TNF-α (5 ng/ml) and IFN-γ (2.5 ng/ml)) in the presence of an anti-CD70 Ab (0.01–1 µg/ml) or anti-CD33 Ab (1 µg/ml) for 16 h (n = 1–5). Specific lysis was calculated based on the anti-IgG Ab (1 µg/ml) control condition. All graphs show the mean ± SEM; statistical analysis: one-way-ANOVA, Bonferroni's multiple comparison; ns $p > 0.05$; *$p < 0.05$; **$p < 0.01$; ***$p < 0.001$; ****$p < 0.0001$.

In contrast, a more refined analysis using primary AML samples revealed differential outcomes depending on the cytokine used. TNF-α exposure led to increased SEA-CD70-mediated cytotoxicity (mean specific lysis: 17.9% vs. 34.3%, n = 13-15, $p = 0.0048$), whereas IFN-γ exposure reduced CD70-mediated cytotoxicity (mean: 17.9% vs. 9.2%, n = 15; **Fig. 21 A** and **Tab. Suppl. 7**). Notably, this suppressive effect of IFN-γ was not dependent on CD70, as CD33-mediated lysis also decreased from 44.2% to 23.2% after IFN-γ exposure (n = 15, $p = 0.0002$; **Fig. 21 B** and **Tab. Suppl. 7**).

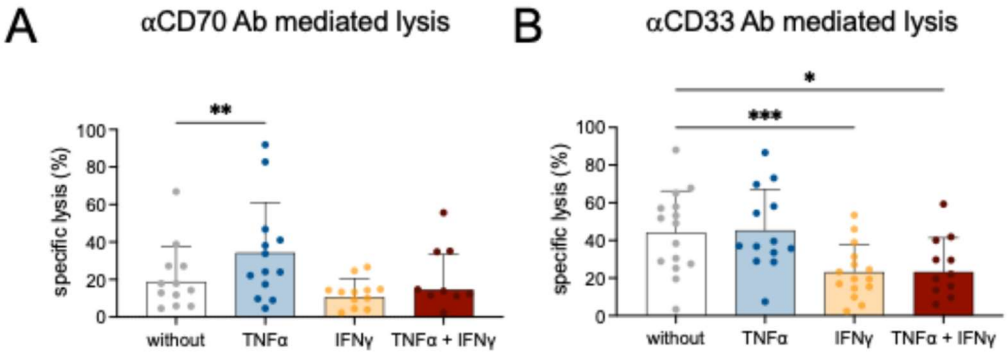

Figure 21: TNF-α increases SEA-CD70-mediated ADCC while IFN-γ decreases ADCC independent of the target
A: Anti-CD70 Ab (1 µg/ml) mediated ADCC against unconditioned primary AML cells (n = 15), or prior exposed to TNF-α (50 ng/ml, n = 13), or IFN-γ (25 ng/ml, n = 15), or both (n =12). **B:** Anti-CD33 Ab- (1 µg/ml) mediated ADCC against unconditioned (n = 15), or those exposed to TNF-α (50 ng/ml, n = 13), IFN-γ (25 ng/ml, n = 15), or both (n = 12). All graphs show the mean ± SEM; statistical analysis: one-way-ANOVA, Bonferroni's multiple comparison; ns $p > 0.05$; *$p < 0.05$; **$p < 0.01$; ***$p < 0.001$; ****$p < 0.0001$.

To determine whether this inhibitory effect was directly mediated by IFN-γ, we utilized MOLM-13 clones lacking IFNGR1. These knockout cells did not show the decrease in ADCC seen in wild-type cells after exposure to IFN-γ (**Fig. 22 A, B**). Similar results were obtained when IFN-γ was neutralized in CM using a mAb targeting IFN-γ (**Fig. 23 A, B**). These findings implicate IFN-γ as a key mediator for lowering ADCC in AML.

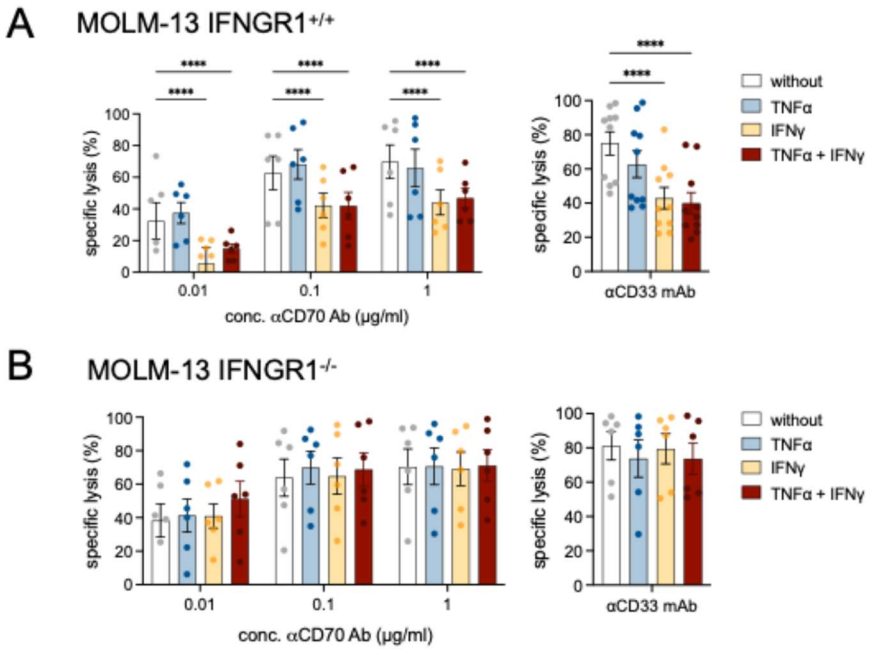

Figure 22: IFN-γ signalling decrease susceptibility to ADCC independent of the target antigen
Anti-CD70 Ab- (0.01–1 µg/ml; left) and anti-CD33 Ab- (right) mediated ADCC against unconditioned, or those exposed to TNF-α (5 ng/ml), IFN-γ (2.5 ng/ml) or both; MOLM-13 were wildtype (A, n = 6) or CRISPR–Cas 9 edited IFNGR1 MOLM-13 knock out clones (B, n = 6). All graphs show the mean ± SEM; statistical analysis: one-way-ANOVA, Bonferroni's multiple comparison; ns $p > 0.05$; *$p < 0.05$; **$p < 0.01$; ***$p < 0.001$; ****$p < 0.0001$.

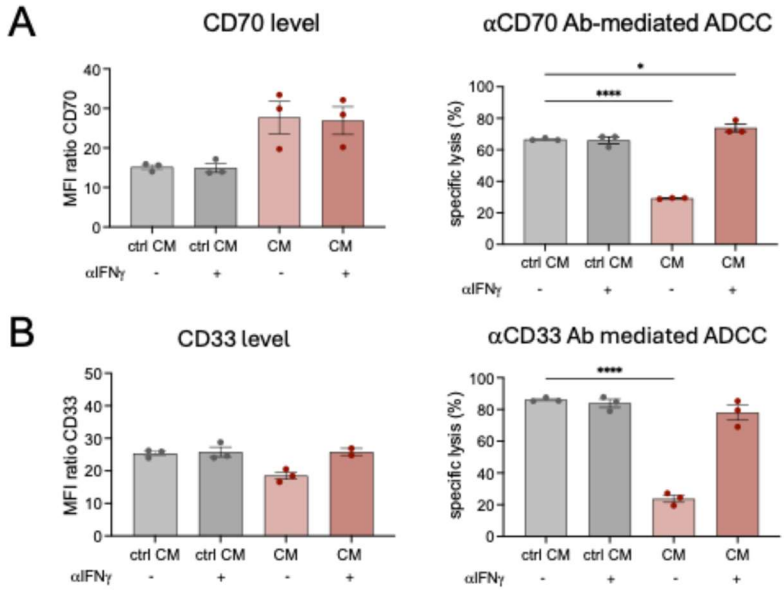

Figure 23: Neutralization of IFN-γ in CM prevents reduction of ADCC
A: Expression level of CD70 and anti-CD70 Ab- (1 µg/ml) mediated ADCC and **B:** Expression level of CD33 and anti-CD33 Ab- (1µg/ml) mediated ADCC against conditioned MOLM-13 cells (supernatant of CD33xCD3 bispecific Ab co-cultures of T cells with MOLM-13 cells in the presence or absence of neutralizing anti-IFN-γ Ab (10 µg/ml, n = 3) for 72 h). All graphs show the mean ± SEM; statistical analysis: one-way-ANOVA, Bonferroni's multiple comparison; ns $p > 0.05$; *$p < 0.05$; **$p < 0.01$; ***$p < 0.001$; ****$p < 0.0001$.

3.5 IFN-γ enhances HLA molecule expression

3.5.1 RNAseq analysis of MOLM-13 cells after TNF-α exposure

Transcriptomic analysis of TNF-α exposed MOLM-13 cells revealed upregulation of genes involved in immune signaling (IL2RG, GBP4), antigen presentation (TAP2, HLA-DQB1), matrix remodeling (MMP9) and cellular adhesion (LIMD2; **Fig. 24).** Interestingly, this analysis showed that TNF-α did not significantly alter CD70 transcript levels.

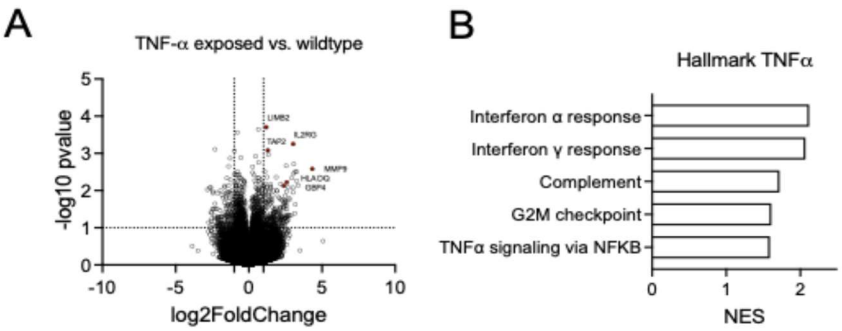

Figure 24: RNAseq analysis of TNF-α exposed MOLM-13 cells
A: Volcano plot of differentially expressed genes (DEGs) in TNF-α exposed MOLM-13 cells (n = 6). **B:** Hallmark gene set analysis of TNF-α exposed MOLM-13 cells; normalized enrichment score (NES; n = 6).

3.5.2 RNAseq analysis of MOLM-13 cells after IFN-γ exposure

RNA-sequencing analysis of IFN-γ-exposed MOLM-13 cells showed an upregulation of immune-regulatory and antigen-presentation genes. Key interferon-stimulated genes, including STAT1, IRF1, and members of the GBP family, were the most significantly induced. Notably, expression of multiple genes involved in antigen processing and presentation, including TAP1, TAP2, and several HLA molecules were increased (**Fig. 24 A-C**).

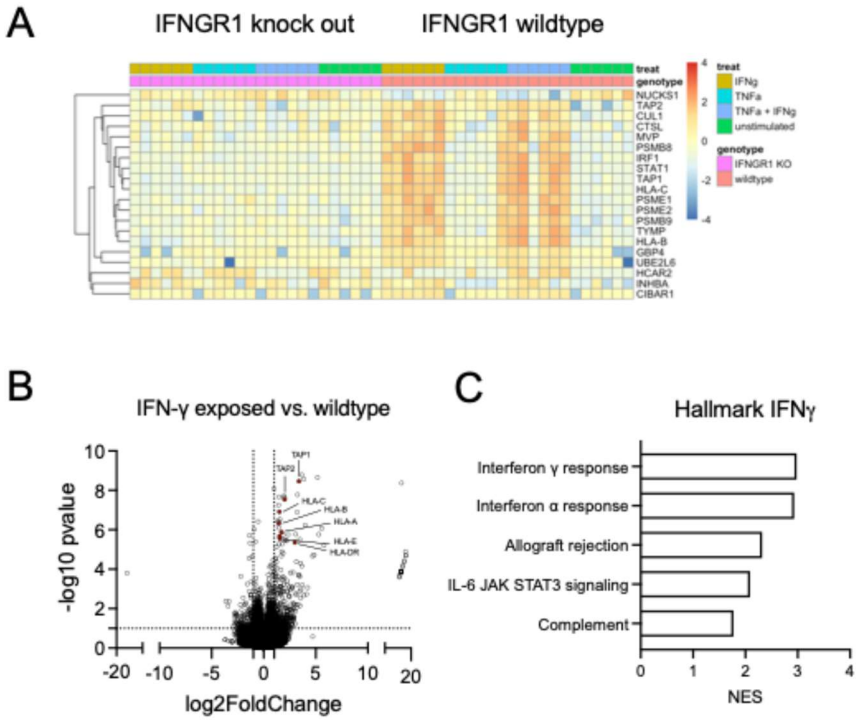

Figure 25: RNAseq analysis of IFN-γ exposed MOLM-13 cells
A: Heatmap of the top 20 de-regulated genes in MOLM-13 wildtype or IFNGR1 knock out clones (n = 6 per group). **B:** Volcano plot of differentially expressed genes (DEGs) in IFN-γ (2.5 ng/ml) conditioned and unconditioned MOLM-13 cells, (n = 6; p = <0.001). **C:** Hallmark gene set analysis of IFN-γ (2.5 ng/ml) exposed and unexposed MOLM-13 cells; normalized enrichment score (NES; n = 6).

3.5.3 Phenotypic changes of MOLM-13 cells after IFN-γ exposure

These transcriptional changes seen by RNAseq analysis were reflected at the protein level detected by MPFC. MOLM-13 cells showed increased expression of both classical (HLA-ABC) and non-classical (HLA-E) class I HLA molecules (MFI ratio HLA-ABC = 55.3 vs. 102.3, n = 7, *p* = 0.0062; MFI ratio HLA-E = 1.6 vs. 3.1, n = 6, *p* = 0.0016; **Fig. 26 A**).

Primary AML cells mirrored these findings, with upregulation of HLA-ABC, HLA-E, HLA-DR, and PD-L1 after exposure to IFN-γ (MFI ratio HLA-ABC: 65.8 vs. 139.1, n = 16, *p* = < 0.0001; HLA-E: 2.4 vs. 4.9, n = 11, *p* = 0.0045; HLA-DR: 19.9 vs. 45.3, n= 11, *p* = 0.0049, MFI ratio PD-L1: 1.6 % vs. 7.5 %, n = 16, *p* = 0.0079; **Fig. 26 B** and **Tab. Suppl. 7**).

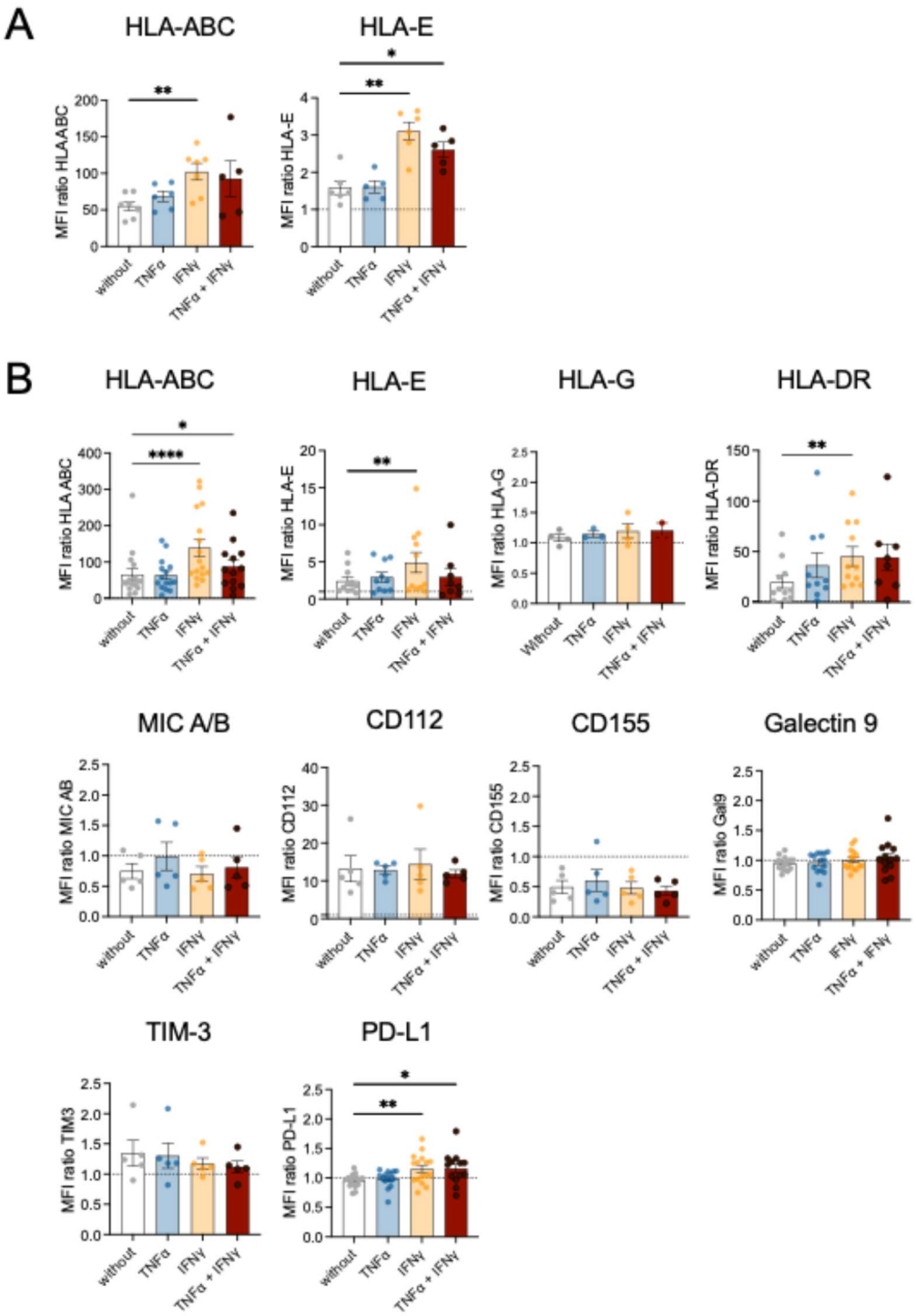

Figure 26: Exposure to IFN-γ increases expression of NK cell inhibitory receptor ligands on protein level in AML
A: Expression level of HLA ABC (ligand for KIR) and HLA-E (ligand for NKG2A) detected by by MPFC on MOLM-13 cells (n= 5-7) with or without exposure (5 ng/ml TNF-α and/or 2.5 ng/ml IFN-γ). **B:** Expression of HLA ABC, HLA-E, HLA-G (ligand for NKG2A), HLA-DR (ligand for LAG-3), MIC A/B (ligand for NKG2D), CD112 (ligand for TIGIT), CD155 (ligand for TIGIT), Galectin 9 (ligand for TIM-3), TIM-3, and PD-L1 detected by MPFC on primary AML cells with or without exposure (50 ng/ml TNF-α and/or 25 ng/ml IFN-γ; n = 3-17). All bar charts show the mean ± SEM; statistical analysis: one-way-ANOVA, Bonferroni's multiple comparison; ns $p > 0.05$; *$p < 0.05$; **$p < 0.01$; ***$p < 0.001$; ****$p < 0.0001$.

Supporting these data, analysis of the TCGA-AML cohort showed that CD70^{high} patients had an enrichment of IFN-γ signaling pathways (p = 3.781^{-10}, **Fig. 27 A**) and increased expression of HLA-related genes (**Fig. 27 B**).

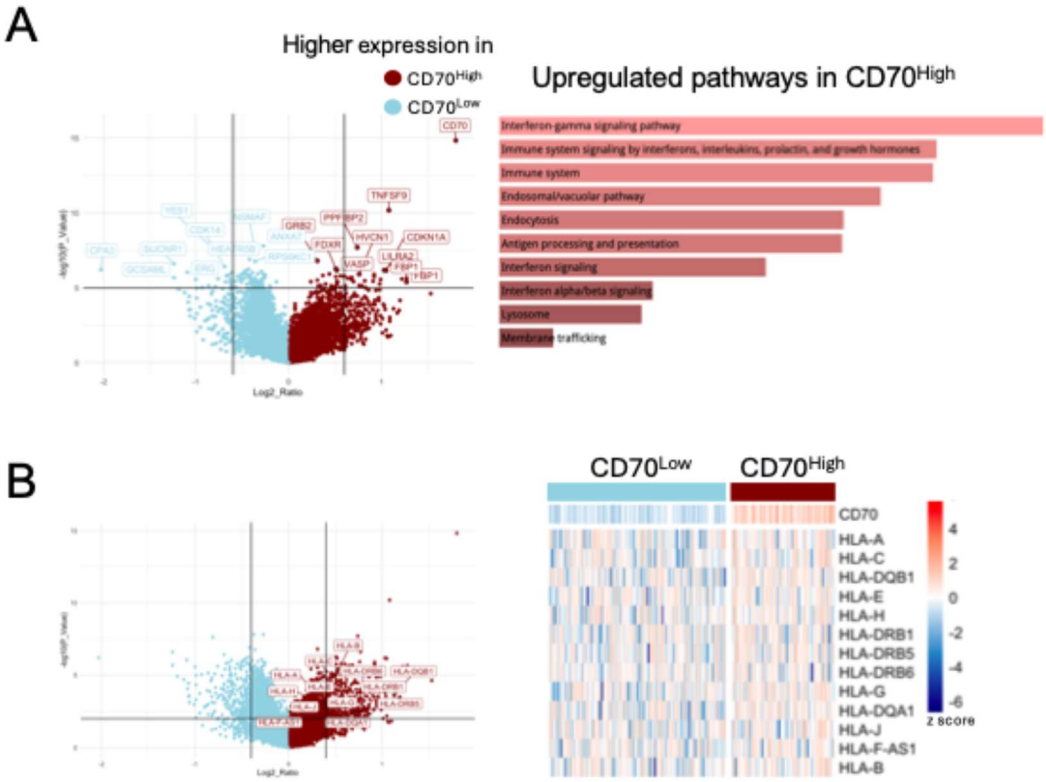

Figure 27: RNAseq analysis of the TCGA-AML cohort in regard of CD70 expression
A: Volcano plot of DEGs (left) and corresponding pathway analysis in AML patients with CD70-high expression profiles (right). **B:** Volcano plot of differential HLA expression (left) and corresponding heatmap in AML patients with CD70-high and CD70-low expression profiles (right).

3.6 Counteracting IFN-γ-induced HLA class I upregulation by KIR and NKG2A blockade

To better understand the mechanism behind IFN-γ-mediated ADCC suppression, we analyzed the expression of NK cell inhibitory receptors. Peripheral blood-derived NK cells expressed high levels of CD158b (KIR2DL2/DL3) and NKG2A (CD158b = 43.3%, NKG2A = 52.7%, n = 9; **Fig. 28 A**) whereas PD-1 expression was barely detectable (< 5%, data not shown). Live-cell microscopy showed that IFN-γ exposure did not impair AML-NK cell conjugate formation (**Figure 28 B, C**), indicating that synapse formation is not defective.

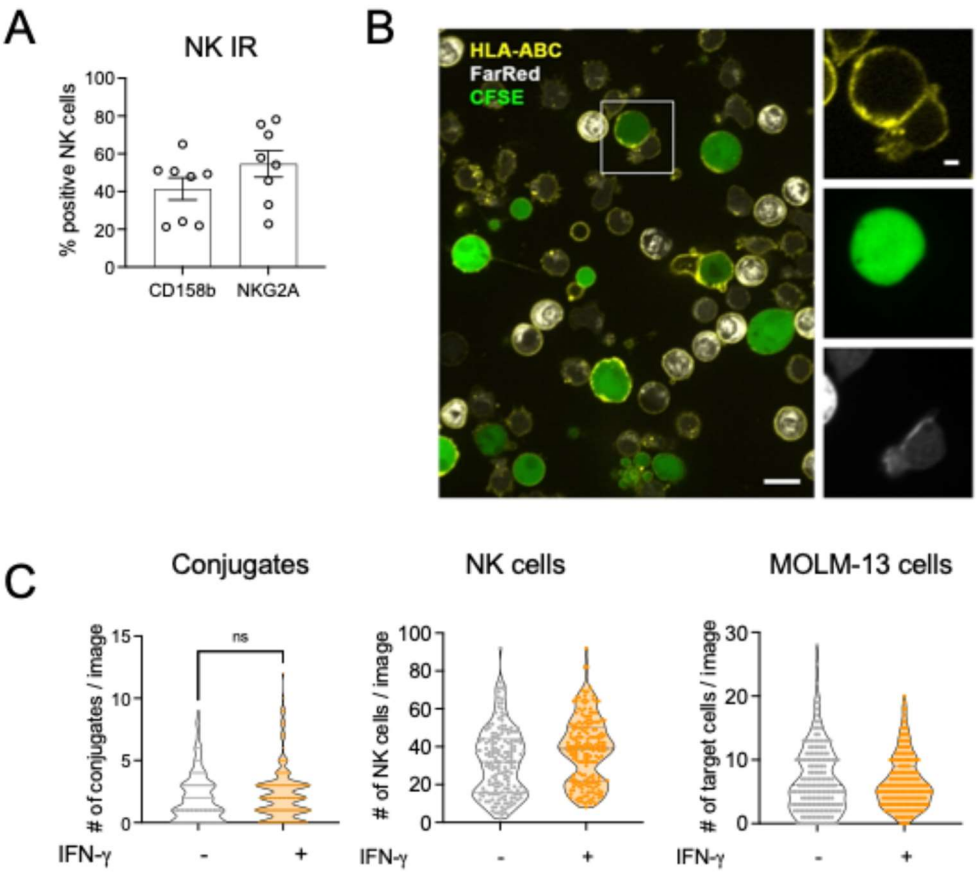

Figure 28: Conjugate formation between MOLM-13 and NK cells
A: Baseline expression of CD158b and NKG2A detected by MPFC on NK cells from healthy donors (n = 9). **B:** Representative fluorescence microscopy images of co-cultures of NK cells (FarRed cell tracer labeled) with IFN-γ (2.5 ng/ml) exposed MOLM-13 cells (CFSE cell tracer labeled) in the presence of anti-CD33 Ab (1µg/ml); scalebars overview = 10 µm, scalebars zoom = 2 µm. The co-culture was immobilized on poly-L-lysine-coated Ibidi cartridges for live cell imaging after 2 h. **C:** Number of conjugates (left) between NK cells (middle) and MOLM-13 cells (right; n = 180 images) with and without exposure to IFN-γ (2.5 ng/ml, n = 189 images) in the presence of an anti-CD33 Ab (1 µg/ml). All graphs show the mean ± SEM; statistical analysis: paired t-test; ns $p > 0.05$; *$p < 0.05$; **$p < 0.01$; ***$p < 0.001$; ****$p < 0.0001$.

Finally, we evaluated whether blocking of HLA-binding inhibitory receptors could rescue ADCC. Blocking CD158b with lirilumab (anti-CD158b mAb) or monalizumab (anti-NKG2A mAb) partially restored cytotoxicity in IFN-γ exposed MOLM-13 cells (SEA-CD70: IFN-γ: 15.3% vs. IFN-γ + aCD158b: 22.2%, IFN-γ + aNKG2A: 25.3%; SEA-CD33: IFN-γ: 25.4% vs. IFN-γ + aCD158b: 41.4%, $p = 0.0226$, IFN-γ + aNKG2A: 51.9%, $p = 0.0024$; n = 6; **Fig 29 A**).

Similar trends were observed in primary AML samples (SEA-CD70: IFN-γ -1.1% vs. IFN-γ + anti-CD158b: 6.5%, IFN-γ + anti-NKG2A: 3.3%, n = 6; SEA-CD33: without 50.6% vs. IFN-γ 16.2% vs. IFN-γ + anti-CD158b: 34.6%, IFN-γ + anti-NKG2A: 29.0%, $p = 0.0409$, n = 6; **Fig. 29 B** and **Tab. Suppl. 7**), providing a rationale for combinatorial strategies involving NK cell checkpoint blockade.

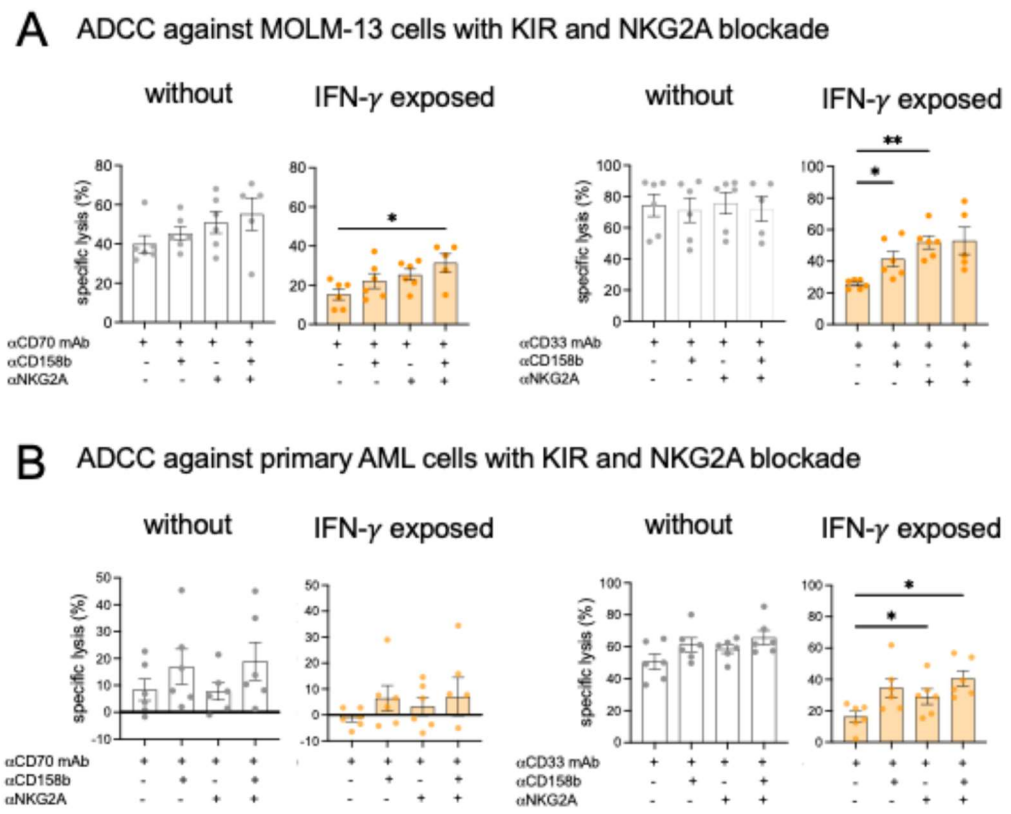

Figure 29: ADCC with KIR and NKG2A blockade

A: Anti-CD70 Ab (left, 1 µg/ml) or anti-CD33 Ab (right, 1µg/ml) mediated ADCC against unconditioned (white bars) or IFN-γ exposed (yellow bars) MOLM-13 cells (2.5 ng/ml, n = 5-6) in the presence of lirilumab (anti-CD158b blocking Ab, 10 µg/ml) and monalizumab (anti-NKG2A blocking Ab, 10 µg/ml). **B:** Anti-CD70 Ab (left, 1 µg/ml) or anti-CD33 Ab (right, 1 µg/ml) mediated ADCC against unconditioned (white bars) or IFN-γ exposed (yellow bars, 25 ng/ml) primary AML cells (n = 6) in the presence of lirilumab (anti-CD158b blocking Ab, 10 µg/ml) and/or monalizumab (anti-NKG2A blocking Ab, 10 µg/ml). All graphs show the mean ± SEM; statistical analysis: one-way-ANOVA, Bonferroni's multiple comparison; ns $p > 0.05$; *$p < 0.05$; **$p < 0.01$; ***$p < 0.001$; ****$p < 0.0001$.

4. Discussion

4.1 CD70 expression and function in AML

The success of target-directed immunotherapy critically depends on the selection of an appropriate antigen. However, identifying an ideal target antigen in AML has been difficult, which has hindered the progress in development of immunotherapies. CD70 has emerged as a promising candidate due to its aberrant expression on AML cells and limited expression on healthy cells (69-71, 115). These characteristics suggest a favorable therapeutic window. However, the reported variability in CD70 expression and the need of a certain antigen density to elicit effective immune responses remain key concerns.

In this study, we first analyzed CD70 expression using publicly available RNAseq databases. Within the TCGA-AML cohort, we identified two subgroups $CD70^{low}$ (63%) and $CD70^{high}$ (37%). To validate and extend these findings to the protein level, we performed MPFC using antibodies targeting CD70 isoform 1. Prior, we analyzed the expression of both CD70 isoforms in AML cell lines and primary AML samples and observed higher levels of isoform 1, indicating that isoform 1 is canonical in AML. Flow cytometry analysis of primary AML samples confirmed the transcriptomic data, revealing that approximately one third of AML patients exceeded the median CD70 expression of 7.0%. Notably, CD70 expression showed high inter-patient heterogeneity, ranging from 0.2 to 89.6%. To further validate our findings, we performed IHC using a different antibody clone. Despite methodological differences, the correlation between IHC intensity score (dime, intermediate, bright) and MPFC results was moderate (r = 0.45), aligning with previously published data comparing IHC with MPFC (115).

We observed a comparable distribution of CD70 positive AML cells in samples from ID (0.2 to 89.6%) and relapsed AML patients (0.3 – 90.3%). Previous reports on CD70 expression utilized various methods, including flow cytometry, PCR, and IHC. Initial studies reported >75% positive AML cells in bulk and LSC populations detected by flow cytometry with low inter-patient variation (69). In contrast, other studies showed a considerable variability in the MFI, although CD70 expression was qualitatively identified in all tested AML samples detected via RT-PCR (70). A preclinical study utilizing CD70-directed CAR T cells showed even greater variability of CD70 expression in AML using both flow cytometry and IHC (71). These observations are consistent with our findings and those of a recent analysis of flow cytometry and IHC-based detection of CD70 in AML, which reported a mean CD70 expression of approximately 30% on AML blasts with high variability (115). While our data did not indicate enrichment of CD70 expression in any specific disease state (ID, relapse), genetic risk group (Fav, Int, Adv) or differentiation stage (bulk or stem/progenitor), prior studies comparing matched diagnosis and relapse samples reported an increase in CD70 expression at relapse (115). This highlights a potential dynamic regulation of CD70 expression.

Epigenetic regulation has been implicated in modulating CD70 expression. Riether et al., demonstrated that HMAs such as azacytidine and decitabine demethylate the CD70 promoter, leading to increased expression in AML (79). Similar results were reported from others (115). While these studies were limited to *in vitro* experiments, we evaluated CD70 expression in primary AML sample from patients treated with azacytidine. No upregulation was observed at early timepoints (days 4-6). However, this conclusion is tempered by the small cohort size (n = 4), the generally low baseline CD70 expression in these patients, and the possibility that CD70 induction may require prolonged exposure or preexisting expression.

Moreover, we found elevated serum levels in AML patients, suggesting active CD27-CD70 signaling. High sCD27 levels were associated with lower overall survival, indicating a role as a negative prognostic marker (70). While we did not detect CD27 on the surface of primary AML cells, prior studies reported that CD27-CD70 interactions promote AML stemness, and that blockade of this axis using mAbs reduced the stem/progenitor compartment (70).

However, when we compared sCD27 levels in bone marrow fluid samples from AML patients at initial diagnosis, remission, and relapse, no significant differences were found. These findings suggest that sCD27 is not regulated in the bone marrow compartment. We therefore hypothesize that peripheral AML cells may interact with naïve T cells, which constitutively express CD27 (**Fig. 10 A**), and that sCD27 is primary derived from T cells rather than from AML cells. Following this idea, we correlated CD70 expression on AML bulk cells and CD27 expression on T cells from the same patients, but no inverse correlation was found.

To evaluate potential immunomodulatory effects of the CD27-CD70 signaling axis on T cell function, we utilized SEA-CD70 for CD70 blockade. In coculture experiments using the AML cell line MOLM-13 and healthy donor T cells in the presence of an BsAb (CD33xCD3), we observed no differences in BsAb-mediated cytotoxicity or T-cell proliferation upon CD70 blockade. However, this model system may not be suitable to assess the specific role of CD27 signaling, as T cells activation in this setting likely dominated by other potent co-stimulatory pathways such as CD28-CD80/CD86, masking CD27-mediated effects.

Beside short-term co-cultures of T cells with MOLM-13 cells, we also performed long-term cocultures of T cells with OCI-Ly1 cells in the presence of BsAb blinatumomab (CD19xCD3). In both short and long-term cocultures, CD70 blockade prevented downregulation of CD27 on BsAb-activated T cells, indicating active CD70-CD27 interaction. However, only minimal differences were observed in BsAb-mediated cytotoxicity, T-cell proliferation, cytokine secretion, or metabolic fitness over 28 days.

Interestingly, cocultures of BsAb-activated T cells and MOLM-13 cells led to increased CD70 expression on MOLM-13 cells. This upregulation was linked to BsAb-induced cytokine secretion, particularly TNF-α, which we have demonstrated to increase CD70 expression in a dose-dependent manner. Using TNFSFR1 KO MOLM-13 clones, we confirmed that TNF-α signaling was required for the increase in CD70 expression. Early studies demonstrated that CD70 is upregulated

during T-cell activation in response to TNF-α, suggesting that a similar TNF-α-mediated mechanism may drive CD70 upregulation in AML cells (57).

Interestingly, RNAseq analysis of TNF-α exposed MOLM-13 cells did not show an increase in CD70 transcript levels, indicating that CD70 upregulation in response to TNF-α occurs predominantly at the protein level. This post-transcriptional regulation is reminiscent of findings in DCs, where CD70 is stored in endosomal compartments alongside HLA class II molecules, enabling a rapid co-stimulation and antigen presentation upon antigen encounter (116).

Supporting a link between inflammation and CD70, gene expression analysis within the $CD70^{high}$ subgroup of the TCGA-AML cohort revealed enrichment of IFN-γ signaling pathways and enhanced expression of HLA class I and II genes. These findings suggest that high CD70 expression in AML is associated with an inflammatory transcriptional signature.

4.2 Preclinical evaluation of SEA-CD70

We validated CD70 as therapeutic target for AML, although its heterogeneous expression across patients is a challenge for immunotherapy. SEA-CD70, a non-fucosylated mAb was evaluated in preclinical modes, demonstrating antigen expression-dependent and dose-dependent cytotoxicity against AML cell lines. In tested primary AML samples, SEA-CD70-mediated cytotoxicity correlated with CD70 surface expression levels. Notably, TNF-α exposure increased CD70 expression which in turn enhanced SEA-CD70-mediated cytotoxicity.

In contrast, exposure of AML cell lines to CM from BsAb-activated T cells, rich in inflammatory cytokines, particular TNF-α and IFN-γ, resulted in reduced SEA-CD70-mediated ADCC, despite upregulation of CD70. These paradoxical finding was linked to IFN-γ-induced upregulation of NK cell inhibitory receptor ligands, including both classical and non-classical HLA class I molecules, which dampen NK cell-mediated cytotoxicity.

One of the most abundant cytokines secreted by activated T cells is IFN-γ, which has a fundamental role in tumor immunity. Over 30 years ago, scientists discovered that IFN-γ increases the expression of the whole antigen processing and presentation pathway including, HLA molecules, which allows rapid recognition of infected tissue by the adaptive immune system (117, 118). Based on these findings, tumors with elevated IFN-γ signaling often showed increased immunogenicity and were classified as “hot” while those with impaired or defective IFN-γ responsiveness may evade immune recognition and were classified as “cold” tumors (119). Despite the crucial role of IFN-γ in promoting immune recognition especially by T cells, it also possesses immunosuppressive properties. One example is the upregulation of PD-L1 an immune checkpoint receptor that inhibits T cell responses (104). Moreover, while increased expression of HLA molecules enhances tumor recognition by T cells, it conversely has suppressive effects on NK cells. NK cells are regulated by a dynamic interplay between activating and inhibitory receptors with the latter include KIRs and NKG2A. These receptors interact with classical (HLA-ABC) and nonclassical

(HLA-E, HLA-G) HLA class I molecules to dampen NK cell activity (92). While activation of NK cells is often depicted as a binary process, their cytotoxic function is in fact shaped by a balance of stimulatory and inhibitory signals. Previous studies have demonstrated that therapeutic efficacy of mAbs such as rituximab (anti-CD20) can be influenced by HLA expression, independent of antigen density (120). In neuroblastoma, responsiveness to anti-GD2 therapy was hampered by HLA-mediated inhibition, which could be overcome by blockade of HLA interaction *in vitro* (121).

Our findings on the IFN-γ-mediated resistance to ADCC align with emerging literature exploring immune evasion strategies used by cancer cells, particularly their ability to upregulate ligands for NK cell inhibitory receptors (122, 123). Importantly, we observed partial recovery of mAb-mediated killing through targeted inhibition of KIR and NKG2A using the blocking antibodies lirilumab and monalizumab, respectively. Lirilumab (IPH2102), an IgG4 antibody that targets KIR2DL1 and KIR2DL2/3, has been shown in preclinical models to enhance cytotoxicity of IL-2-activated NK cells against HLA-C-matched AML cells (124). Despite a good safety profile in early-phase clinical trials, lirilumab did not show therapeutic benefit as a single agent or in combination with chemotherapy in subsequent studies (125-128). NKG2A, an inhibitory receptor containing an ITIM, is expressed not only on subsets of NK cells but also on cytotoxic $CD8^+$ T cells (129, 130). Moreover, tumor-infiltrating NK cells express NKG2A at high levels (131). Its ligand HLA-E is frequently overexpressed in various tumors and correlates with unfavorable clinical outcomes (132-136). Monalizumab, an IgG4 monoclonal antibody developed to block NKG2A, has demonstrated potential in enhancing immune responses in cancer. In a phase II trial (NCT026435509) involving patients with squamous cell carcinoma of the head and neck (SCCHN), monalizumab combined with cetuximab showed a response rate of 27.5%, outperforming cetuximab monotherapy, which had a historical response rate of only 13% (137, 138). Notably, genetic deletion of NKG2A via CRISPR-Cas9 in *ex vivo* expanded NK cells led to superior anti-leukemic activity compared to antibody blockade, both *in vitro* and in xenograft mouse models (139). These insights underscore the potential of augmenting ADCC by disrupting inhibitory HLA-NK cell receptor interactions, either through therapeutic antibodies or gene editing strategies to enhance NK cell effector function.

5. Summary and Conclusion

In this preclinical study, we investigated the therapeutic potential and resistance mechanisms of a CD70-targeting mAb in the context of NK cell-based treatment strategy in AML. Using a non-fucosylated anti-CD70 monoclonal IgG1 antibody, we demonstrated that both antigen density and antibody concentration determine the degree of NK cell-mediated ADCC. Notably, CD70 expression was increased by TNF-α, resulting in enhanced anti-CD70 mAb- (SEA-CD70) mediated ADCC.

However, co-exposure to IFN-γ, which is frequently secreted alongside TNF-α, led to increased expression of classical and non-classical HLA class I molecules. This upregulation impaired NK cell-mediated ADCC through engagement of inhibitory receptors, thereby counteracting the benefit of increased CD70 expression. Importantly, this immunomodulatory effect of IFN-γ was not restricted to CD70-targeting mAbs. Similar resistance was observed with an anti-CD33 mAb, indicating that IFN-γ-driven HLA upregulation represents a recurrent mechanism by which AML cells evade NK cell-mediated ADCC. These findings highlight the dual role of inflammatory cytokines in modulating both target antigen availability and immune resistance.

Considering ongoing clinical trials involving ADCC-based therapies against various AML antigens, our data underscore the importance of cytokine profiling and biomarker-driven patient stratification to predict therapeutic responsiveness and to design rationale combination therapies.

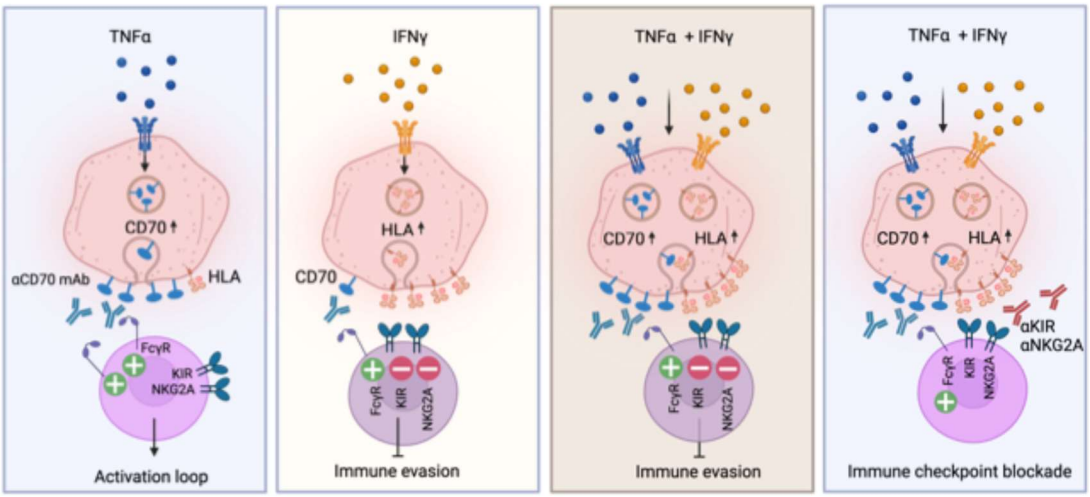

Figure 30: TNF-α- and IFN-γ-mediated modulation of surface receptor expression and ADCC in AML
Exposure of AML cells to TNF-α enhances the expression of the target antigen CD70, resulting in improved susceptibility to ADCC. Activated NK cells can secrete TNF-α, potentially creating a positive feedback loop. In contrast exposure to IFN-γ upregulates inhibitory ligands for NK cell receptors, particularly classical and non-classical HLA class I molecules, which dampens ADCC. When both TNF-α and IFN-γ are present, the immunosuppressive effect of IFN-γ dominates, shifting the balance toward NK cell inhibition resulting in immune evasion. However, this evasion mechanism can be counteracted by therapeutic mAbs targeting inhibitory NK cell receptors such as KIR and NKG2A, thereby restoring ADCC activity. Figure was created with Biorender.

References

1. Sasaki K, Ravandi F, Kadia TM, DiNardo CD, Short NJ, Borthakur G, et al. De novo acute myeloid leukemia: A population-based study of outcome in the United States based on the Surveillance, Epidemiology, and End Results (SEER) database, 1980 to 2017. Cancer. 2021;127(12):2049-61.

2. Sill H, Olipitz W, Zebisch A, Schulz E, Wölfler A. Therapy-related myeloid neoplasms: pathobiology and clinical characteristics. British Journal of Pharmacology. 2011;162(4):792-805.

3. Papaemmanuil E, Gerstung M, Bullinger L, Gaidzik VI, Paschka P, Roberts ND, et al. Genomic Classification and Prognosis in Acute Myeloid Leukemia. New England Journal of Medicine. 2016;374(23):2209-21.

4. Döhner H, Weisdorf DJ, Bloomfield CD. Acute Myeloid Leukemia. New England Journal of Medicine. 2015;373(12):1136-52.

5. Yates JW, Wallace HJ, Jr., Ellison RR, Holland JF. Cytosine arabinoside (NSC-63878) and daunorubicin (NSC-83142) therapy in acute nonlymphocytic leukemia. Cancer Chemother Rep. 1973;57(4):485-8.

6. Vogler WR, Velez-Garcia E, Weiner RS, Flaum MA, Bartolucci AA, Omura GA, et al. A phase III trial comparing idarubicin and daunorubicin in combination with cytarabine in acute myelogenous leukemia: a Southeastern Cancer Study Group Study. Journal of Clinical Oncology. 1992;10(7):1103-11.

7. Oran B, Weisdorf DJ. Survival for older patients with acute myeloid leukemia: a population-based study. Haematologica. 2012;97(12):1916.

8. Döhner H, Estey E, Grimwade D, Amadori S, Appelbaum FR, Büchner T, et al. Diagnosis and management of AML in adults: 2017 ELN recommendations from an international expert panel. Blood, The Journal of the American Society of Hematology. 2017;129(4):424-47.

9. Lancet JE, Uy GL, Cortes JE, Newell LF, Lin TL, Ritchie EK, et al. CPX-351 (cytarabine and daunorubicin) liposome for injection versus conventional cytarabine plus daunorubicin in older patients with newly diagnosed secondary acute myeloid leukemia. Journal of Clinical Oncology. 2018;36(26):2684-92.

10. Shlush LI, Mitchell A, Heisler L, Abelson S, Ng SWK, Trotman-Grant A, et al. Tracing the origins of relapse in acute myeloid leukaemia to stem cells. Nature. 2017;547(7661):104-8.

11. Weiden PL, Flournoy N, Thomas ED, Prentice R, Fefer A, Buckner CD, et al. Antileukemic effect of graft-versus-host disease in human recipients of allogeneic-marrow grafts. New England Journal of Medicine. 1979;300(19):1068-73.

12. Grimwade D, Freeman SD. Defining minimal residual disease in acute myeloid leukemia: which platforms are ready for “prime time”? Blood, The Journal of the American Society of Hematology. 2014;124(23):3345-55.

13. DiNardo CD, Jonas BA, Pullarkat V, Thirman MJ, Garcia JS, Wei AH, et al. Azacitidine and Venetoclax in Previously Untreated Acute Myeloid Leukemia. N Engl J Med. 2020;383(7):617-29.

14. Pratz KW, Cherry M, Altman JK, Cooper BW, Podoltsev NA, Cruz JC, et al. Gilteritinib in Combination With Induction and Consolidation Chemotherapy and as Maintenance Therapy: A Phase IB Study in Patients With Newly Diagnosed AML. J Clin Oncol. 2023;41(26):4236-46.

15. Stone RM, Mandrekar SJ, Sanford BL, Laumann K, Geyer S, Bloomfield CD, et al. Midostaurin plus chemotherapy for acute myeloid leukemia with a FLT3 mutation. New England Journal of Medicine. 2017;377(5):454-64.

16. DiNardo CD, Stein EM, de Botton S, Roboz GJ, Altman JK, Mims AS, et al. Durable Remissions with Ivosidenib in IDH1-Mutated Relapsed or Refractory AML. N Engl J Med. 2018;378(25):2386-98.

17. DiNardo CD, Schuh AC, Stein EM, Montesinos P, Wei AH, de Botton S, et al. Enasidenib plus azacitidine versus azacitidine alone in patients with newly diagnosed, mutant-IDH2 acute myeloid

leukaemia (AG221-AML-005): a single-arm, phase 1b and randomised, phase 2 trial. Lancet Oncol. 2021;22(11):1597-608.

18. Tiong IS, Wei AH. New drugs creating new challenges in acute myeloid leukemia. Genes, Chromosomes and Cancer. 2019;58(12):903-14.

19. Ott PA, Hodi FS, Robert C. CTLA-4 and PD-1/PD-L1 Blockade: New Immunotherapeutic Modalities with Durable Clinical Benefit in Melanoma Patients. Clinical Cancer Research. 2013;19(19):5300-9.

20. Ballantyne A, Dhillon S. Trastuzumab emtansine: first global approval. Drugs. 2013;73:755-65.

21. Castaigne S, Pautas C, Terré C, Raffoux E, Bordessoule D, Bastie J-N, et al. Effect of gemtuzumab ozogamicin on survival of adult patients with de-novo acute myeloid leukaemia (ALFA-0701): a randomised, open-label, phase 3 study. The Lancet. 2012;379(9825):1508-16.

22. Jen EY, Ko C-W, Lee JE, Del Valle PL, Aydanian A, Jewell C, et al. FDA approval: gemtuzumab ozogamicin for the treatment of adults with newly diagnosed CD33-positive acute myeloid leukemia. Clinical cancer research. 2018;24(14):3242-6.

23. Daver NG, Montesinos P, DeAngelo DJ, Wang ES, Papadantonakis N, Todisco E, et al. Pivekimab sunirine (IMGN632), a novel CD123-targeting antibody–drug conjugate, in relapsed or refractory acute myeloid leukaemia: a phase 1/2 study. The Lancet Oncology. 2024;25(3):388-99.

24. McLaughlin P, Grillo-Lopez AJ, Link BK, Levy R, Czuczman MS, Williams ME, et al. Rituximab chimeric anti-CD20 monoclonal antibody therapy for relapsed indolent lymphoma: half of patients respond to a four-dose treatment program. Journal of clinical oncology. 1998;16(8):2825-33.

25. Piccart-Gebhart MJ, Procter M, Leyland-Jones B, Goldhirsch A, Untch M, Smith I, et al. Trastuzumab after adjuvant chemotherapy in HER2-positive breast cancer. New England Journal of Medicine. 2005;353(16):1659-72.

26. Lonial S, Weiss BM, Usmani SZ, Singhal S, Chari A, Bahlis NJ, et al. Daratumumab monotherapy in patients with treatment-refractory multiple myeloma (SIRIUS): an open-label, randomised, phase 2 trial. The Lancet. 2016;387(10027):1551-60.

27. Topp MS, Gökbuget N, Stein AS, Zugmaier G, O'Brien S, Bargou RC, et al. Safety and activity of blinatumomab for adult patients with relapsed or refractory B-precursor acute lymphoblastic leukaemia: a multicentre, single-arm, phase 2 study. The lancet oncology. 2015;16(1):57-66.

28. Gökbuget N, Dombret H, Bonifacio M, Reichle A, Graux C, Faul C, et al. Blinatumomab for minimal residual disease in adults with B-cell precursor acute lymphoblastic leukemia. Blood, The Journal of the American Society of Hematology. 2018;131(14):1522-31.

29. Krupka C, Kufer P, Kischel R, Zugmaier G, Bögeholz J, Köhnke T, et al. CD33 target validation and sustained depletion of AML blasts in long-term cultures by the bispecific T-cell–engaging antibody AMG 330. Blood, The Journal of the American Society of Hematology. 2014;123(3):356-65.

30. Ravandi F, Subklewe M, Walter RB, Vachhani P, Ossenkoppele G, Buecklein V, et al. Safety and tolerability of AMG 330 in adults with relapsed/refractory AML: a phase 1a dose-escalation study. Leukemia & Lymphoma. 2024;65(9):1281-91.

31. Ravandi F, Stein AS, Kantarjian HM, Walter RB, Paschka P, Jongen-Lavrencic M, et al. A phase 1 first-in-human study of AMG 330, an anti-CD33 bispecific T-cell engager (BiTE®) antibody construct, in relapsed/refractory acute myeloid leukemia (R/R AML). Blood. 2018;132:25.

32. Uy GL, Rettig MP, Vey N, Godwin J, Foster MC, Rizzieri DA, et al. Phase 1 cohort expansion of flotetuzumab, a CD123× CD3 bispecific Dart® protein in patients with relapsed/refractory acute myeloid leukemia (AML). Blood. 2018;132:764.

33. Martin-Liberal J, Ochoa de Olza M, Hierro C, Gros A, Rodon J, Tabernero J. The expanding role of immunotherapy. Cancer Treatment Reviews. 2017;54:74-86.

34. Locke FL, Neelapu SS, Bartlett NL, Siddiqi T, Chavez JC, Hosing CM, et al. Phase 1 results of ZUMA-1: a multicenter study of KTE-C19 anti-CD19 CAR T cell therapy in refractory aggressive lymphoma. Molecular Therapy. 2017;25(1):285-95.

35. Rives S, Maude SL, Hiramatsu H, Baruchel A, Bader P, Bittencourt H, et al. S112: tisagenlecleucel in pediatric and young adult patients (PTS) with relapsed/refractory (R/R) B-cell acute lymphoblastic leukemia (B-ALL): final analyses from the Eliana Study. HemaSphere. 2022;6:13-4.

36. Plaks V, Rossi JM, Chou J, Wang L, Poddar S, Han G, et al. CD19 target evasion as a mechanism of relapse in large B-cell lymphoma treated with axicabtagene ciloleucel. Blood, The Journal of the American Society of Hematology. 2021;138(12):1081-5.

37. Philipp N, Kazerani M, Nicholls A, Vick B, Wulf J, Straub T, et al. T-cell exhaustion induced by continuous bispecific molecule exposure is ameliorated by treatment-free intervals. Blood. 2022;140(10):1104-18.

38. Ehninger A, Kramer M, Rollig C, Thiede C, Bornhauser M, von Bonin M, et al. Distribution and levels of cell surface expression of CD33 and CD123 in acute myeloid leukemia. Blood Cancer J. 2014;4(6):e218.

39. Dinndorf PA, Andrews RG, Benjamin D, Ridgway D, Wolff L, Bernstein ID. Expression of normal myeloid-associated antigens by acute leukemia cells. Blood. 1986;67(4):1048-53.

40. Griffin JD, Linch D, Sabbath K, Larcom P, Schlossman SF. A monoclonal antibody reactive with normal and leukemic human myeloid progenitor cells. Leuk Res. 1984;8(4):521-34.

41. Munoz L, Nomdedéu JF, López O, Carnicer MJ, Bellido M, Aventín A, et al. Interleukin-3 receptor alpha chain (CD123) is widely expressed in hematologic malignancies. Haematologica. 2001;86(12):1261-9.

42. Perna F, Berman SH, Soni RK, Mansilla-Soto J, Eyquem J, Hamieh M, et al. Integrating proteomics and transcriptomics for systematic combinatorial chimeric antigen receptor therapy of AML. Cancer cell. 2017;32(4):506-19. e5.

43. Carow CE, Levenstein M, Kaufmann SH, Chen J, Amin S, Rockwell P, et al. Expression of the hematopoietic growth factor receptor FLT3 (STK-1/Flk2) in human leukemias. 1996.

44. Rosnet O, Bühring H, Marchetto S, Rappold I, Lavagna C, Sainty D, et al. Human FLT3/FLK2 receptor tyrosine kinase is expressed at the surface of normal and malignant hematopoietic cells. Leukemia. 1996;10(2):238-48.

45. Morsink LM, Walter RB, Ossenkoppele GJ. Prognostic and therapeutic role of CLEC12A in acute myeloid leukemia. Blood Reviews. 2019;34:26-33.

46. Hofmann S, Schubert M-L, Wang L, He B, Neuber B, Dreger P, et al. Chimeric antigen receptor (CAR) T cell therapy in acute myeloid leukemia (AML). Journal of clinical medicine. 2019;8(2):200.

47. Gottschlich A, Thomas M, Grunmeier R, Lesch S, Rohrbacher L, Igl V, et al. Single-cell transcriptomic atlas-guided development of CAR-T cells for the treatment of acute myeloid leukemia. Nat Biotechnol. 2023;41(11):1618-32.

48. Denoeud J, Moser M. Role of CD27/CD70 pathway of activation in immunity and tolerance. Journal of Leukocyte Biology. 2010;89(2):195-203.

49. Akiba H, Nakano H, Nishinaka S, Shindo M, Kobata T, Atsuta M, et al. CD27, a Member of the Tumor Necrosis Factor Receptor Superfamily, Activates NF-κB and Stress-activated Protein Kinase/c-Jun N-terminal Kinase via TRAF2, TRAF5, and NF-κB-inducing Kinase *. Journal of Biological Chemistry. 1998;273(21):13353-8.

50. Keller AM, Schildknecht A, Xiao Y, van den Broek M, Borst J. Expression of costimulatory ligand CD70 on steady-state dendritic cells breaks CD8+ T cell tolerance and permits effective immunity. Immunity. 2008;29(6):934-46.

51. Arens R, Tesselaar K, Baars PA, Van Schijndel GM, Hendriks J, Pals ST, et al. Constitutive CD27/CD70 interaction induces expansion of effector-type T cells and results in IFNγ-mediated B cell depletion. Immunity. 2001;15(5):801-12.

52. Hintzen RQ, de Jong R, Hack CE, Chamuleau M, de Vries EF, ten Berge IJ, et al. A soluble form of the human T cell differentiation antigen CD27 is released after triggering of the TCR/CD3 complex. The Journal of Immunology. 1991;147(1):29-35.

53. Kato K, Chu P, Takahashi S, Hamada H, Kipps TJ. Metalloprotease inhibitors block release of soluble CD27 and enhance the immune stimulatory activity of chronic lymphocytic leukemia cells. Experimental Hematology. 2007;35(3):434-42.

54. Tesselaar K, Xiao Y, Arens R, van Schijndel GMW, Schuurhuis DH, Mebius RE, et al. Expression of the Murine CD27 Ligand CD70 In Vitro and In Vivo4. The Journal of Immunology. 2003;170(1):33-40.

55. Kashii Y, Giorda R, Herberman RB, Whiteside TL, Vujanovic NL. Constitutive Expression and Role of the TNF Family Ligands in Apoptotic Killing of Tumor Cells by Human NK Cells1. The Journal of Immunology. 1999;163(10):5358-66.

56. Sanchez PJ, McWilliams JA, Haluszczak C, Yagita H, Kedl RM. Combined TLR/CD40 Stimulation Mediates Potent Cellular Immunity by Regulating Dendritic Cell Expression of CD70 In Vivo1. The Journal of Immunology. 2007;178(3):1564-72.

57. Lens S, Baars P, Hooibrink B, Van Oers M, Van Lier R. Antigen-presenting cell-derived signals determine expression levels of CD70 on ‘qc primed T cells. Immunology. 1997;90(1):38-45.

58. Ranheim EA, Cantwell MJ, Kipps TJ. Expression of CD27 and its ligand, CD70, on chronic lymphocytic leukemia B cells. 1995.

59. Soares H, Waechter H, Glaichenhaus N, Mougneau E, Yagita H, Mizenina O, et al. A subset of dendritic cells induces CD4+ T cells to produce IFN-γ by an IL-12–independent but CD70-dependent mechanism in vivo. Journal of Experimental Medicine. 2007;204(5):1095-106.

60. Xiao Y, Peperzak V, Keller AM, Borst J. CD27 Instructs CD4+ T Cells to Provide Help for the Memory CD8+ T Cell Response after Protein Immunization1. The Journal of Immunology. 2008;181(2):1071-82.

61. Hendriks J, Gravestein LA, Tesselaar K, van Lier RAW, Schumacher TNM, Borst J. CD27 is required for generation and long-term maintenance of T cell immunity. Nature Immunology. 2000;1(5):433-40.

62. Coquet JM, Ribot JC, Bąbała N, Middendorp S, van der Horst G, Xiao Y, et al. Epithelial and dendritic cells in the thymic medulla promote CD4+Foxp3+ regulatory T cell development via the CD27–CD70 pathway. Journal of Experimental Medicine. 2013;210(4):715-28.

63. Laouar A, Haridas V, Vargas D, Zhinan X, Chaplin D, van Lier RAW, et al. CD70+ antigen-presenting cells control the proliferation and differentiation of T cells in the intestinal mucosa. Nature Immunology. 2005;6(7):698-706.

64. Ghosh S, Köstel Bal S, Edwards ES, Pillay B, Jiménez Heredia R, Erol Cipe F, et al. Extended clinical and immunological phenotype and transplant outcome in CD27 and CD70 deficiency. Blood, The Journal of the American Society of Hematology. 2020;136(23):2638-55.

65. Han BK, Olsen NJ, Bottaro A, editors. The CD27–CD70 pathway and pathogenesis of autoimmune disease. Seminars in arthritis and rheumatism; 2016: Elsevier.

66. Glouchkova L, Ackermann B, Zibert A, Meisel R, Siepermann M, Janka-Schaub GE, et al. The CD70/CD27 pathway is critical for stimulation of an effective cytotoxic T cell response against B cell precursor acute lymphoblastic leukemia. The Journal of Immunology. 2009;182(1):718-25.

67. Jacobs J, Deschoolmeester V, Zwaenepoel K, Rolfo C, Silence K, Rottey S, et al. CD70: An emerging target in cancer immunotherapy. Pharmacology & therapeutics. 2015;155:1-10.

68. Flieswasser T, Camara-Clayette V, Danu A, Bosq J, Ribrag V, Zabrocki P, et al. Screening a broad range of solid and haematological tumour types for CD70 expression using a uniform IHC methodology as potential patient stratification method. Cancers. 2019;11(10):1611.

69. Perna F, Berman SH, Soni RK, Mansilla-Soto J, Eyquem J, Hamieh M, et al. Integrating Proteomics and Transcriptomics for Systematic Combinatorial Chimeric Antigen Receptor Therapy of AML. Cancer Cell. 2017;32(4):506-19.e5.

70. Riether C, Schürch CM, Bührer ED, Hinterbrandner M, Huguenin A-L, Hoepner S, et al. CD70/CD27 signaling promotes blast stemness and is a viable therapeutic target in acute myeloid leukemia. Journal of Experimental Medicine. 2017;214(2):359-80.

71. Sauer T, Parikh K, Sharma S, Omer B, Sedloev D, Chen Q, et al. CD70-specific CAR T cells have potent activity against acute myeloid leukemia without HSC toxicity. Blood, The Journal of the American Society of Hematology. 2021;138(4):318-30.

72. Font J, Pallares L, Martorell J, Martinez E, Gaya A, Vives J, et al. Elevated soluble CD27 levels in serum of patients with systemic lupus erythematosus. Clinical immunology and immunopathology. 1996;81(3):239-43.

73. Van Oers M, Pals S, Evers L, Van der Schoot C, Koopman G, Bonfrer J, et al. Expression and release of CD27 in human B-cell malignancies. 1993.

74. Huang J, Jochems C, Anderson AM, Talaie T, Jales A, Madan RA, et al. Soluble CD27-pool in humans may contribute to T cell activation and tumor immunity. The Journal of Immunology. 2013;190(12):6250-8.

75. Phillips T, Barr PM, Park SI, Kolibaba K, Caimi PF, Chhabra S, et al. A phase 1 trial of SGN-CD70A in patients with CD70-positive diffuse large B cell lymphoma and mantle cell lymphoma. Investigational new drugs. 2019;37:297-306.

76. Owonikoko TK, Hussain A, Stadler WM, Smith DC, Kluger H, Molina AM, et al. First-in-human multicenter phase I study of BMS-936561 (MDX-1203), an antibody-drug conjugate targeting CD70. Cancer chemotherapy and pharmacology. 2016;77:155-62.

77. Massard C, Soria J-C, Krauss J, Gordon M, Lockhart AC, Rasmussen E, et al. First-in-human study to assess safety, tolerability, pharmacokinetics, and pharmacodynamics of the anti-CD27L antibody-drug conjugate AMG 172 in patients with relapsed/refractory renal cell carcinoma. Cancer chemotherapy and pharmacology. 2019;83:1057-63.

78. Tannir NM, Forero-Torres A, Ramchandren R, Pal SK, Ansell SM, Infante JR, et al. Phase I dose-escalation study of SGN-75 in patients with CD70-positive relapsed/refractory non-Hodgkin lymphoma or metastatic renal cell carcinoma. Investigational new drugs. 2014;32:1246-57.

79. Riether C, Pabst T, Höpner S, Bacher U, Hinterbrandner M, Banz Y, et al. Targeting CD70 with cusatuzumab eliminates acute myeloid leukemia stem cells in patients treated with hypomethylating agents. Nature medicine. 2020;26(9):1459-67.

80. Ochsenbein AF, Riether C, Bacher U, Müller R, Höpner S, Banz Y, et al. Argx-110 targeting CD70, in combination with azacitidine, shows favorable safety profile and promising anti-leukemia activity in newly diagnosed AML patients in an ongoing phase 1/2 clinical trial. Blood. 2018;132:2680.

81. Grieselhuber NR, Baratam P, Advani AS, Yacoub A, Stevens DA, Aribi A, et al. PF-08046040 (SEA-CD70), a Nonfucosylated CD70-Directed Antibody, in Combination with Azacitidine for Patients with Myelodysplastic Syndromes (MDS): A Phase 1 Dose-Finding and Dose Expansion Study. Blood. 2024;144:1840.

82. Pabst T, Vey N, Adès L, Bacher U, Bargetzi M, Fung S, et al. Results from a phase I/II trial of cusatuzumab combined with azacitidine in patients with newly diagnosed acute myeloid leukemia who are ineligible for intensive chemotherapy. Haematologica. 2023;108(7):1793.

83. D'Silva SZ, Singh M, Pinto AS. NK cell defects: implication in acute myeloid leukemia. Frontiers in Immunology. 2023;14:1112059.

84. Bianchi M, Reichen C, Croset A, Fischer S, Eggenschwiler A, Grübler Y, et al. The CD33xCD123xCD70 multispecific CD3-engaging DARPin MP0533 induces selective T cell–mediated killing of AML leukemic stem cells. Cancer immunology research. 2024;12(7):921-43.

85. Tu S, Zhou X, Guo Z, Huang R, Yue C, He Y, et al. CD19 and CD70 dual-target chimeric antigen receptor T-cell therapy for the treatment of relapsed and refractory primary central nervous system diffuse large B-cell lymphoma. Frontiers in oncology. 2019;9:1350.

86. Pal SK, Tran B, Haanen JB, Hurwitz ME, Sacher A, Tannir NM, et al. CD70-targeted allogeneic CAR T-cell therapy for advanced clear cell renal cell carcinoma. Cancer discovery. 2024;14(7):1176-89.

87. Burris HA, Infante JR, Ansell SM, Nemunaitis JJ, Weiss GR, Villalobos VM, et al. Safety and activity of varlilumab, a novel and first-in-class agonist anti-CD27 antibody, in patients with advanced solid tumors. Journal of Clinical Oncology. 2017;35(18):2028-36.

88. Melsen JE, Lugthart G, Lankester AC, Schilham MW. Human circulating and tissue-resident CD56bright natural killer cell populations. Frontiers in immunology. 2016;7:262.

89. Cooper MA, Bush JE, Fehniger TA, VanDeusen JB, Waite RE, Liu Y, et al. In vivo evidence for a dependence on interleukin 15 for survival of natural killer cells. Blood, The Journal of the American Society of Hematology. 2002;100(10):3633-8.

90. Bryceson YT, March ME, Ljunggren H-G, Long EO. Synergy among receptors on resting NK cells for the activation of natural cytotoxicity and cytokine secretion. Blood. 2006;107(1):159-66.

91. Gasser S, Orsulic S, Brown EJ, Raulet DH. The DNA damage pathway regulates innate immune system ligands of the NKG2D receptor. Nature. 2005;436(7054):1186-90.

92. Berrien-Elliott MM, Jacobs MT, Fehniger TA. Allogeneic natural killer cell therapy. Blood. 2023;141(8):856-68.

93. Vivier E, Nunès JA, Vély F. Natural killer cell signaling pathways. Science. 2004;306(5701):1517-9.

94. Hicklin DJ, Marincola FM, Ferrone S. HLA class I antigen downregulation in human cancers: T-cell immunotherapy revives an old story. Molecular medicine today. 1999;5(4):178-86.

95. Buckle I, Guillerey C. Inhibitory receptors and immune checkpoints regulating natural killer cell responses to cancer. Cancers. 2021;13(17):4263.

96. Lizana-Vasquez GD, Torres-Lugo M, Dixon RB, Powderly JD, Warin RF. The application of autologous cancer immunotherapies in the age of memory-NK cells. Frontiers in Immunology. 2023;14:1167666.

97. Li Y, Hermanson DL, Moriarity BS, Kaufman DS. Human iPSC-derived natural killer cells engineered with chimeric antigen receptors enhance anti-tumor activity. Cell stem cell. 2018;23(2):181-92. e5.

98. Beilhack A, Schulz S, Baker J, Beilhack GF, Wieland CB, Herman EI, et al. In vivo analyses of early events in acute graft-versus-host disease reveal sequential infiltration of T-cell subsets. Blood. 2005;106(3):1113-22.

99. Denman CJ, Senyukov VV, Somanchi SS, Phatarpekar PV, Kopp LM, Johnson JL, et al. Membrane-bound IL-21 promotes sustained ex vivo proliferation of human natural killer cells. PloS one. 2012;7(1):e30264.

100. Liu E, Tong Y, Dotti G, Shaim H, Savoldo B, Mukherjee M, et al. Cord blood NK cells engineered to express IL-15 and a CD19-targeted CAR show long-term persistence and potent antitumor activity. Leukemia. 2018;32(2):520-31.

101. Liu E, Marin D, Banerjee P, Macapinlac HA, Thompson P, Basar R, et al. Use of CAR-transduced natural killer cells in CD19-positive lymphoid tumors. New England Journal of Medicine. 2020;382(6):545-53.

102. Janjic A, Wange LE, Bagnoli JW, Geuder J, Nguyen P, Richter D, et al. Prime-seq, efficient and powerful bulk RNA sequencing. Genome Biol. 2022;23(1):88.

103. Krupka C, Kufer P, Kischel R, Zugmaier G, Bogeholz J, Kohnke T, et al. CD33 target validation and sustained depletion of AML blasts in long-term cultures by the bispecific T-cell-engaging antibody AMG 330. Blood. 2014;123(3):356-65.

104. Marcinek A, Brauchle B, Rohrbacher L, Hanel G, Philipp N, Markl F, et al. Correction to: CD33 BiTE((R)) molecule-mediated immune synapse formation and subsequent T-cell activation is determined by the expression profile of activating and inhibitory checkpoint molecules on AML cells. Cancer Immunol Immunother. 2023;72(7):2513-4.

105. Bonato V, Tang SY, Hsieh M, Zhang Y, Deng S. Experimental design considerations and statistical analyses in preclinical tumor growth inhibition studies. Pharm Stat. 2024.

106. Herrmann M, Krupka C, Deiser K, Brauchle B, Marcinek A, Ogrinc Wagner A, et al. Bifunctional PD-1 x alphaCD3 x alphaCD33 fusion protein reverses adaptive immune escape in acute myeloid leukemia. Blood. 2018;132(23):2484-94.

107. Schmid-Burgk JL, Schmidt T, Gaidt MM, Pelka K, Latz E, Ebert TS, et al. OutKnocker: a web tool for rapid and simple genotyping of designer nuclease edited cell lines. Genome Res. 2014;24(10):1719-23.

108. Andrews S. FastQC: a quality control tool for high throughput sequence data. Cambridge, United Kingdom; 2010.

109. Martin M. Cutadapt removes adapter sequences from high-throughput sequencing reads. 2011. 2011;17(1):3.

110. Parekh S, Ziegenhain C, Vieth B, Enard W, Hellmann I. zUMIs-A fast and flexible pipeline to process RNA sequencing data with UMIs. Gigascience. 2018;7(6):giy059.

111. Renaud G, Stenzel U, Maricic T, Wiebe V, Kelso J. deML: robust demultiplexing of Illumina sequences using a likelihood-based approach. Bioinformatics. 2015;31(5):770-2.

112. Roboz GJ, Pabst T, Aribi A, Brandwein JM, Döhner H, Fiedler W, et al. Safety and Efficacy of Cusatuzumab in Combination with Venetoclax and Azacitidine (CVA) in Patients with Previously Untreated Acute Myeloid Leukemia (AML) Who Are Not Eligible for Intensive Chemotherapy; An Open-Label, Multicenter, Phase 1b Study. Blood. 2021;138:369.

113. Riether C, Pabst T, Hopner S, Bacher U, Hinterbrandner M, Banz Y, et al. Targeting CD70 with cusatuzumab eliminates acute myeloid leukemia stem cells in patients treated with hypomethylating agents. Nat Med. 2020;26(9):1459-67.

114. Borst J, Hendriks J, Xiao Y. CD27 and CD70 in T cell and B cell activation. Current Opinion in Immunology. 2005;17(3):275-81.

115. Marques-Piubelli ML, Kumar B, Basar R, Panowski S, Srinivasan S, Norwood K, et al. Increased expression of CD70 in relapsed acute myeloid leukemia after hypomethylating agents. Virchows Archiv. 2024:1-5.

116. Keller AM, Groothuis TA, Veraar EA, Marsman M, de Buy Wenniger LM, Janssen H, et al. Costimulatory ligand CD70 is delivered to the immunological synapse by shared intracellular trafficking with MHC class II molecules. Proceedings of the National Academy of Sciences. 2007;104(14):5989-94.

117. Amaldi I, Reith W, Berte C, Mach B. Induction of HLA class II genes by IFN-gamma is transcriptional and requires a trans-acting protein. J Immunol. 1989;142(3):999-1004.

118. Shirayoshi Y, Burke PA, Appella E, Ozato K. Interferon-induced transcription of a major histocompatibility class I gene accompanies binding of inducible nuclear factors to the interferon consensus sequence. Proc Natl Acad Sci U S A. 1988;85(16):5884-8.

119. Castro F, Cardoso AP, Goncalves RM, Serre K, Oliveira MJ. Interferon-Gamma at the Crossroads of Tumor Immune Surveillance or Evasion. Front Immunol. 2018;9:847.

120. Borgerding A, Hasenkamp J, Engelke M, Burkhart N, Trumper L, Wienands J, et al. B-lymphoma cells escape rituximab-triggered elimination by NK cells through increased HLA class I expression. Exp Hematol. 2010;38(3):213-21.

121. Tarek N, Le Luduec JB, Gallagher MM, Zheng J, Venstrom JM, Chamberlain E, et al. Unlicensed NK cells target neuroblastoma following anti-GD2 antibody treatment. J Clin Invest. 2012;122(9):3260-70.

122. Dufva O, Gandolfi S, Huuhtanen J, Dashevsky O, Duan H, Saeed K, et al. Single-cell functional genomics reveals determinants of sensitivity and resistance to natural killer cells in blood cancers. Immunity. 2023;56(12):2816-35 e13.

123. Dubrot J, Du PP, Lane-Reticker SK, Kessler EA, Muscato AJ, Mehta A, et al. In vivo CRISPR screens reveal the landscape of immune evasion pathways across cancer. Nat Immunol. 2022;23(10):1495-506.

124. Lorig-Roach N, Harpell NM, DuBois RM. Structural basis for the activity and specificity of the immune checkpoint inhibitor lirilumab. Sci Rep. 2024;14(1):742.

125. Vey N, Karlin L, Sadot-Lebouvier S, Broussais F, Berton-Rigaud D, Rey J, et al. A phase 1 study of lirilumab (antibody against killer immunoglobulin-like receptor antibody KIR2D; IPH2102) in patients with solid tumors and hematologic malignancies. Oncotarget. 2018;9(25):17675-88.

126. Carlsten M, Korde N, Kotecha R, Reger R, Bor S, Kazandjian D, et al. Checkpoint Inhibition of KIR2D with the Monoclonal Antibody IPH2101 Induces Contraction and Hyporesponsiveness of NK Cells in Patients with Myeloma. Clin Cancer Res. 2016;22(21):5211-22.

127. Benson DM, Jr., Bakan CE, Zhang S, Collins SM, Liang J, Srivastava S, et al. IPH2101, a novel anti-inhibitory KIR antibody, and lenalidomide combine to enhance the natural killer cell versus multiple myeloma effect. Blood. 2011;118(24):6387-91.

128. Romagne F, Andre P, Spee P, Zahn S, Anfossi N, Gauthier L, et al. Preclinical characterization of 1-7F9, a novel human anti-KIR receptor therapeutic antibody that augments natural killer-mediated killing of tumor cells. Blood. 2009;114(13):2667-77.

129. Le Drean E, Vely F, Olcese L, Cambiaggi A, Guia S, Krystal G, et al. Inhibition of antigen-induced T cell response and antibody-induced NK cell cytotoxicity by NKG2A: association of NKG2A with SHP-1 and SHP-2 protein-tyrosine phosphatases. Eur J Immunol. 1998;28(1):264-76.

130. Braud VM, Allan DS, O'Callaghan CA, Soderstrom K, D'Andrea A, Ogg GS, et al. HLA-E binds to natural killer cell receptors CD94/NKG2A, B and C. Nature. 1998;391(6669):795-9.

131. Sun C, Xu J, Huang Q, Huang M, Wen H, Zhang C, et al. High NKG2A expression contributes to NK cell exhaustion and predicts a poor prognosis of patients with liver cancer. Oncoimmunology. 2017;6(1):e1264562.

132. Talebian Yazdi M, van Riet S, van Schadewijk A, Fiocco M, van Hall T, Taube C, et al. The positive prognostic effect of stromal CD8+ tumor-infiltrating T cells is restrained by the expression of HLA-E in non-small cell lung carcinoma. Oncotarget. 2016;7(3):3477-88.

133. Andersson E, Poschke I, Villabona L, Carlson JW, Lundqvist A, Kiessling R, et al. Non-classical HLA-class I expression in serous ovarian carcinoma: Correlation with the HLA-genotype, tumor infiltrating immune cells and prognosis. Oncoimmunology. 2016;5(1):e1052213.

134. Mamessier E, Sylvain A, Thibult ML, Houvenaeghel G, Jacquemier J, Castellano R, et al. Human breast cancer cells enhance self tolerance by promoting evasion from NK cell antitumor immunity. J Clin Invest. 2011;121(9):3609-22.

135. Gooden M, Lampen M, Jordanova ES, Leffers N, Trimbos JB, van der Burg SH, et al. HLA-E expression by gynecological cancers restrains tumor-infiltrating CD8(+) T lymphocytes. Proc Natl Acad Sci U S A. 2011;108(26):10656-61.

136. de Kruijf EM, Sajet A, van Nes JG, Natanov R, Putter H, Smit VT, et al. HLA-E and HLA-G expression in classical HLA class I-negative tumors is of prognostic value for clinical outcome of early breast cancer patients. J Immunol. 2010;185(12):7452-9.

137. Andre P, Denis C, Soulas C, Bourbon-Caillet C, Lopez J, Arnoux T, et al. Anti-NKG2A mAb Is a Checkpoint Inhibitor that Promotes Anti-tumor Immunity by Unleashing Both T and NK Cells. Cell. 2018;175(7):1731-43 e13.

138. Vermorken JB, Trigo J, Hitt R, Koralewski P, Diaz-Rubio E, Rolland F, et al. Open-label, uncontrolled, multicenter phase II study to evaluate the efficacy and toxicity of cetuximab as a single agent in patients with recurrent and/or metastatic squamous cell carcinoma of the head and neck who failed to respond to platinum-based therapy. J Clin Oncol. 2007;25(16):2171-7.

139. Gong Y, Germeraad WTV, Zhang X, Wu N, Li B, Janssen L, et al. NKG2A genetic deletion promotes human primary NK cell anti-tumor responses better than an anti-NKG2A monoclonal antibody. Mol Ther. 2024;32(8):2711-27.

Appendix

Table Supplementary 1: Characteristics of AML patients used for evaluation of CD70 isoform 1 and 2

Patient	Sex	Age	Diagnosis	Blasts	Cytogenetics	Genetic abnormalities
1	male	58	ID	52%	46, XY	NPM1+, FLT3-ITD+
2	male	56	ID	75%	46, XY	NPM1+, FLT3-ITD, RUNX1-RUNX1T1 Translocation t(8;21)
3	male	59	ID	84%	46, XY	NPM1+, FLT3-ITD+
4	male	74	ID	94%	46, XY	-
5	female	55	ID	90%	46, XX	IDH2+
6	female	49	ID	88%	46, XX	NPM1+, FLT3-ITD
7	male	59	ID	N/A	N/A	N/A
8	female	73	ID	81%	47,XX,+8(13)/46, XX(9)	NPM1+, FLT3-ITD+, Trisomy 8
9	male	39	relapse	81%	N/A	N/A
10	male	42	ID	80%	46, XY	CEBPA+2
11	female	64	ID	53%	46,XX, der(3)t(3;11)(q26;?);del(11)(q14-22)(10)	FLT3-ITD+, FLT3-TKD, hTERC del
12	male	58	ID	84%	46, XY	FLT3-ITD+
13	male	21	ID	87%	48,XY,+13,der(14)t(1;14)(q12;q32),+20(6)/46,XY(5)	-
14	female	56	ID	87%	46,XX, der(18)t(18;19)(q2?;q13),der(19)t(11;19)(q13;q13)(13)	KMT2A-PTD
15	female	43	ID	N/A	46, XX	NPM1+

16	N/A	N/A	N/A	N/A	N/A	N/A
17	female	51	ID	77%	46,XX	FLT3-ITD+, FLT3-TKD+, RUNX1+
18	male	46	ID	N/A	46,XY	FLT3-ITD+, NPM1+
19	female	N/A	ID	87%	46, XX	-

ID = initial diagnosis, N/A = not available

Table Supplementary 2: Characteristics of AML patients used for evaluation of CD70 expression (Ab clone REA-292)

Patient	Sex	Age	Diagnosis	Blasts	Cytogenetics	Genetic abnormalities
1	male	67	ID	32%	46, XY	NPM1+, FLT3-ITD
2	male	85	ID	47%	46, XY	NPM1+
3	male	67	ID	65%	46, XY	-
4	male	58	ID	77%	46, XY	NPM1+,FLT3-TKD, IDH1, IDH2
5	female	31	ID	32%	46, XX	NPM1+, CEBPA+1
6	female	59	ID	96%	46, XX	NPM1+, IDH2
7	male	32	ID	96%	46,XY,t(9;11)(p21.3;q23.3)(3)/55,sl,+3,+8,+der(11)t(9;11)(p21.3;q23.3)+12,+13,+14,+18,+19,+20(13)	MECOM, KMT2A, ETV6, KMT2a-MLLT3, RUNX1T1
8	female	86	ID	84%	46, XX	NPM1+, FLT3-ITD
9	male	20	ID	44%	46,XY,del(9)(q?13?22)(11)/46,XY(12)	CEBPA+2,
10	female	65	ID	72%	46, XX	KMT2A-PTD, CEBPA+1, IDH2+
11	male	61	ID	28%	45,XY,7(13)/47,XX,+8(8)/46,XY(2)	Trisomy 8, CEBPA+1, ASXL1
12	female	58	ID	77%	46, XX	NPM1+, FLT3-ITD, IDH1

13	male	63	ID	36%	46, XY	-
14	female	83	ID	82%	46, XX	NPM1+, FLT3-TKD
15	female	74	ID	96%	46, XX	NPM1+, FLT3-ITD
16	female	72	ID	51%	47, XX,+i(4)(p10)(15)	NPM1+, FLT3-ITD
17	male	71	ID	70%	46, XY	IDH2
18	female	60	ID	94%	46, XX	NPM1+, FLT3-ITD, IDH2
19	female	54	ID	81%	46, XX	NPM1+, IDH2
20	female	72	ID	80%	46,XX,i(5)(p10),+11,-17(5)/46,XX(8)	Monosomy 17, 5p15 and deletion 5q31, IDH1
21	female	80	ID	82%	46, XX	NPM1+
22	female	78	ID	85%	46, XX	NPM1+, FLT3-TKD
23	female	60	ID	72%	46, XX	NPM1+, FLT3-ITD
24	male	92	ID	50%	46, XY	CEBPA+2
25	male	63	ID	89%	47,XY,+8(19)/46, XY(3)	NPM1+, FLT3-ITD, Trisomy 8
26	female	89	ID	34%	46,XX,del(9)(q1?3q?22)(6)/46,XX(10)	NPM1+
27	male	81	ID	70%	45,XY7(9)/46,XY(2)	Monosomy 7, CE-BPA+2
28	male	70	ID	58%	aberrant, complex	5q31 deletion, 7q31 deletion, BCR-ABL, BCR-ABL, TP53
29	male	76	ID	51%	45, X, Y (19)/46, XY (1) aberrant	NPM1+
30	male	56	ID	75%	46, XY	NPM1+, FLT3-TKD, Trisomy 8, RUNX1T1, FLT3-ITD
31	female	46	ID	63%	46, XX	-
32	male	81	ID	32%	45,XY,-7(8)/46,XY(2)	Monosomy 7, ASXL1

33	female	48	ID	71%	46,XX,der(5)t(5;11)(q35;q13)(8/47,XX+11(1)/46,XX(2)	7q31 deletion, Trisomy 11, ASXL1, IDH2
34	female	63	ID	69%	46, XX	NPM1+, FLT3-ITD, CEBPA+1
35	male	59	ID	84%	46, XY	NPM1+, FLT3-ITD
36	male	57	ID	4%	-	-
37	female	56	ID	22%	46, XX	ASXL1
38	male	52	ID	50%	-	FLT3-ITD, KMT2A-PTD, IDH2, RUNX1
39	male	58	ID	78%	46,XY,der(3)t(3;8)(p25;q22)der(8)(t(8;21)(q22;q22),der()t(3;21)(p25;q22)(9)/45,X,sl, -Y(11)	RUNX1-RUNX1T1
40	female	55	ID	90%	-	-
41	male	57	ID	61%	46, XY	NPM1+, FLT3-ITD
42	male	42	ID	55%	46, XY	CEBPA+2
43	male	52	ID	56%	46, XY	NPM1+
44	female	70	ID	77%	46, XX	FLT3-ITD, KMT2A-PTD
45	male	81	ID	69%	46,XY,i(7)(p10)(5)/47,sl,+8(2)/46,XY(4)	7q31 deletion
46	male	57	ID	-		NPM1+, RUNX1-RUNX1T1, Trisomy 8, Trisomy 21
47	female	77	ID	77%	46,Xxi(17)(q10)(16)//46,XX(4)	TP53 del, Monosomy 7, ASXL1, RUNX1, CEBPA2+
48	male	67	ID	43%	47,XY,+8(3)/46,XY(17)	Trisomy 8, RUNX1T1, ASXL1
49	female	43	ID	92%	46,XX,t(9;11)(p22;q23)(10)/46,XX(8)	KMT2A rearrangement, KMT2A-

						MLLT3 fusiontran-script
50	female	85	ID	83%	46,XX,r(18)(p?q?)(10)	NPM1+, FLT3-ITD
51	male	86	ID	61%	46,XY	NPM1+
52	male	86	ID	-	46,XY	NPM1+, FLT3-ITD
53	male	66	ID	-	47,XY,+13,(18)/46,XY(2)	RUNX1+
54	female	51	ID	58%	aberrant, complex	KMT2A del, ETV6 del, 7q31 del
55	female	62	ID	34%	46,XX	RUNX1+, ASXL1+, SRSRF2+
56	male	50	ID	71%	46,XY	NPM1+, FLT3-ITD, FLT3-TKD, IDH2
57	male	68	ID	58%	46,XY	ASXL1 (2)
58	female	74	ID	52%	aberrant, complex	RUNX1T1, TP53
59	male	53	ID	76%	46,XY	FLT3-ITD, FLT3-TKD, IDH2
60	male	60	ID	81%	46,XY,inv(16)(p13.1q22)(10)/46,XY(2)	CBFB-MYH11 rearangement
61	female	74	ID	72%	46,XX	FLT3-ITD
62	female	51	ID	93%	46,XX	FLT3-TKD, RUNX1
63	male	63	ID	70%	complex	Monosomy 5, 7, TP53 del, RUNX1
64	male	85	ID	75%	46,XY	NPM1+
65	female	21	ID	84%	46,XX	NPM1+, FLT3-ITD, CEBPA+1
66	female	40	ID	29%	46,XX	NPM1+
67	female	77	ID	89%	46,XY	NPM1+, FLT3-ITD
68	female	57	ID	55%	46,XX,t(9;22)(q34;q11)(16)	BCR-ABL1 rearrangement, KMT2A rearrangement
69	male	83	ID	70%	46,XY	RUNX1+, FLT3-ITD

70	female	36	ID	63%	46,XX,del(9)(q13q22)(15)/46,XX(3)	
71	femae	51	ID	68%	47,XX,+X(15)	
72	female	64	ID	48%	46,XX,der(3(t(3;11)(q26);del(11)(q14-22)(10)	hTERC, FLT3-TKD
73	female	56	ID	52%	aberrant, complex	CBFB
74	female	46	ID	81%	46,XX	NPM1+, FLT3-ITD, ASXL1
75	male	67	ID	22%	47,XY,+8(2)/46,XY(20)	Trisomy 8, FLT3-ITD, ASXL1, RUNX1
76	male	63	ID	98%	46,XY	NPM1+, FLT3-ITD
77	female	43	ID	58%	46,XX,t(9;11)(p22;q23)(9)/46,XX	KMT2A-MLLT3
78	male	54	ID	92%	47,XY,+8,der(8)t(8;17)(p21;?q)x2(4)/47,sl,der,(10)t(8;10)(q21;q26)(5)/46	NPM1+, Trisomy 8, FLT3-TKD
79	male	79	ID	74%	47,XY,+11(16)/46,XY(1)	Trisomy 11, KMT2A-PTD, FLT3-TKD
80	female	28	ID	96%	46,XX	NPM1+, FLT3-ITD
81	male	85	ID	76%	46,XY,t(5;6)(q35;q25-27)(13)	FLT3-ITD, CE-BPA+1
82	male	61	ID	33%	46,XY	-
83	male	64	ID	25%	46,XY	RUNX1+
84	male	77	ID	28%	46,XY	FLT3-ITD, KMT2A-PTD, ASXL1, RUNX1, IDH1
85	male	76	ID	30%	-	NPM1+, Trisomy 8
86	female	52	ID	91%	46,XX	FLT3-ITD
87	female	53	relapse	40%	46,XX,t(3;3)(q21.3;q26.2)(19)/46,XX(1).ish der(2)t(2;11)(q3?7;q23)(KMT2A+)(3/14)	MECOM rearrangement, KMT2A

88	male	45	relapse	59%	-	-
89	female	76	relapse	18%	46, XX	NPM1+, IDH1
90	male	36	relapse	23%	46,XY,t(6;9)p22;q34)(7)/46,XY(3)	Dek-NUP214 rearangement
91	male	61	relapse	29%	46,XY,inv(16)(p13.1q22)(7)/46,XY(7)	CBFB-MYH11 rearangement
92	male	81	relapse	85%	47,XY,+13(5)/48,XY,+13,+15(6)/46,XY(5)	Trisomy 13, PML-RARA, RUNX1, FLT3-ITD, IDH1
93	male	50	relapse	20%	46, XY	IDH2
94	male	67	relapse	82%	47,XY,der(7)t(7;11)(q?22;q23),+13(9)/46,XY(2)	7q31 deletion, Trisomy 13
95	male	38	relapse	69%	45,XY,7(1)/45,sl,inv(3)(q21.3q26.2),del(11)(p12p15)(10)	MECOM rearrangement, Monosomy 7
96	female	77	relapse	29%	46, XX	IDH2, PTD
97	female	54	relapse	87%	-	NPM1+, FLT3-ITD
98	male	76	relapse	15%	-	NPM1+, FLT3-ITD
99	male	43	relapse	70%	46,XY	FLT3-ITD
100	male	55	relapse	78%	45,XY,8inv(16)(p13.1q22),der(17)(10)	RUNX1T1, CBFB-MYH11 fusiontranscript

ID = initial diagnosis, , N/A = not available

Table Supplementary 3: Characteristics of AML patients used for evaluation of CD70 expression (Ab clone h1F6)

Patient	Sex	Age	Diagnosis	Blasts	Cytogenetics	Genetic abnormalities
1	male	59	ID	N/A	N/A	-
2	male	74	ID	94%	46, XY	-
3	male	65	ID	68%	46, XY	NPM1+
4	male	61	ID	33%	46, XY	-

5	male	36	ID	55%	47,XY,t(1;8)(q21;q21),dup(17)(q21),+19(8)/48,sl,+8(3)/46,XY(3)	RUNX1-RUNX1T1 Trasnlocation t(8;21), Trisomy 8
6	male	28	ID	70%	46,XY,add(2)(q37),der(22)t(9;22)(q34.1;q11.2)(18)der(2)t(2;22)(q37;q11.2)(BCR+),der(9)(ABL1 dim),der(22)z(9;22)q34.1;q11.2)(BCR+,ABL1+)(24)/50,sl,+4,+6,+10,der(22)t(9;22)(q34.1;q11.2)	-
7	female	49	ID	88%	46, XX	NPM1+, FLT3-ITD
8	male	56	ID	75%	46, XY	NPM1+, FLT3-ITD, RUNX1-RUNX1T1 Trasnlocation t(8;21)
9	male	59	ID	84%	46, XY	NPM1+, FLT3-ITD
10	male	42	ID	80%	46, XY	CEBPA+2
11	male	75	ID	98%	46, XY	FLT3-ITD, RUNX1+
12	female	64	ID	53%	46,XX,der(3)t(3;11)(q26;?);del(11)(q14-22)(10)	FLT3-ITD, FLT3-TKD, hTERC del
13	male	54	ID	92%	47,XY,+8,der(8)z(8;17)(p21;?q)x2(4)/47,sl,der(10)t(8;10)(q?21;q2?6)(5)/46,XY(5)	NPM1+, FLT3-TKD, Trisomy 8
14	male	77	ID	28%	46, XY	FLT3-ITD, RUNX1+, KMT2a-PTD, ASXL1+, IDH1+

15	male	58	ID	52%	46, XY	NPM1+, FLT3-ITD
16	female	38	ID	78%	N/A	NPM1+, FLT3-ITD
17	female	55	ID	90%	46, XX	IDH2+
18	male	54	ID	70%	46, XY	NPM1+, FLT3-ITD+
19	female	73	ID	81%	47,XX,+8(13)/46,XX(9)	NPM1+, FLT3-ITD+, Trisomy 8
20	male	21	ID	87%	48,XY,+13,der(14)t(1;14)(q12;q32),+20(6)/46,XY(5)	-
21	female	56	ID	87%	46,XX,der(18)t(18;19)(q2?;q13),der(19)t(11;19)(q13;q13)(13)	KMT2A-PTD
22	male	39	relapse	81%	N/A	-
23	male	58	ID	84%	46, XY	FLT3-ITD+
24	female	43	ID	N/A	46, XX	NPM1+
25	female	86	ID	N/A	46, XX	NPM1+, FLT3-ITD+ (low)
26	female	40	ID	29%	46, XX	NPM1+
27	male	77	ID	89%	46, XY	NPM1+, FLT3-ITD+
28	female	76	ID	87%	46, XX	-

ID = initial diagnosis, N/A not available

Table Supplementary 4: Characteristics of AML patients used for evaluation of CD70 expression pre/post azacytidine treatment

Patient	Sex	Age	Diagnosis	Blasts	Cytogenetics	Genetic abnormalities
1	male	37	relapse	43%	46, XY, inv (16)(p13q22)[14]	CBFß-MYH11
2	male	85	ID	91%	46,XY,der(7)t(7;13)(q11;q12)[19]/45,XY,7[7]/46,X	-

					Y,der(7)del(7)(p12)del(7)(q11)[2]/46,XY[2]	
3	female	82	ID	31%	46,XX,del(5)(q22q33),+8t(10;14)(q22;q11),del(12)(p13[5]/46,sl,-7,der(22)t(7;22)(?p11)[5]/46,XX[2]	5q31 del, 7q31 del, ETV6 del, Trisomy 8, TP53mut
4	male	74	relapse	14%	N/A	N/A

ID = initial diagnosis, N/A = not available

Table Supplementary 5: Characteristics of AML patients used for evaluation of soluble CD27 in peripheral serum

Patient	Sex	Age	Diagnosis	Blasts	Cytogenetics	Genetic abnormalities
1	male	65	ID	68%	46, XY	NPM1+
2	male	61	ID	33%	46, XY	-
3	male	59	ID	76%	46, XY	CEBPA+2, WT1+
4	female	39	ID	65%	N/A	NPM1+, FLT3-ITD+, Trisomy 8
5	male	84	ID	44%	45,XY[12]/46,sl,+8[3]	Trisomy 8
6	male	66	ID	77%	47,XY,+8[2]/47,sl,der(18)t(3;18)(q21;q23)[6]/46,XY[6]	NPM1+, ASXL1+, Trisomy 8
7	male	62	ID	79%	46, XY	FLT3-ITD+, NPM1+
8	female	73	ID	N/A	N/A	N/A
9	female	69	ID	87%	46, XX	FLT3-TKD+, NPM1+, IDH2+
10	male	39	relapse	81%	N/A	N/A
11	female	82	ID	47%	N/A	N/A

ID = initial diagnosis, N/A = not available

Table Supplementary 6: Characteristics of AML patients used for evaluation of soluble CD27 in bone marrow fluid

Patient	Sex	Age	Diagnosis	Blasts	Cytogenetics	Genetic abnormalities
1	male	32	ID	61%	N/A	N/A
2	N/A	N/A	N/A	N/A	N/A	N/A
3	female	19	ID	92%	46,XX	FLT3-ITD+,CE-BPA2+
4	female	27	ID	63%	46,XX,der(7)t(7;13)(q3?;q?),inv(16)(p13q22)[11]/46,XX,dup(11)(q13q25),inv(16)(p13q22)[3]/46,XX[2]	FLT3-TKD+, CBFß-MYH11
5	male	56	ID	29%	N/A	N/A
6	male	59	ID	N/A	46, XY	-
7	female	51	ID	77%	46, XX	FLT3-ITD+, FLT3-TKD+, RUNX1+,
8	female	68	ID	55%	46, XX	-
9	female	73	ID	81%	47, XX,+8[13]/46,XX[9]	FLT3-ITD+, NPM1+
10	female	65	ID	32%	46, XX	FLT3-ITD+, NPM1+
11	male	79	ID	74%	45,X,Y,del(20)(q11)20	FLT3-ITD+, RUNX1+
12	male	46	ID	55%	46, XY	CEBPA+2
13	male	71	ID	49%	46,XY,der(12)t(10;12)(q11;p1?1)[10]/46,XY[10]	CEBPA+1
14	female	69	ID	N/A	N/A	FLT3-ITD+, NPM1+, IDH2

15	female	56	ID	90%	47,XX,+11[18]/46,XX[2]	FLT3-ITD+, KMT2A-PTD+, IDH2+
16	male	64	ID	60%	N/A	KMT2A-PTD+, RUNX1+, IDH2+
17	male	63	ID	40%	47,XY,+13[3]/46,XY[18]	RUNX1+
18	male	78	ID	24%	46,XY	ASXL1+
19	female	69	ID	72%	46,XX,t(8;12)(q12;p13)[8]/46,XX[4	FLT3-ITD+, NPM1+
20	male	66	ID	N/A	46, XY	CEBPA+1
21	female	64	ID	58%	46,XX,t(15;17)(q24;q21)[5]/46,sl, der(21)t(8;21)(q1?;p11)[8]	PML-RARA, FLT3-ITD+,
22	male	86	ID	52%	46, XY	FLT3-ITD+, NPM1+
23	N/A	N/A	N/A	N/A	N/A	N/A
24	female	28	ID	N/A	N/A	N/A
25	male	46	ID	40%	43,XY,del(5)(q13),del(6)(p22),i(8)(q10),-15,der(16)t(15;16)(q22;q21),-17,-18[8]/44~45,XY,del(5)(q13),+der(8)t(8;15)(p2?1;q22),+del(8)(p11),i(8)(q10),-15,der(16)t(15;16)(q22;q21),-17,-18[cp3]	TP53mut
26	male	25	ID	33%	46,XX	FLT3-TKD+, NPM1+

27	male	74	ID	58%	47,XY,+8,der(16)inv(16)(p13q22)del(16)(q22q22)[5]/47,XY,der(16)inv(16)(p13q22)del(16)(q22q22),+22[2]/46,XY[1]	CBFß-;MYH11
28	female	19	ID	92%	46,XX	FLT3-ITD+
29	female	77	ID	99%	46,XX	FLT3-ITD+, NPM1+, IDH1+
30	male	62	ID	79%	46,XY	FLT3-ITD+, NPM1+
31	male	76	ID	84%	46,XY,der(7)del(7)(p1?)del(7)(q11)[2]/46,XY,der(4)t(4;9)(p1?6;?),der(6)t(6;11)(q1?;q23)[5]/46,XY[4]	ASXL1+, RUNX1+
32	female	68	ID	N/A	N/A	IGH-rearrange-ment, tetrasomy 17 with TP53 deletion
33	male	68	ID	62%	46,XY,del(12)(p13)[14].ish del(12)(p13p13)(ETV6-)[21/21]/46,XY[4]	FLT3-TKD+, RUNX1+, ASXL1+
34	female	40	ID	60%	49,XX,inv(7)(p11q11.23),+8,inv(16)(p13.1q22),+21,+22	CBFß-MYH11
35	male	82	ID	97%	47,XY,+11[18]	FLT3-ITD+
36	female	56	relapse	42%	49,XX,inv(7)(p11q11.23),+8,inv(16)(p13.1q22),+21,+22	CBFß deletion
37	male	32	relapse	19%	46,XY,inv(16)(p13q22)[12]/46,XY[10]	CBFß-MYH11
38	male	39	relapse	81%	N/A	N/A

39	female	82	relapse	<10%	N/A	N/A
40	male	24	relapse	26%	N/A	N/A

ID = initial diagnosis, N/A = not available

Table Supplementary 7: Characteristics of AML patients used for *ex vivo* studies

Patient	Sex	Age	Diagnosis	Blasts	Cytogenetics	Genetic abnormalities
1	male	28	ID	70%	46,XY,add(2)(q37),der(22)t(9;22)(q34.1;q11.2)(18).ish der(2)t(2;22)(q37;q11.2)(BCR+),der(9)(ABL1 dim),der(22)z(9;22)q34.1;q11.2)(BCR+,ABL1+)(24)/50,sl,+4,+6,+10,der(22)t(9;22)(q34.1;q11.2)	BCR-ABL1 rearrange-ment
2	male	39	relapse	81%	N/A	-
3	male	77	ID	89%	46, XY	NPM1+, FLT3-ITD+
4	female	86	ID	N/A	46, XX	NPM1+, FLT3-ITD+
5	female	40	ID	29%	46, XX	NPM1+
6	male	56	ID	N/A	N/A	N/A
7	male	32	ID	96%	46,XY,t(9;11)(p21.3;q23.3)(3)/55,sl,+3,+8,+der(11)t(9;11)(p21.3;q23.3)+12,+13,+14,+18,+19,+20(13)	MECOM, KMT2A, ETV6, KMT2a-MLLT3, RUNX1T1
8	male	63	ID	89%	47,XY,+8(19)/46,XY(3)	NPM1+, FLT3-ITD+, Trismoy 8
9	male	54	ID	70%	46, XY	NPM1+, FLT3-ITD+
10	male	42	ID	80%	46, XY	CEBPA+2
11	female	75	ID	N/A	46, XX	N/A
12	male	59	ID	84%	46, XY	NPM1+, FLT3-ITD+

13	male	51	ID	N/A	N/A	N/A
14	male	53	ID	N/A	N/A	N/A
15	N/A	N/A	ID	N/A	N/A	N/A
16	N/A	N/A	ID	N/A	N/A	N/A
17	male	56	ID	61%	46,XY,-5,+8,t(12;22)(p13;q12)[2]/46,XY,del(2)(q22~q24),der(5)t(2;5)(q22~q24;q35),t(12;22)(p13;q12)[2]/46,XY,t(9;22;15)(q?21;q13;q2?2),t(12;22)(p13;q12)[7]	ETV6 rearrangement,
18	male	55	ID	67%	N/A	FLT3-ITD+

ID = initial diagnosis, N/A = not available

Acknowledgements

In first line, I would like to express my deep gratitude to Marion Subklewe, for letting me contribute to her research. I am especially thankful to her, for giving me lots of freedom, and the opportunity to attend local and international scientific conferences.

I was fortunate to be welcomed into a team of highly motivated and great scientists. I would like to thank the entire group for their assistance whenever I had a question about my research and for cheering me up when I was frustrated. Moreover, I would like to thank them for being remarkable and lovely people. I enjoyed our lunch breaks, parties, and hiking trips.

I want to thank Prof. Dr. Elfriede Nößner and Prof. Dr. Anne Krug who agreed to be my thesis advisory committee for their support and experimental ideas.

It was a pleasure to collaborate with Daniel Diolaiti and Sherif Abdelhamed from Seattle Genetics/Pfizer. Thank you for all the meetings and discussion on the project, but especially for performing the *in vivo* experiments and for providing the corresponding data.

I want to thank Prof. Dr. Martina Rudleius from the Pathology of the University Hospital LMU for collaborating with us and helping us to identify CD70 by immunohistochemistry.

I greatly appreciate the support from Prof. Dr. Wolfgang Enard and his team (Daniel Richter and Eva Briem) from the Faculty of Biology, Anthropology and Human Genomics for helping with RNA sequencing, and Dr. Tobias Straub from the Bioinformatics Unit at LMU for his support in data processing and analysis.

I am grateful for working in collaboration with Prof. Dr. Veit Hornung and his team (Andreas Linder, Ignazio Piseddu, Niklas Kuhl) on gene editing using CRISPR-Cas9.

I want to thank Prof. Dr. Heinrich Leonhardt and his team (Hartmann Harz and Andreas Maiser) for their support in the imaging experiments and editing of the images.

Finally, I would like to thank my family for believing in me and supporting me during my entire study period. Even though it was a challenging time for me, I am highly motivated to move on and contribute to new exciting research questions.

Affidavit

LMU LUDWIG-MAXIMILIANS-UNIVERSITÄT MÜNCHEN

Dean's Office Medical Faculty
Faculty of Medicine

Affidavit

Sponheimer, Monika

Surname, first name

I hereby declare, that the submitted thesis entitled

TNF-α and IFN-γ Differentially Regulate AML Cell Susceptibility to CD70-Antibody-Mediated Cytotoxicity

is my own work. I have only used the sources indicated and have not made unauthorised use of services of a third party. Where the work of others has been quoted or reproduced, the source is always given.

I further declare that the dissertation presented here has not been submitted in the same or similar form to any other institution for the purpose of obtaining an academic degree.

Munich, 8th of Feb 2026

Place, Date

Monika Sponheimer

Signature doctoral candidate

Confirmation of congruency

LMU LUDWIG-MAXIMILIANS-UNIVERSITÄT MÜNCHEN

Dean's Office Medical Faculty
Doctoral Office

Confirmation of congruency between printed and electronic version of the doctoral thesis

Sponheimer, Monika

Surname, first name

I hereby declare that the electronic version of the submitted thesis, entitled

TNF-α and IFN-γ Differentially Regulate AML Cell Susceptibility to CD70-Antibody-Mediated Cytotoxicity

is congruent with the printed version both in content and format.

Munich, 8th of Feb 2026

Place, Date

Monika Sponheimer

Signature doctoral candidate

List of publications

1. Philipp N, Kazerani M, Nicholls A, Vick B, Wulf J, Straub T, Scheurer M, Muth A, Hänel G, Nixdorf D, **Sponheimer M**, Ohlmeyer M, Lacher SM, Brauchle B, Marcinek A, Rohrbacher L, Leutbecher A, Rejeski K, Weigert O, von Bergwelt-Baildon M, Theurich S, Kischel R, Jeremias I, Bücklein V, Subklewe M. T-cell exhaustion induced by continuous bispecific molecule exposure is ameliorated by treatment-free intervals. Blood. 2022;140(10):1104-18.

2. Nixdorf D, **Sponheimer M**, Berghammer D, Engert F, Bader U, Philipp N, Kazerani M, Straub T, Rohrbacher L, Wange L. Adapter CAR T cells to counteract T-cell exhaustion and enable flexible targeting in AML. Leukemia. 2023;37(6):1298-310.

3. Hänel G, Schönle A, Neumann A-S, Nixdorf D, Philipp N, **Sponheimer M**, Leutbecher A, Emhardt A-J, Magno G, Bücklein V. Combining venetoclax and azacytidine with T-cell bispecific antibodies for treatment of acute myeloid leukemia: a preclinical assessment. Leukemia. 2024;38(2):398-402.

4. Nair R, Salinas-Illarena A, **Sponheimer M**, Wullkopf I, Schreiber Y, Côrte-Real JV, del Pozo Ben A, Marterer H, Thomas D, Geisslinger G. Novel Vpx virus-like particles to improve cytarabine treatment response against acute myeloid leukemia. Clinical and Experimental Medicine. 2024;24(1):155.